Design and Implementation of a Clutch and Brake System for a Single Wheel Indoor Tire Testing Rig

Aamir Khusru Khan

Thesis submitted to the Faculty of the
Virginia Polytechnic Institute and State University
in partial fulfillment of the requirements for the degree of

Master of Science
in
Mechanical Engineering

Corina Sandu, Chair
Saied Taheri
Robert L. West

September 19, 2017
Blacksburg, Virginia

Keywords: terramechanics, tires, tire testing, brake, clutch

Design and Implementation of a Clutch and Brake System for a Single Wheel Indoor Tire Testing Rig

Aamir Khusru Khan

ABSTRACT

The primary goal of this work is to design and implement a clutch and brake system on the single tire Terramechanics rig of Advanced Vehicle Dynamics Laboratory (AVDL) at Virginia Tech. This test rig was designed and built to study the performance of tires in off-road conditions on surfaces such as soil, sand, and ice. Understanding the braking performance of tires is crucial, especially for terrains like ice, which has a low coefficient of friction. Also, rolling resistance is one of the important aspects affecting the tractive performance of a vehicle and its fuel consumption. Investigating these experimentally will help improve tire models performance. The current configuration of the test rig does not have braking and free rolling capabilities. This study involves modifications on the rig to enable free rolling testing when the clutch is disengaged and to allow braking when the clutch is engaged and the brake applied. The first part of this work involves the design and fabrication of a clutch system that would not require major changes in the setup of the test rig; this includes selecting the appropriate clutch that would meet the torque requirement, the size that would fit in the space available, and the capability to be remotely operated. The test rig's carriage has to be modified in order to fit a pneumatic clutch, its adapter, a new transmission shaft, and the mounting frame for the clutch system. The components of the actuation system consisting of pneumatic lines, the pressure regulator, valves, etc., have to be installed. Easy operation of the clutch from a remote location is enabled through the installation of a solenoid valve. The second part of this work is to design, fabricate, and install a braking system. The main task is to design a customized braking system that satisfies the various physical and functional constraints of the current configuration of the Terramechanics rig. Some other tasks are the design and fabrication of a customized rotor, selection of a suitable caliper, and design and fabrication of a customized mounting bracket for the caliper. A hydraulic actuation system is selected since it is suitable for this configuration and enables remote operation of the brakes. Finally, the rig is upgraded with the assembly of these two systems onto it.

Design and Implementation of a Clutch and Brake System for a Single Wheel Indoor Tire Testing Rig

Aamir Khusru Khan

GENERAL AUDIENCE ABSTRACT

The main goal of this project is to increase the testing capabilities of the single tire Terramechanics rig of Advanced Vehicle Dynamics Laboratory (AVDL) at Virginia Tech. The first task is to enable the rig to have the tire in free rolling condition. This will allow to study rolling resistance of the tire on various off-road conditions such as soil, sand, etc. The free rolling capability will also allow evaluation of the rolling radius of a tire. A customized clutch system was designed to achieve this free rolling requirement. The second task of this project was to implement braking capabilities to the rig. Apart from the traction performance of tires on off-road conditions such as ice, the other parameter is its performance during braking as it is an important factor leading to safety on roads. A customized disc brake system is designed to add braking capabilities to the rig. This free rolling and braking systems has to implemented taking into account the various physical and functional constraints of the rig. The work involves the design and fabrication of various customized components followed by the assembly of these components along with their actuation systems.

Dedication

To the memory of a beloved and cheerful friend Rajat Bhan who left us all at a very young age. You are missed and will always be missed.

To the 32 beautiful souls of Virginia Tech who left us all 10 years ago in a tragic incident. You will not be forgotten.

Acknowledgments

I would like to extend my sincerest gratitude to my advisor, Dr. Corina Sandu. It was an honor to work under her guidance. She has been a source of inspiration for me to push myself and work harder. Her guidance throughout my tenure as a graduate student has helped me grow from strength to strength. I feel lucky and blessed for having had the opportunity to be her student. I am indebted for all her help and support. I would also like to express my deepest gratitude to Dr. Saied Taheri and Dr. Robert West, for their teachings and guidance. Their courses helped me build up on my knowledge and learn valuable lessons in the respective topics.

I take this opportunity to thank all my colleagues at AVDL and CenTiRe for their help and support. A big thanks to Emilio Jimenez, Rui He, Sebastien Corner, Tan Li, Hoda Mousavi, Sterling McBride and Sunish Vadakkeveetil. Special thanks to Ms. Diana Israel for helping me place the order of all the materials as and when required. Her help enabled me to stick to my timeline for the project. I would also like to thank all the personnel from the ME machine shop. I am really thankful to Mr. Timothy Kessinger, Mr. Bill Songer, and Mr. Phillip Long for their valuable help in all the machining and fabrication work. I would like to thank Dr. Qing Li for helping us place the order for the clutch from China. My warmest gratitude to Ms. Jenna Dixon for being a friend, a mentor, a colleague, and a supervisor. She helped me learn many new things. The work of developing and maintaining the ISTVS website with her was a productive time away from books and laboratory work. I would like to thank CenTiRe for partially supporting me financially.

I would also like to express my deepest and sincerest gratitude to parents and grandparents. This would not have been possible if it were not for them. Their constant support and encouragement has motivated me to pursue my goals. Their blessings and guidance has helped me to stay focused.

This is an opportunity to thank my mentors and teachers from my undergraduate school. My sincerest regards to Dr. Rollin Fernandes, Prof. Thomas Mathewlal, Prof. Prasad Bari and many others for helping me become who I am. Your constant challenges and push, helped me to work harder and better.

Contents

List of Figures

List of Tables

Chapter 1

Introduction

This chapter introduces the work that was carried out as part of this research. The chapter briefly discusses the motivation for this research, the objectives of this study and the approach that was followed. The first section introduces the motivation for this work.

1.1 Motivation

The single tire Terramechanics test rig at Advanced Vehicle Dynamics Laboratory(AVDL) at Virginia Tech was built in 2007 for studying various tire parameters for off−road conditions like ice, sand, etc. The current configuration of the test rig enables to measure the drawbar pull and the lateral forces under various slip conditions. A comparison of different tires for traction performance on soil and ice can be achieved using this[6]. One of the other important aspects of the tire, which is currently a topic of active research, is the rolling resistance. Studying this factor experimentally for off−road conditions, such as soil and ice, can help in improving tire models for the same. The current setup has motors driving the wheel and carriage separately. In order to study rolling resistance, it is important that the

tire undergoes pure rolling action, i.e., under towing mode. There was a need to introduce a mechanism to isolate the motor from the tire as per requirement. Apart from traction, the other important aspect of tires is its performance during braking operation, especially on conditions such as ice surface. This motivated to investigate the feasibility of incorporating a braking system on the Terramechanics rig and implement the same.

1.2 Objectives

As discussed in the previous section, for off−road conditions, rolling resistance, and braking performance are also some of the important aspects in terms of tire modeling. To enable measurement of these parameter using the Terramechanics rig, it was necessary to incorporate few modifications to it. The objective involved investigating the feasibility of such systems which would allow free rolling or towing motion of the tire on the rig and braking application to the wheel.

The first objective of this work is to investigate the means of positively isolating the tire driving motor from the tire; further, design a system based on the investigation and finally fabricate and install it on the test rig.

The second objective of this study was to investigate means of implementing braking system to the Terramechanics rig and consequently design a customized brake system for the rig. This would follow with the fabrication and installation of this system onto the rig.

The last task would involve the calibration and testing of this system to validate these modifications.

1.3 Approach

The initial work involved studying few other testing facilities which were developed for testing of tires. Further, study how the braking and power isolation is achieved in actual automobiles and investigate the feasibility of having a similar system onto the Terramechanics rig.

The first task was to study clutch system which is a commonly used mechanical component for isolation of power from the engine to the wheel. Study the feasibility of having such a system on the Terramechanics rig based on the current configuration of the rig. One of the key aspects of this study was to have minimum modification to the rig. It involved designing a framework to install such a system without causing major modifications to the test rig. Having investigated and designed such a system, the next work would be to fabricate all the parts of the system and assemble it on the rig. Finally, test the system with this new modification and calibrate it.

The second objective involved the study of brake systems and required identifying which of them would best suit the rig; investigate and identify locations for installation of such a brake system. Once a system has been finalized, the next activity would be to design a customized braking system that would not cause major modifications to the configuration of the rig. Once the design is completed, the following task would be to fabricate and install it on the Terramechanics rig. Finally just like the clutch system, the braking system will be tested and the rig will be calibrated.

Chapter 2

Literature Review

In this chapter, some of the most relevant existing testing facilities of tires are discussed in terms of their testing capabilities and features. This chapter also discusses the braking systems and clutch systems in case of automobiles and how it can be incorporated into a testing facility such as the Terramechanics rig at AVDL [6]. The main sections of this chapter are as follows:

- Indoor Tire Testing Facilities
- Clutch System
- Brake System

2.1 Overview of Indoor Tire Testing Facilities

Various indoor and outdoor tire testing facilities have been developed all around the world to study the tire parameters under different conditions. These include test rigs devel-

oped for planetary exploration rover's wheel development, off−road tire performance, agricultural tire performance, etc. Some of the facilities which are similar to the Terramechanics rig at AVDL are discussed below:

UPM Indoor Tire Traction Testing Facility

The testing facility at Universiti Putra Malaysia (UPM) [1] was developed to test agricultural tires on tropical soil. It consists of a moving carriage mounted on rails above a soil tank. The tire to be tested is mounted as a cantilever arrangement as shown in the schematic Figure 2.1 [1].

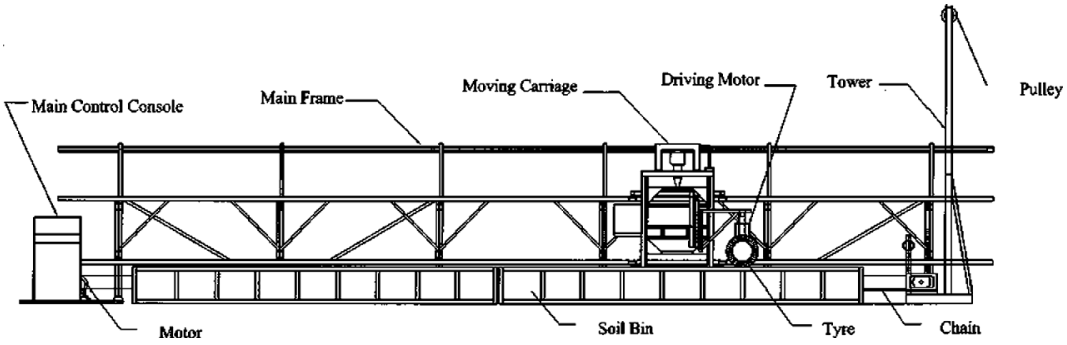

Figure 2.1: Schematic diagram of the UPM Indoor Tire Traction Facility, Figure 1 [1], Used under fair use, 2017; Fair use determination attached.

The carriage can be set moving at a speed from 0.053 m/s (0.12 mph) to 0.547 m/s (1.22 mph). The test rig has two modes of operation, i.e., towing test mode and driving test mode. The testing facility has two soil tanks of size 6.4 m x 0.6 m x 0.8 m. There are two individual motors that drive the carriage and wheel. In the towing mode, the carriage motor was active and it pulled the wheel on the soil bin surface. In the driving test mode, the wheel motor powers the wheel and pulls the carriage with an additional pull provided by a cable−pulley arrangement. The motor is connected to the respective shafts in all the modes. The towing test is used to study tire motion resistance whereas the driving mode

is used for tractive efficiency studies. This facility doesn't have any active method to study the tire performance during braking operation.

Single Wheel Tester, Off−Road Dynamics Research Laboratory, Cranfield University

The single wheel tester at Off−Road Dynamics Laboratory at Cranfield University consists of soil placement unit which is 45 m long and 5 m wide with a variable depth of 0.75 m upto 35 m length and 1.5 m for the rest 10 m length. The wheel tester is fixed on a Claas Xerion tractor [7]. Normal load is applied through a hydraulic system. A winch mounted on the platform is used to add restraint or drive to the wheel and has a capacity of 50 kN pull for upto 50 m. The tester is used for tires sizes from 0.5 m to 1.4 m and can be steered in both directions upto 20deg. A control system uses the torque, load and speed measurements to follow a pre−defined torque and slip control as well as maintain the normal load independent of the vertical motion of the tire.

Portable Tire Test Rig, Intelligent Transportation Laboratory, Virginia Tech

The Portable Tire Test Rig has been developed by Intelligent Transportation Laboratory at Virginia Tech [2], for collecting tire data on various on− and off−road surfaces. The arrangement and setup is somewhat similar to an in−house testing facility. It consists of load frame which is mounted inside the trailer of size 2.44 m x 9.75**m** (8 ft x 32 ft) and the tire is lowered from a cut out of size 1.22 m x 2.44 m (4 ft x 8 ft) as shown in Figure 2.2 [2].

This trailer is pulled by a truck with high drawbar pull capacity. All the hardware and the software is powered by a gasoline generator placed on this truck. The test tire

Figure 2.2: Tire access to the ground, Portable Tire Test Rig, Figure 4.2 [2], Used under fair use, 2017; Fair use determination attached.

simply rolls due to the towing action and no power is provided to the test tire. There is an arrangement for vertical load application through air−springs. The load frame has a servo mechanism setup to provide steering to the tire. It provides tire slip angle between −20 degrees to +20 degrees under the assumption the trailer is towed in a straight line. An additional arrangement using a servo motor provides camber angle. A *Kistler* force hub is used for tire force and moment measurement. This setup also has a braking system in the form of disc brake operated using mechanical pedal effort.

Soil−Tire Interaction Testbed (MIT)

This is single wheel test bed developed by Field and Space Robotics Laboratory (FSRL) of the Massachusetts Institute of Technology (MIT) [8] for studying planetary rovers. The test bed has all the measurement systems installed to measure the forces, moments, velocities. It has two motors: one driving the carriage and the other driving the wheel. By

controlling the velocity of the carriage and the rotational velocity of the wheel, various slip ratios are achieved.

All-terrain Vehicle (ATV) Tire Traction Research Machine for use on Soil Bins

Another indoor single tire testing facility developed at USDA−ARS National Soil Dynamics Lab, Auburn [3] to measure motion resistance and traction properties of all terrain vehicle tires. The normal loading is in the form of dead load upto a maximum load of 2700 N (600 *lbs.*) The ATV machine is designed for maximum overall tire diameter of 0.69 m and a maximum width of 0.28 m. There are six load cells in the three axes to measure the forces in the longitudinal, vertical and lateral direction. A hydraulic motor drives the wheel through chain and sprocket arrangement. It does not have a provision for changing the camber or the toe angle of the wheel. A Traction Research Vehicle (TRV) drives this setup similar to a carriage in the previous sections as shown in Figure 2.3 [3].

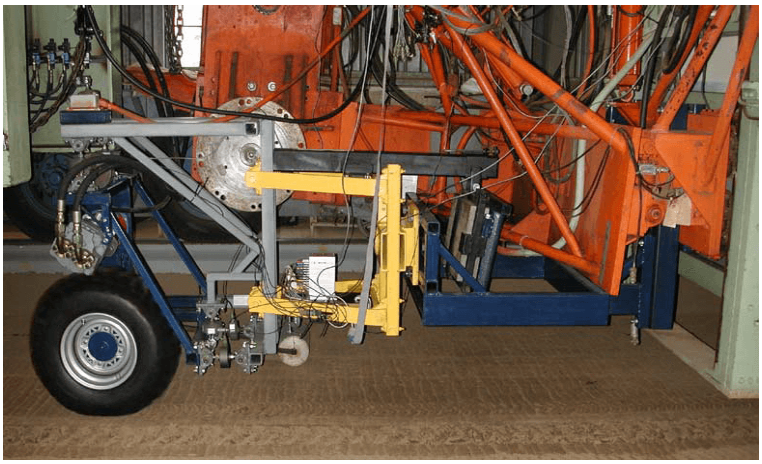

Figure 2.3: All−Terrain Vehicle (ATV) Tire Traction Research Machine, Figure 6 [3], Used under fair use, 2017; Fair use determination attached.

Indoor Traction Measurement System, Kyoto University

An indoor testing facility developed at Kyoto University consisted of a single wheel tester, a traction load device, a mixing and compacting device as shown in Figure 2.4 [4].

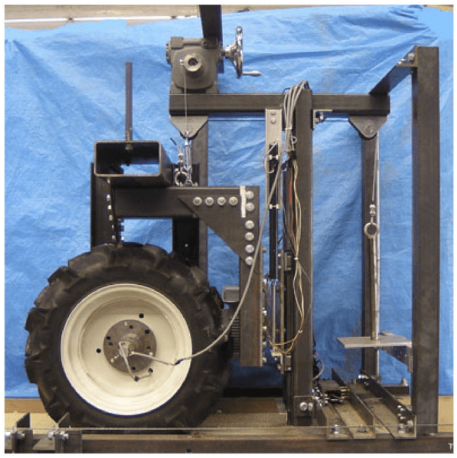

Figure 2.4: Single Wheel Tester, Figure 3 [4], Used under fair use, 2017; Fair use determination attached.

The mixing device and the wheel tester move along a soil bin which 3.015 m long, 0.48 m wide and 0.605 m deep. An electric motor pulls the wheel assembly in the longitudinally through a steel wire. A constant traction is achieved using the traction load device. The tire is driven using an electric motor through a reduction gear unit and an inverter unit controls the motor's revolution speed. The displacement of the wheel is measured using a rotary encoder to the pulley measures of the single wheel tester and a linear potentiometer measures the tire sinkage. The drawbar pull is measured using an octagonal ring transducer.

Most of the testing facilities reviewed had a unique design serving the purpose of their functional requirements. The capabilities of interest was the ability to study tractive performance, braking performance and achieve free rolling of the tire to study motion resistance. A majority of the facilities had one or two of these capabilities described above. Thus, it was imperative to come up with a design unique to the Terramechanics Rig at AVDL so as

to achieve the above three capabilities.

In automobiles, the clutch facilitates the isolation of power from the engine to the wheels. When the gears are shifted or when the brakes are applied to a running vehicle, the first operation is actuating the clutch. Similarly, in our intent to study free rolling and braking, it is important that the power from the wheel motor is isolated from the wheel. The following sections is a brief review of automobile and industrial clutches and brakes.

2.2 Clutch System

A clutch is a mechanical component that couples or decouples power/torque from a driver shaft to a driven shaft. In automobiles, a clutch performs the function of isolating the power coming from the engine to the wheels. The clutches in automobiles have transformed from manual transmission type to the latest automatic transmission. Most of the clutches function on load being transmitted through frictional force between two mating surface. Cone clutch, single plate, multiple plate clutch etc., are some of the clutches that work on the principle of friction. Cone clutch has the friction contact surface in conical shape where the driving part would precisely fit into a conical shaped flywheel. These were used in the early Daimler cars [9]. There is an inherent problem due to the conical shape. It has a tendency to lock up due to expansion. Later, with the development of the clutch plate, the design and types of clutch increased. The single plate clutch is a type of dry friction clutch with a very simple design. It comprises of a metallic disc with a friction material layer on it. In the engaged mode, it is in contact with the output hub using the axial force through springs. To disengage the clutch, a pedal effort linked through levers acts against this springs thereby disengaging the clutch. Initially, helical springs and coil springs were used. Later diaphragm spring clutch became popular since it provided lower pedal effort. This spring

is a Belleville shaped metal disc and is still very common in manual transmission clutches. Multi−plate clutch functions similar to the single plate clutch with a variation in design. It has a series of clutch plates instead of just one. Initial multi−plate clutches had their clutch plates immersed in oil for lubrication. It is lubricated to reduce the wear and tear and improve the cooling capacity. The reduction in the coefficient of friction due to the presence of a lubricating medium is compensated by the multiple number of plates.

Working of a Clutch

The engine crankshaft is connected to the flywheel which has a frictional surface on the gearbox side of the transmission line. When the clutch is engaged, power is transmitted from the flywheel to the clutch plate and then to the gearbox. The clutch plate comprises of a hub connected to a splined shaft. A pressure plate is bolted to the flywheel and it rotates with the flywheel. The clutch plate is held in position in between the flywheel and this pressure plate. The diaphragm springs applies force at the outer circumferential area of the pressure plate. This engages the clutch plate against the flywheel. A splined shaft connected to the pressure plate serves as the output. When the gear has to be shifted, the power has to be cut off from the engine to the gearbox. In order to do that, pedal effort is applied, which is transmitted using mechanical linkages or using hydraulic forces to the clutch. This manual effort is translated through lever mechanism which is connected to a release bearing. This causes the release bearing to move in and apply a force on the inner circumferential area of the diaphragm spring. This spring is pivoted at a ring held between the inner and the outer circumference. Due to this action, the diaphragm outer circumference moves outward from the clutch plate. This disengages the clutch plate from the flywheel. Releasing the pedal effort, causes the diaphragm spring to flip the other way to apply force on the pressure plate which again engages the clutch.

Dry Clutch and Wet Clutch

Clutch engagement is a process where the driven component gradually attains a speed close to the speed of the driving component. While the driving component runs at a constant velocity, the driven component's speed rises from zero to somewhere close to the driving component's speed. During this time period there is a frictional loss in form of heat. Additionally, it also causes the wearing of the frictional surface. This is fundamentally how a dry clutch works. As against this, there are clutches that are lubricated with oil. This lubrication helps in cooling the clutch plate and the pressure plate. However, it also causes the engagement time to increase since the coefficient of friction is reduced. Thus, in order to increase the power transmission capacity, wet clutches are usually multiple plate type. Hele−Shaw clutch [9] was one of the initial wet clutches developed in the 1900s. These clutches were costly and the design was complex. It required proper maintenance, properly designed housings etc. With the advent of better friction material, dry clutches gained popularity since they were inherently free from all the problems that the wet clutch caused.

Non−Slip Clutches

In a friction based clutch, power is transmitted to the driven shaft through frictional force. As mentioned previously, the driven shaft through the clutch plate tries to attain the speed of the driving shaft. This difference in speed causes slip [9]. In some applications, mostly industrial, this slip is undesirable. For this reason, various forms of non−slip clutches have been developed. The dog clutch is one such type of non−slip clutch. The driving and the driven part of the clutch perfectly lock into each other. The driving component of the clutch has a gear profile while the driven component has a negative gear profile. When in engaged position, the two components lock on each other. This is similar to the synchromesh

gearbox. The other type of non−slip clutch is the toothed clutch. Similar to the dog clutch, the toothed clutch also has a profile on the driving component and the negative profile on the driven component. However, the profile is in the radial direction as against the axial gear profile on the circumference in the case of a dog clutch. Unlike the friction type clutch, these clutches do not encounter the phenomenon of slip. The engagement process is usually actuated by electromagnetic forces or pneumatic forces.

Electromagnetic Clutches

Unlike the friction or the non−slip type of clutch, these are non−contact type clutches. They develop the torque due to electromagnetic forces [10]. Some of the types of electromagnetic clutches are magnetic particle clutch, hysteresis clutch, eddy current clutch etc. These clutches are sometimes a combination of brakes and clutch. In the magnetic particle type of clutch, the input shaft is attached to a drum which encloses another smaller cylinder/drum which is connected to the output shaft. The region between these two drums is filled with magnetic particle. The electromagnetic field is generated when coil outside the outer drum (placed concentrically) is energized. This links the outer and inner drum using the magnetic particles. The stresses in these links resist the relative rotation between the driver and the driven shaft and thus transmits the torque. The transmitted torque depends on the energy or the current in the coil and is independent of the speed of the driver [10]. In case of a hysteresis clutch, there are two cup shaped members instead of drums, connected to the driver and the driven shaft respectively. The outer member is grooved on the inner side (axial slots called wells) and the inner cup has the same wells on its outer surface. These wells act as alternating poles when they are energized by the current through the coils at their base. The output shaft is connected to the inner cup and the driving shaft is connected to the outer cup. The energization of the coils causes the formation magnetic poles in the slots. These

magnetic poles keeps changing polarity resulting in hysteresis. At any instant, the polarity in the walls of the outer cup is such that it forces the inner cup to remain stationary relative to the input shaft, i.e., no relative rotation. In this way, the torque is transmitted from the input to the output shaft. The eddy current clutch operates on the principle of eddy current and is similar in functioning as the hysteresis type clutch.

2.3 Brake System

In automobiles, braking is an action of slowing down or bringing the automobile to a complete stop, maintaining speed on a downgrade or keeping it stationary [11]. The resistive or braking force develops between the tire treads and the road surface. This force depends on the normal load and the coefficient of friction between the tire and the road surface. This force to be transmitted between the tire treads and the road surface, cannot be more than the product of the normal load and the coefficient of friction [11]. In terms of energy, the kinetic energy of the automobile is required to be converted to some other form (heat in case of brakes) in order to slow it down or bring it to rest. Similar to the clutch, brakes generally use frictional force to generate the braking force/torque. The friction based brake systems in case of automobile are primarily of two types − drum brakes and disc brakes.

Drum Brakes

Drum brakes were used quite extensively in almost all the vehicles. Drum brakes consists of drum which is connected to the wheels. A set of internal shoes are pivoted inside which have a frictional material on it. A set of hydraulic piston or cam is in contact with the shoes at their free end. The pedal effort is translated to this hydraulic pistons or cams. The action of the cam/piston causes the shoes move outward such that the frictional material

comes in contact with the inner circumference of the drum. This generates a frictional force (brake torque), which slows down the automobile and eventually brings it to rest. Depending on how the shoes are pivoted inside the housing, the drum brakes can be self locking or self energizing type. When the frictional torque aids the actuating torque, it is called self energizing brakes. Self locking brakes is a situation when no more actuating force is required to apply the brake. Drum brakes with two shoes pivoted at two locations are called dual−anchor brakes [11]. Further, these dual−anchor brakes are of different types viz. cam brake, wedge brake, simplex brake and duplex brake. These are the types based on how the actuating force is applied to the shoes, either through a cam or a wedge etc. Another type of arrangement having a single anchor point with two shoes is the Bendix brake [11]. None of the shoe is permanently fixed and it shifts locations depending on the rotation of the drum. The arrangement is such that one of the shoes is pivoted to the anchor point and other shoe is pivoted to the first shoe and adjusted using an adjusting screw. This enables the entire patch of the friction material right from the head to toe to have a uniform wear of the friction pad.

Disc Brakes

The other category of the friction based brakes which is highly popular nowadays is the disc brake system. The disc brake has two major components − a disc or brake rotor which is mounted on the wheel hub, and a brake caliper which clamps the rotor with a pair of frictional brake pads. The major advantage of disc brake over drum brake is its ability to have greater heat dissipation and decreased fading of the frictional materials [11]. The major disadvantage of disc brake over drum brake is the larger actuation force that is required to put the brake in action. Some of the larger earth moving equipment have multiple disc brakes housed in an oil bath. This is done to keep the dirt away and also for

better heat dissipation. Unlike drum brakes, disc brakes have less susceptibility to brake fade. In case of a regular heavy braking, there are chances of brake fade in the case of disc brakes. This is counteracted using vaned or ventilated disc rotors. The vanes help in better heat dissipation and improves the rotor's life. Further, the calipers have a linear relationship between the brake torque and the coefficient of friction between brake pad and rotor [11]. These calipers for automobile applications usually don't have the self energizing modes like the drum brakes. The caliper is bolted to a rigid or a fixed body relative to the brake rotor. Depending on the design, the number of pistons in a caliper varies. The outward motion of the pistons forces the brake pads onto the brake rotor. This is known as the clamping force. There are generally two types of caliper − fixed caliper and floating caliper. The fixed caliper has pistons on both sides of the break rotor. The brake line pressure acts on the both the pistons which move outwards pushing the brake pads and thus clamping the brake rotor. The floating type caliper has piston on the inner side also called the inboard side. The caliper is mounted on a pin that is bolted onto the rigid part. When the pressure is applied on the piston. The piston moves out the the inboard side brake pad starts applying force on the brake rotor. On further application of pressure, the piston can't move more which offers resistance and causes the caliper to move inward on the sliding pins. This causes the brake pads on the outboard or wheel side to come in contact with the brake rotor.

Electromagnetic Brakes

These brakes work on the similar concept as the electromagnetic clutches [10]. Some of the types of the electromagnetic brakes are same as the clutches, i.e., magnetic particle brakes, hysteresis brakes, eddy current brakes, etc. The only difference when it comes to brakes as against the clutch is that unlike the clutch which has two moving parts, the brakes just have one moving part. In the magnetic particle brake, one of the drum is stationary

and the other is rotating part, i.e., the inner part. When the electricity is passed through the coil, the linkages are formed via the magnetic particles and they take the stress, i.e., the shear and tensile stresses [10]. This resists the rotating motion of the inner drum thereby slowing it down and eventually stopping the motion. A similar action occurs in the other two, i.e., hysteresis and the eddy current brakes, where one of the moving parts is stationary and these electromagnetic forces then try to slow down the rotating member.

Actuation Mechanism

In the previous sections, various types of brake systems were described briefly. The basic idea was that two surfaces come in contact to each other creating frictional force which eventually caused the braking torque. Now the mechanical force which pushes the brake pad or brake shoes on the metallic rotor or the drum, is caused by various other medium. One of the medium is hydraulic force. Hydraulic fluid pressure is used to push the piston out in case of brake calipers. This hydraulic pressure is created by a mechanical pedal effort into the master cylinder which is a piston−cylinder arrangement. This pressure created by the pedal effort is transmitted through brake hose to the brake caliper pistons. The other medium that is used is compressed air. In air brakes, the action of pushing the piton out is carried out by compressed air. A tank in the automobile stores the compressed air. This tank is constantly filled with by compressing the air using some power from the motion of the vehicle. When the brake pedals are applied, compressed air is released from the tanks that reach the brake pistons. Some of the other types of the actuation includes mechanical linkages. In general for an automobile, even if all the wheels have disc brakes, the rear end tires would have a dual type of rotor which has an offset at the hub region. This serves as a drum for the parking brake system. The actuation is generally through mechanical linkages applied to the cam or wedge in the drum brakes. One more type of brake actuation is the

electric brake where the braking action is still frictional but the actuating part uses electrical components for pushing out the piston similar to the working of a solenoid.

Chapter 3

Theoretical Aspects of Free Rolling and Braking of a Tire

3.1 Rolling Resistance and Free Rolling of a Tire

3.1.1 Rolling Resistance

The various forces and moments that act on the tire includes the normal force, the longitudinal force, the lateral force, the aligning torque, the overturning moment and the rolling resistance moment based on the axis systems defined by Society of Automotive Engineers (SAE) [12] is shown in the Figure 3.1. The longitudinal axis is defined by the X−axis, the lateral axis is defined by the Y−axis and the vertical axis point pointing up as shown by the Z−axis. The tire on the Terramechanics rig represents the left front wheel and thus, the transformed axes is as shown in Figure 3.2.

When a tire rolls over a surface under the weight of the vehicle, a section of the tire

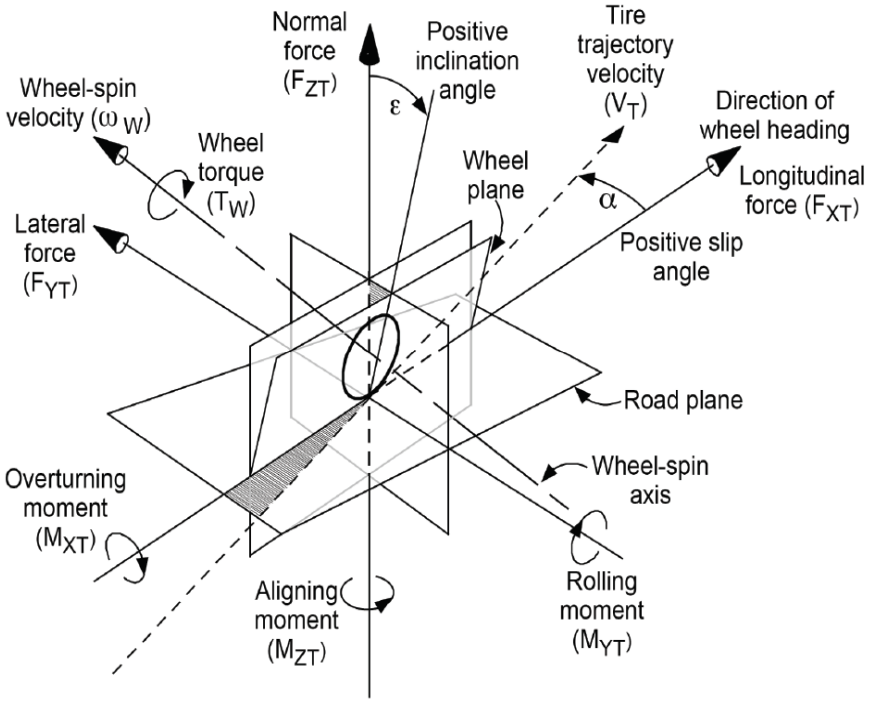

Figure 3.1: Tire force and moment system from SAE − Z axis up, Vehicle Dynamics Terminology: SAE J670, 2008, Used under fair use, 2017; Fair use determination attached.

undergoes deformation. This deformation occurs as the tire enters the contact patch and is recovered when it leaves the contact patch. Since rubber is a deformable material, it experiences hysteresis. A fraction of the energy spent in deformation is not recovered after relaxation. This causes a shift in the center of the normal pressure in the direction of the rolling motion. This shift in the center of the normal pressure in the longitudinal direction causes the rolling resistance moment. Now considering a free rolling tire where no torque is applied to the tire, a counteractive force must act at the tire−terrain interface to maintain equilibrium and this longitudinal force is called rolling resistance. The coefficient of rolling resistance is the ratio of the rolling resistance to the normal load. There are many factors that affect the rolling resistance in the case of a pneumatic which includes factors related to the construction of the tire and the factors related to the operating conditions of a tire [5].

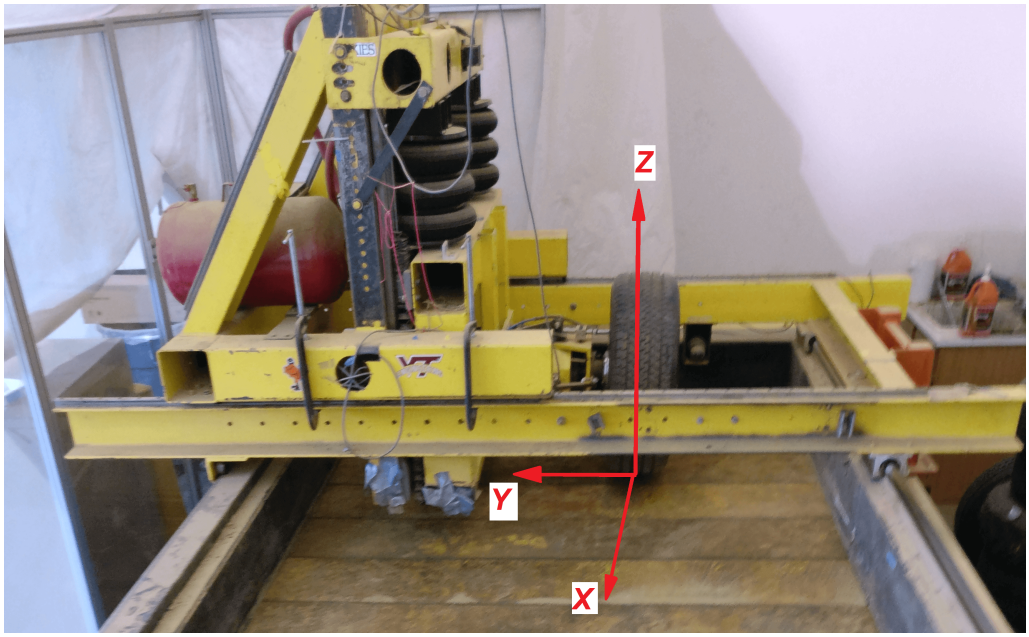

Figure 3.2: Axis system for the Terramechanics rig

The construction of tires, i.e., radial ply or bias ply, the construction of treads, the size of the tire, the composition of the rubber compounds and the operational conditions such as the tire pressure and the speed of the tire, operating temperature, etc. contributes to the rolling resistance. The other parameter important in contributing to rolling resistance is the surface on which the tire is running. In general, the coefficient of rolling resistance on smooth surfaces, such as concrete roads, are low. The value of the coefficient of rolling resistance becomes significant when the tire runs on soft deformable surfaces such as sand and soil. This is due to the tire causing penetration of the deformable surfaces, which adds to the rolling resistance. For experimental study of rolling resistance, it is a primary requirement that the tire is free rolling, i.e., the power to the wheel has to be isolated.

3.1.2 Longitudinal Slip and Rolling Radius Tire

When a torque is applied to a tire, there is a difference in the velocity of the center of the wheel and the velocity at the contact patch. As the torque is applied to the tire, the tread element in front of the contact patch, i.e., the leading edge are compressed whereas the treads at the back of the contact patch, i.e., the trailing edge have tension. Due to this, the distance that the tire moves is less that in the case if no torque was applied to the tire. This difference in the speed is called longitudinal slip and is given by Eq. (3.1) [5].

$$i = (1 - \frac{V}{r\omega}) \tag{3.1}$$

Where i represents the longitudinal slip ratio, V represents the velocity of the wheel center, r is the rolling radius of a free rolling tire and ω is the angular speed of the tire. The percentage slip is simply multiplying this slip ratio by 100. The effective rolling radius on the other hand is the ratio of the velocity of the center of the tire and the angular velocity of the tire as shown in given by Eq. (3.2)

$$r_e = \frac{V}{\omega} \tag{3.2}$$

Where r_e represents the effective rolling radius. This reduces the longitudinal slip ratio formula as shown in Eq. (3.3).

$$i = (1 - \frac{r_e}{r}) \tag{3.3}$$

Positive slip is the case when torque is applied to the tire which causes $r\omega$ to be greater than the linear velocity of the wheel. This slipping can increase a lot on surfaces

with low coefficient of friction such as ice, where there are chances of the tires to slip 100%. Conversely, when a braking torque is applied, what we see is the reverse of this process. The tread elements at the trailing edge are undergoing compression and the tension at the leading edge and the tire center is still moving in the forward direction with a velocity textitV. Due to this action the velocity, $r\omega$ gets smaller than the velocity of the center of the wheel. Under this scenario Eq. (3.1) gives a negative longitudinal slip or longitudinal skid. To express this ratio as a positive number, Eq. (3.3) is modified to represent skid during braking operation and given by Eq. (3.4).

$$i_s = (1 - \frac{r}{r_e}) \tag{3.4}$$

Where i_s represents the longitudinal skid in case of braking operation. For all this calculation, one of the important parameters to be determined is the free rolling radius of the tire. This can be achieved only when the tire is free rolling and in that case, the effective rolling radius and the free rolling radius are the same. All these factors are important because of the fact that the tractive force or the braking force depends on the longitudinal slip. Generally the tractive force increases with an increase in the longitudinal slip, reaches a peak value and then starts decreasing till the longitudinal slip is 100 %, where the wheel is simply sliding/spinning with no longitudinal motion. The aim here is to have the maximum tractive force. Experimental work is done to evaluate this peak value and from few studies, it is found that, for non−deformable surface this peak tractive force is reached for slip ratios between 15 % and 20 %. The peak value also depends on the coefficient of friction between the tire−terrain interface. Therefore, during experimental evaluation where the slip ratios are controlled, the primary task is to evaluate the rolling radius of tire.

In case of the Terramechanics rig, the longitudinal slip ratio is achieved by controlling

the speed of the wheel motor with respect to the speed of the motor that moves the carriage longitudinally using a two axis *PicPro* motion controller. The code for the controller is written in ladder programming. The value of the longitudinal velocity V is kept constant during a test. This is also verified during each test using a distance measurement system and measuring the time taken by the carriage to move a particular distance during each test. The speed of the motor of the wheel depends on the evaluation of the rolling radius of a free rolling tire (r). For the Terramechanics rig, Naranjo [13, 14, 15] developed the *Wireless Internal Tire Sensors (WITS)* system to measure the radius, specifically the deflected radius of the tire. It comprised of 8 infrared emitting diodes (IRED) placed at equal intervals on the wheel rim. The rolling radius of a free rolling tire has been obtained using the *WITS* system for different tire sizes and normal loads. Based on the required slip ratio and using Eq. (3.3), the value of the effective rolling radius (r_e) is determined. The value of r_e and V is then substituted in Eq. (3.2) to evaluate the value of angular speed (ω) that will give the desired slip ratio. The value of ω is then used in the ladder program that controls the motion of the wheel motor. Thus the value of r dictates the setting of the longitudinal slip for the Terramechanics rig. Accurate knowledge of the free rolling radius of the tire will lead to accurate setting of the longitudinal slip and thereby accurate evaluation of the peak tractive effort.

3.2 Braking

Braking is the action of slowing down a vehicle, bringing it to complete stop or holding it stationary on an inclined surface. The necessary forces to bring these changes occurs at the tire contact patch. Now to understand the nature and amount of braking force required, we look at a simplified vehicle model with brake forces applied to both the front and rear

wheels as shown in Figure 3.3.

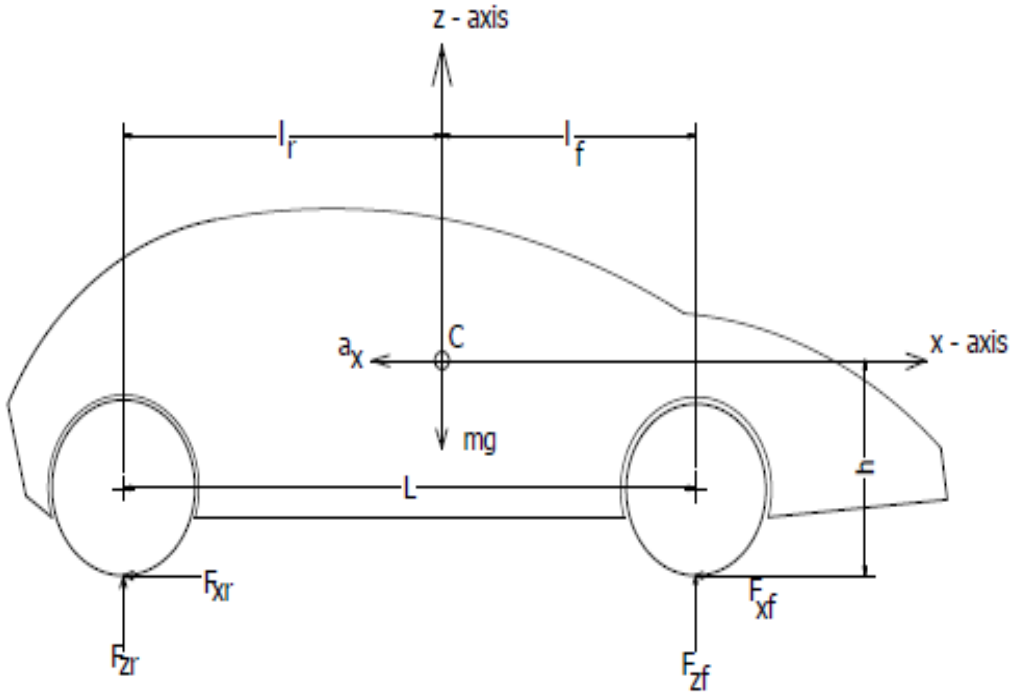

Figure 3.3: Simplified vehicle model

Here m is the mass of the vehicle, g represents the acceleration due to gravity, C is the center of gravity (C.G.), and a_x is the deceleration. F_{zf} is the normal force under the front tires, F_{zr} is the normal force under the rear tires, F_{xf} is the longitudinal brake force at the tire terrain contact patch of the front tires, and F_{zr} represents the longitudinal brake force at the tire−terrain contact patch of the rear tires. l_f is the distance between the front axle and the C.G., l_r is the distance between the C.G. and the rear axle, h is the distance of the C.G. from the ground level, and L is the wheelbase. Using the Newtons equation for the decelerating body, and static equilibrium conditions of force in the $z-$direction and

moment/roll about the $y-$ axis equal to zero, we get:

$$\begin{gathered}\sum F_x = ma_x \\ F_{xf} + F_{xr} = ma_x \\ \sum F_z = 0 \\ F_{zf} + F_{zr} - mg = 0 \\ \sum M_y = 0 \\ F_{zf} l_f - F_{zr} l_r - (F_{xf} + F_{xr})h = 0\end{gathered} \tag{3.5}$$

Using the above equations, the normal loads can be written as shown in Eq. (3.6).

$$\begin{aligned}F_{zf} &= \frac{1}{L}(mgl_r + mg\frac{ha_x}{g}) \\ F_{zr} &= \frac{1}{L}(mgl_f - mg\frac{ha_x}{g})\end{aligned} \tag{3.6}$$

The first term is the static part and the second term is the dynamic part due to the acceleration/deceleration. The dynamic part in case of acceleration adds the force to the rear wheels and subtracts from the front wheels. In case of braking, the dynamic part adds to the front wheels and subtracts from the rear wheels. The maximum longitudinal brake force cannot exceed the product of the normal load and the friction coefficient at the tire terrain interface [5]. Thus, the longitudinal brake forces can be written as shown in Eq. (3.7)

where μ is the coefficient of friction at the tire−terrain interface.

$$\begin{aligned} F_{xf} &= \mu F_{zf} \\ F_{xf} &= \frac{\mu}{L}(mgl_r + mg\frac{ha_x}{g}) \\ F_{xr} &= \mu F_{zr} \\ F_{xr} &= \frac{\mu}{L}(mgl_f - mg\frac{ha_x}{g}) \end{aligned} \tag{3.7}$$

Further, the Newtons equation can be modified as shown in Eq. (3.8) which gives the relation between the acceleration/deceleration and the coefficient of friction.

$$\begin{aligned} \mu(F_{zf} + F_{zr}) &= ma_x \\ \mu(mg) &= ma_x \\ a_x &= \mu g \end{aligned} \tag{3.8}$$

Thus, using Eq. (3.8) and Eq. (3.7), we get the braking force in the front and rear wheels as shown in Eq. (3.9)

$$\begin{aligned} F_{xf} &= \frac{\mu mg}{L}(l_r + h\mu) \\ F_{xr} &= \frac{\mu mg}{L}(l_f - h\mu) \end{aligned} \tag{3.9}$$

We can see that for the same friction coefficient and required deceleration, the maximum brake force requirement is larger for the front wheels as compared to the rear wheels. Further, this maximum force will cause the rear wheels to lock. So under under all conditions, it has to be ensured that the forces remain under the maximum values to avoid locking of the wheels. A ratio of the longitudinal forces at the front and rear wheels, as shown in Eq.

(3.10), helps to understand the difference in the brake force for the rear and front wheels.

$$\frac{F_{xf}}{F_{xr}} = \frac{l_r + h\mu}{l_f - h\mu} \tag{3.10}$$

The difference in the brake force for the front and rear wheels is dependent on the C.G. location with respect to the ground and the C.G. location from the axles. A lower C.G. and closer to rear axle C.G. can ensure similar braking force on both the front and rear wheels. This ratio enables the brake balance. If there is unbalance in this ratio, then either the front wheels or the rear wheels would lock up first. If the front wheels lock up first, the front wheels will slide and the driver will lose control to steer the vehicle. However, if the rear wheels are locked, a small amount of lateral force will cause a yaw moment which will cause the vehicle to lose direction stability. Thus it is imperative that when hard brakes are applied, the front wheels lock first as against the rear wheels. Once the wheels starts sliding, the frictional force available reduces and this will lead to longer stopping time and distance. As mentioned earlier, the braking forces are developed at the tire contact patch similar to the tractive effort explained earlier. As against the compression of the tire treads before entering the contact patch, in case of braking, the tread elements are under tension at the leading edge. The braking force increases as the skid increases and reaches a peak value and then drops to a lower till the wheels are locked, i.e., 100% skid [5]. In case of braking, it is essential that the wheels are not locked and the tire's contact patch produce the peak braking force. Thus, the goal of any brake system is to keep the brake force at the peak value. For this, it is important to know slip/skid ratio which gives the maximum braking force.

Chapter 4

Design of Clutch System

Majority of this chapter has been published in paper [16] by Khan, A. and Sandu, C. with permission from ASME publications.

The Terramechanics rig shown in Figure 4.1 consists of a carriage with a tire frame moving longitudinally over a soil/ice bin. The test tire frame (rectangular mounting frame in Figure 4.1) of the carriage supports all the major components such as the gearbox, its mounting plate, the small knuckle, big knuckle, etc. There are two vertical box channels welded to the frame supports the gearbox mounting plate. The components in front of the plate includes the small knuckle, which is used to set the camber angle of the wheel. The component right in front of the small knuckle is the constant velocity (C.V.) joint. The big knuckle which follows next helps to set the toe angle of the wheel. The big knuckle also supports the *Jeep* hub, mounting adapter, and a six axes wheel force measurement system, i.e., P650 *Kistler* system.

The existing power transmission system of the Terramechanics rig includes two motors, one to supply torque to the wheel and the other to move the carriage along the rig,

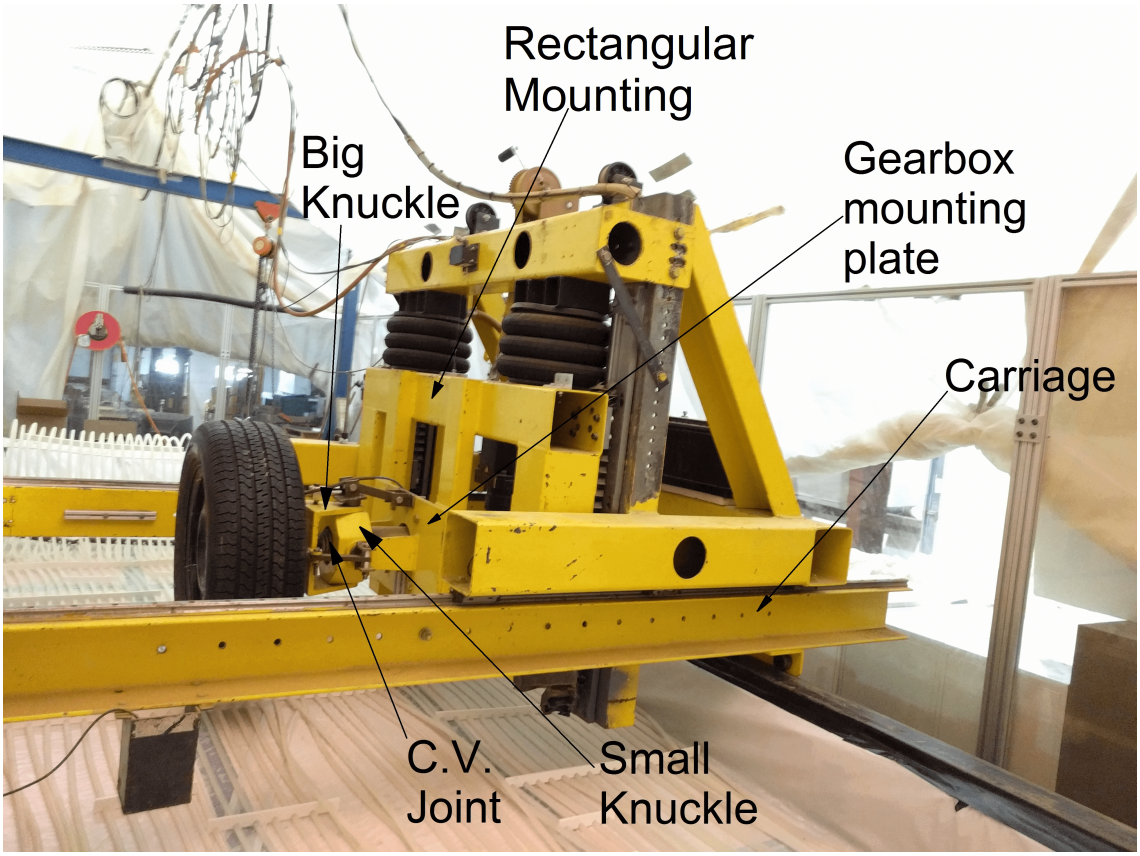

Figure 4.1: Single tire test rig (Terramechanics rig) at Advanced Vehicle Dynamics Laboratory (AVDL). Reprinted Figure 1 from [16] with permission from ASME publications.

as mentioned earlier. The relative adjustment in the applied torque to these two motors allows testing tires at different slip ratios. The wheel is driven by an electric motor passing through a 60:1 gear box [6]. One of the capabilities to be added to the rig was to be able to perform free rolling tests. This motivated a design change in the configuration of the rig, which would enable rolling the tire freely on any surface.

4.1 Concept Generation

There was a need to come up with a robust solution to meet our requirement without making major modifications to the carriage or the rig in general. An initial concept was to set

the motor that drives the wheel in the neutral mode or switch it off and just use the carriage motor, thereby enabling the free rolling. Although it looked like a quick and easy solution to the problem of free rolling, it had its inherent hindrances. There was no active method of switching off the wheel motor. Further, due to the high gearing ratio of the gearbox, the rolling induced by the translational motion of the carriage could potentially damage the gearbox and eventually the electric motor that drives the tire. Thus, an alternative methodology was required to isolate the power from the motor driving the wheel.

4.1.1 Clutch

The ideal way of isolating power from an engine to a shaft is to install a clutch in the transmission line. For our test rig, the installation of a clutch on the transmission shaft posed a great challenge due to the design of the carriage. The first aspect to consider was the location of the clutch and the space available. Next, it was necessary to find out how this modification would affect the testing span of the test rig and whether or not that is the best solution. Lateral side view and the isometric view of the tire test frame is shown in the below in Figure 4.2.

The clutch cannot be mounted in front of the big knuckle due to lack of space for a mounting support. The best location where there is enough space is the mounting plate where the gearbox is currently mounted. Another mounting plate at an offset to create enough space for the clutch and the gearbox has to be installed. The entire support structure and the location depend on the type of clutch selected. The next task was to investigate the type of clutch, the size of clutch and its other configuration which might be suitable for the required purpose.

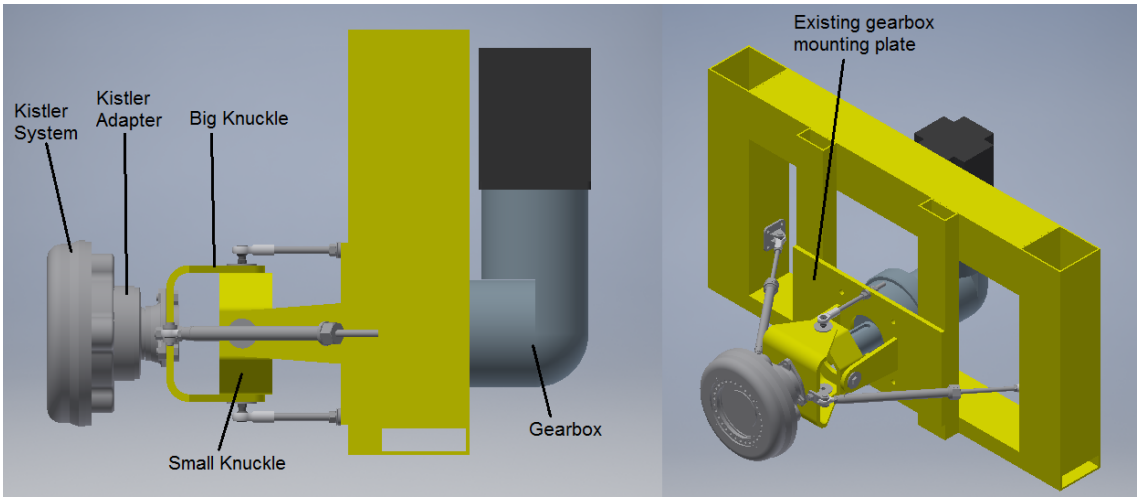

Figure 4.2: Tire Test Frame: Lateral side view and isometric view.

4.2 Selection of Clutch

In general, major criteria for selection of a clutch are the maximum operating speed, maximum operating torque, type of actuation, type of engagement, thermal capacity, and response time [10]. The selection of the clutch depends on the mode of operation of the clutch, the overall size of the clutch, and the maximum torque it can transfer. Since the longitudinal speed of the carriage is about 2 *mph* [6], the maximum speed criteria can be neglected. The clutch is to be mounted on a rig that is in motion and unmanned. For remote operation of the clutch, the available options are electromagnetic and pneumatic clutches. The electromagnetic clutch is generally used for low torque applications. There are electromagnetic clutches available for higher torque values but they are too bulky for this application and also very expensive. It was decided to procure a pneumatic clutch which meets the necessary requirements. In addition to the maximum torque that a particular clutch can transmit, another important criterion is the engaging speed. There is always an upper limit for the speed at which a clutch can safely engage and disengage without causing damage to its structure. In the case of the Terramechanics rig, due to its low speed, this

criterion is eliminated as a factor for the selection. The rig has capabilities of precisely controlling the longitudinal slip. In a friction−based clutch, the driven shaft receives power through frictional force. The driver is at a constant speed and the driven shaft connected through the clutch plate tries to attain that speed. This difference in speed causes slip [10]. This is undesirable in the case of the Terramechanics rig. Thus, a clutch based on principles other than friction had to be selected. Two other important criteria were the maximum torque transmission capacity and the physical size of the clutch. The maximum torque that needs to be transmitted is 1900 Nm (about 1400 $lbf.ft$). Various vendors were contacted for a quotation on the same. One of the type of specialty clutch is the toothed clutch. A combination of toothed clutch that is pneumatically operated is not a readily available product in the market. Most clutches available around this torque were too big and too expensive. Finally after going through lot of catalogs, *Shanghai Long Bright Mechanical and Electrical Equipment Co. Ltd.* offered a clutch model **LLTC−200** which met our requirement. The dimensional and technical specifications of the clutch are as shown in Table 4.1.

Table 4.1: Clutch Model: LLTC−200 by Shanghai Long Bright Mechanical and Electrical Equipment Co. Ltd.

Type of Clutch	Toothed Clutch
Mode of Operation	Pneumatic
Maximum Torque	2000 Nm (1475 $lbf.ft$)
Operating Pressure	0.6 MPa (87 psi)
Length	14.5 cm (5.7 in)
Bore Diameter	75 mm (2.95 in)
Outer Diameter	23.2 cm (9.13 in)

As per the catalog, the clutch model **LLTC-200** was meant for an input shaft of 80 mm (3.14 in). The manufacturer was consulted and it agreed to manufacture the same model for an input shaft of 75 mm (2.95 in). The vendor offered this product for $1400 which

was cheaper than the other manufacturers. The order was placed and the clutch procured is shown in Figure 4.3.

Figure 4.3: Pneumatic clutch − LLTC−200: as received.

This clutch operates at a pneumatic pressure of 0.6 MPa (87 psi). The Advanced Vehicle Dynamics Laboratory is equipped to supply compressed air at 1.03 MPa (100 psi). The operation of the clutch and its components is explained in the later sections. The next major task in the design of the clutch system for the Terramechanics rig at AVDL involved a mounting frame and finalizing the exact location of the clutch w.r.t to the carriage.

4.3 Design of Mounting Frame

The location selected for mounting the clutch was between the existing mounting plate and the gearbox as shown in Figure 4.4. However, given the existing structure of the carriage, there was a need to modify and add additional supports, etc., to support and

mount the clutch. Looking at the existing construction of the carriage where the gearbox is mounted as shown in Figure 4.4.

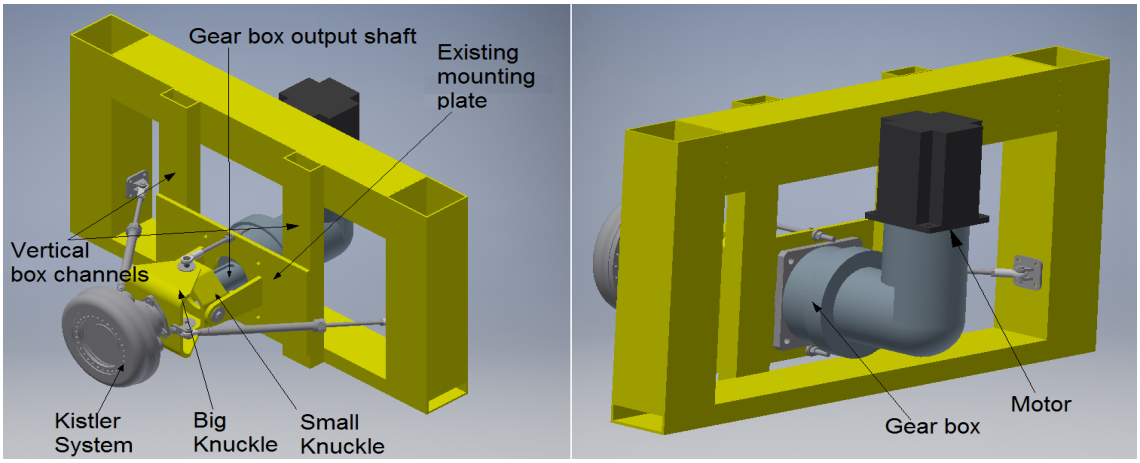

Figure 4.4: Existing carriage construction where the gear box is mounted. Reprinted Figure 2 and Figure 3 from [16] with permission from ASME publications.

It can seen that there is no space where the clutch can be directly placed between the gear box and the mounting plate without adding new members and modification to the existing structure. It was clear that a new mounting plate will be required at an offset from the existing mounting plate which would create space for the clutch and the gear box. A new mounting plate cannot be directly mounted on the rectangular frame. The solution identified was to have two new vertical box channels to be welded at the rear end of the frame as shown in Figure 4.5. These channels shall support the new mounting plate as shown in Figure 4.5.

In order to make the assembly and disassembly easier and convenient, it was necessary that this new mounting plate isn't welded to the new box channels. The final decision was that the new mounting plate will be bolted to the new box channels, not welded. Thus, the existing structure is transformed as shown in Figure 4.6.

The load that these newly added components to the rig have to sustain, as compared

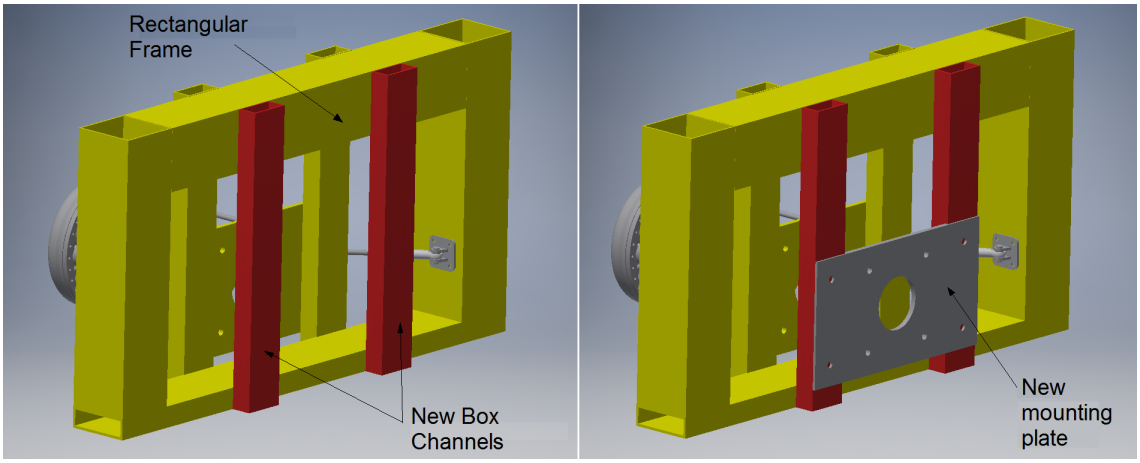

Figure 4.5: New box channels and mounting plate at the rear end of the carriage's rectangular frame. Reprinted Figure 5 from [16] with permission from ASME publications.

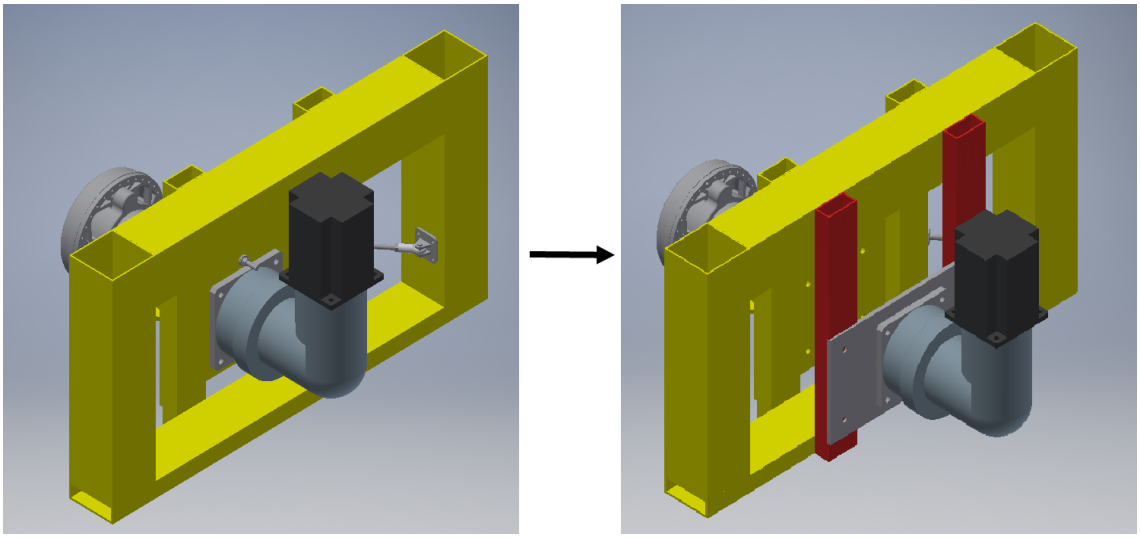

Figure 4.6: Modifications to the existing structure. Reprinted Figure 6 from [16] with permission from ASME publications.

to the previous mounting plate, is just the additional dead weight of the clutch, its adapter, and the shaft (discussed in following sections). A stress analysis was conducted to check whether the stresses remain under a limit or the design needs to be modified. The stress analysis was carried out on Abaqus software. The Von Mises stresses induced for the plate and box channels were well within the yield strength limit for carbon steel material, as shown in Figure 4.7.

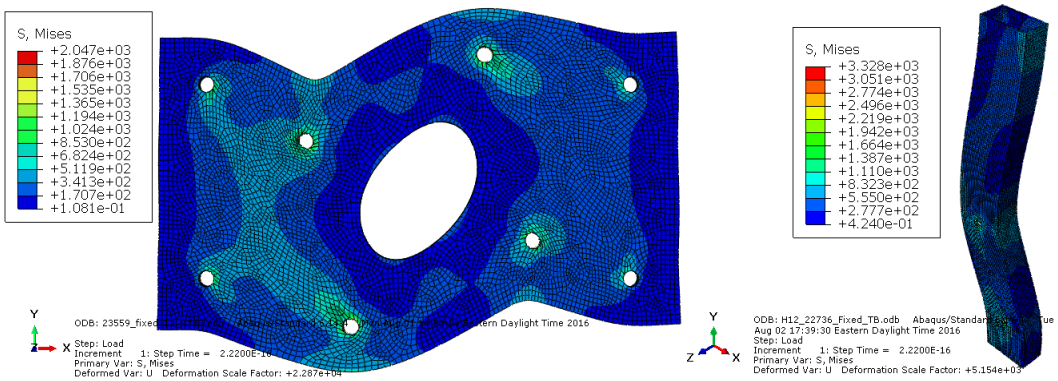

Figure 4.7: Stress analysis of the new mounting plate and vertical box channels. Reprinted Figure 7 from [16] with permission from ASME publications.

This concluded the design of the mounting frame for the new clutch. The raw material for the box channels was standard structural steel. The mounting plate was to be fabricated out of 1018 steel. The machining of these materials was done in the machine shop at Virginia Tech. The finished mounting plate and the box channels are shown in Figure 4.8. The next task in the design of the clutch system for the Terramechanics rig involved design of an adapter and a new shaft.

4.4 Design of Adapter and Shaft

The driver and the driven sides of the clutch are shown in Figure 4.9. The driver end has a static part that has to be locked to prevent its rotation. A simple bracket was designed to lock the static part at the slot provided on the clutch.

In order to enable any minor adjustments if required later during assembly, the support bracket is made in two parts as shown in Figure 4.10. The lower part as shown in section (a) of Figure 4.10 shall be welded to the rectangular frame of the carriage. Part (b) of the support shall be bolted on the part (a).

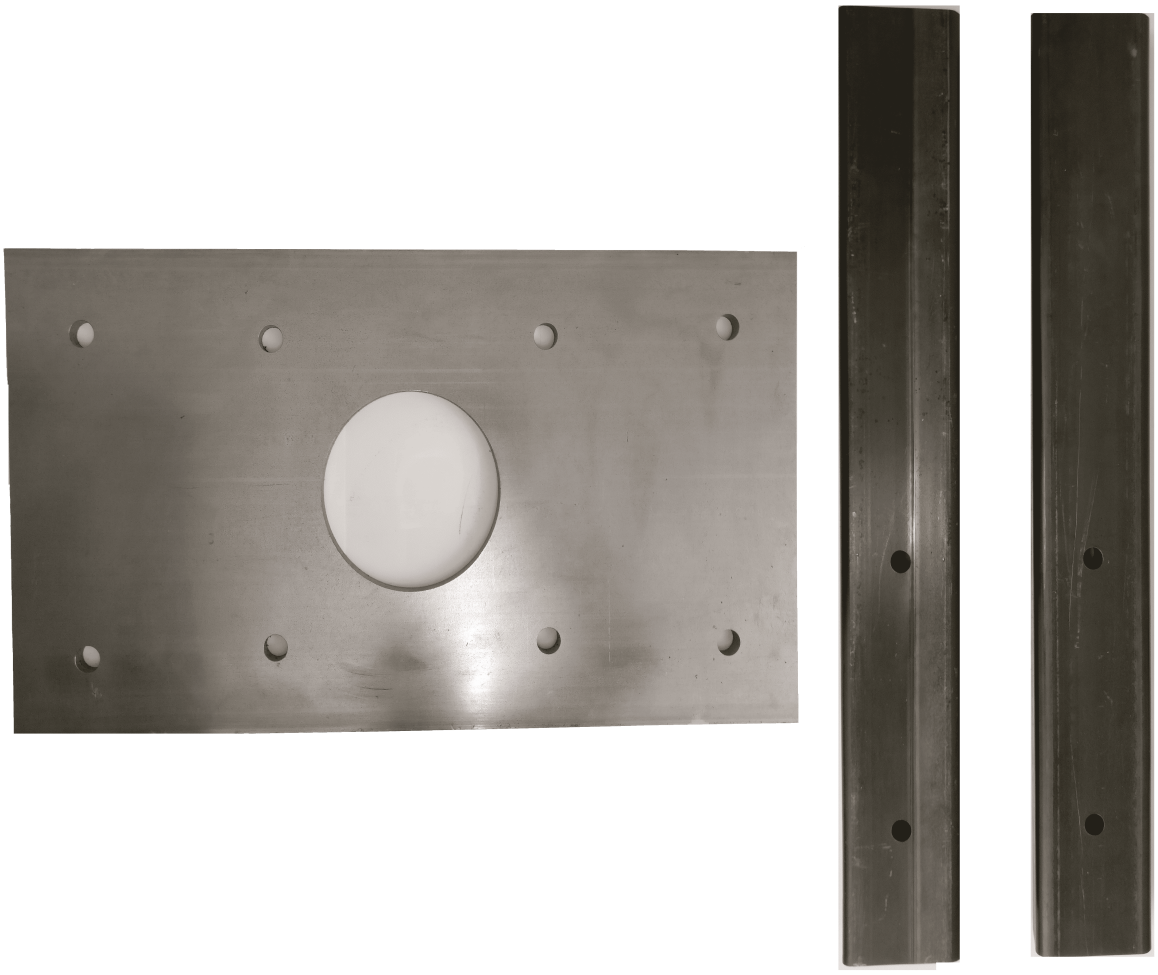

Figure 4.8: New mounting plate and Box Channels for the gearbox

The new mounting plate created a lateral space of 25.4 *cm* (10 *in*) between the old mounting plate and a new mounting plate shown in Figure 4.11. This space would be enough to place the clutch (lateral dimension of 14.5 *cm*, i.e., 5.8 *in*) and design a new adapter for the same that would fit in this space. The clutch would be mounted on the gearbox shaft and the driver side face would flush with the new mounting plate. For the driven side, a new shaft cannot be directly connected to the clutch. An adapter had to be designed which would be bolted to the clutch on the driven side and a new shaft would then couple with this clutch adapter.

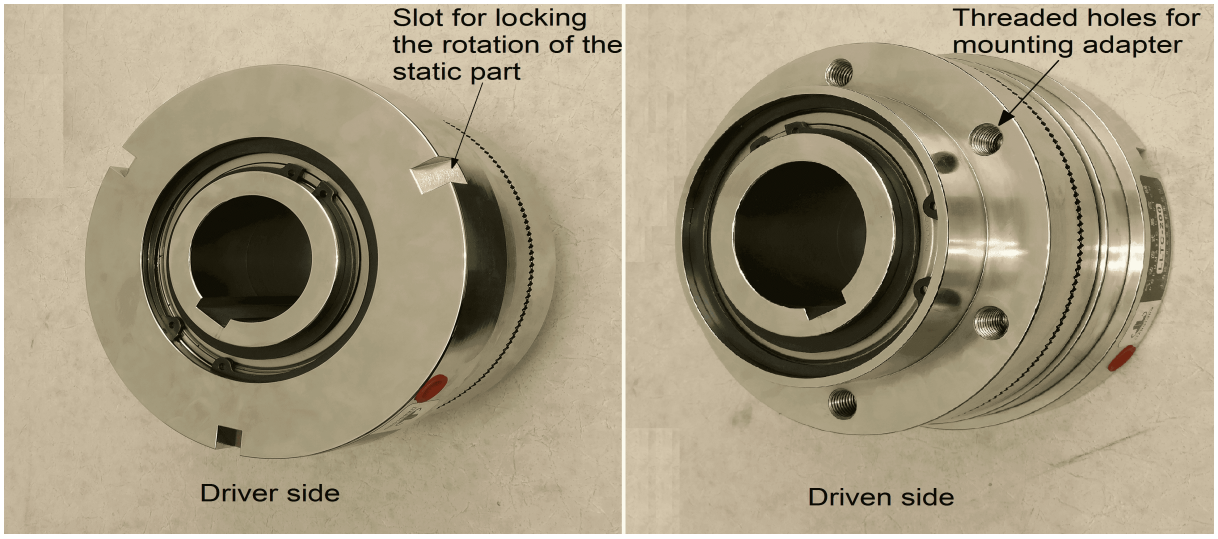

Figure 4.9: Driver and driven side of the clutch. Reprinted Figure 8 from [16] with permission from ASME publications.

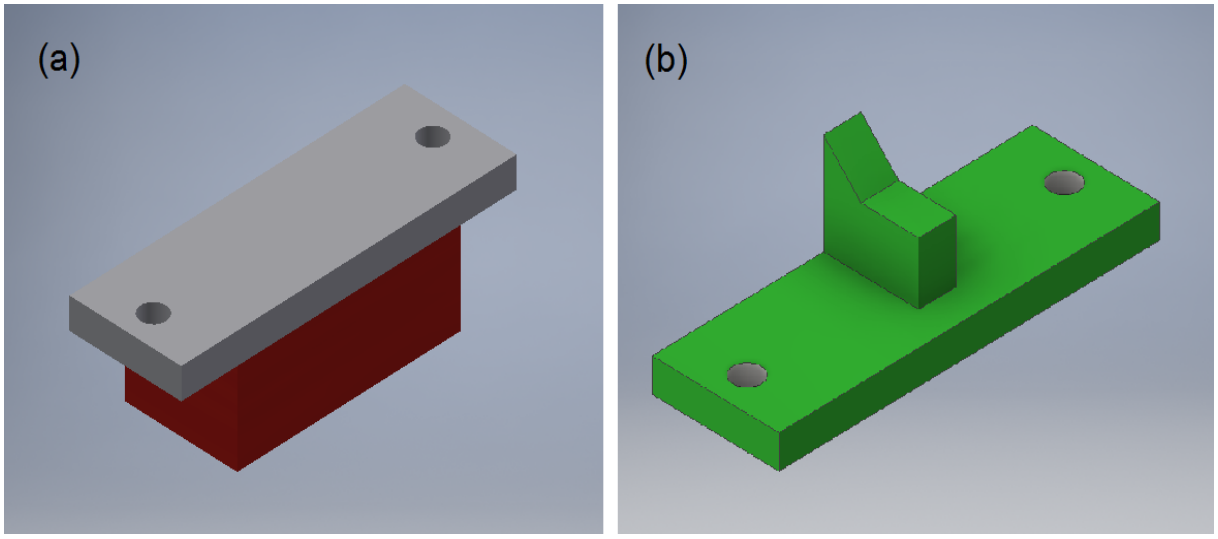

Figure 4.10: Clutch support to lock rotation of the static part.

The adapter has to perfectly mate with the clutch such that the only portion that comes in contact with the clutch should be the radial area where the clutch is bolted to it. Further, the output hole of the adapter should be for a shaft of 75 mm (2.95 in). The new shaft shall be keyed to the adapter. Thus, the adapter should have the proper sized key−way for the specified shaft diameter. To allow for axial adjustment of the shaft during

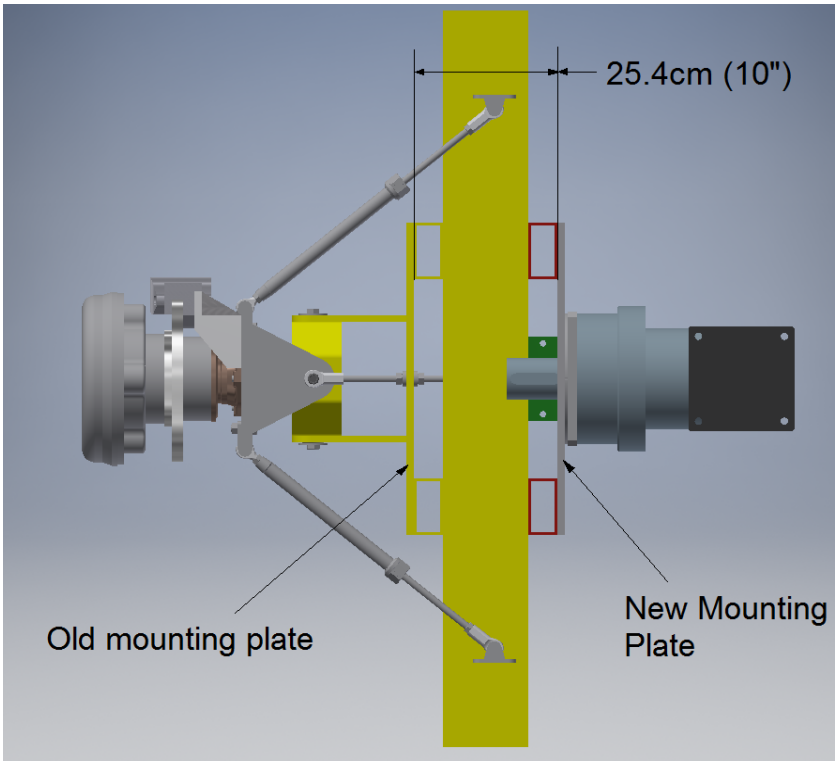

Figure 4.11: Top view: Assembly of new mounting plate and box channels.

assembly, a tapped hole for a setscrew locks the shaft at the adjusted location. In the current configuration of the Terramechanics rig, a sleeve houses the shaft from the gearbox and couples it to the constant velocity (C.V.) joint. In order to keep that system intact, the length of the adapter must be flushed with this sleeve. Therefore, the lateral size of the adapter is such that one face flushes with the mounting location on the clutch and the other face flushes with the sleeve face. Keeping all this into consideration, the adapter shown in Figure 4.12, was designed.

The shaft had to be 75 mm (2.95 in) in diameter, since it would couple with the sleeve that connects it to the C.V. joint. The length would be based on two components. The length that goes inside the shaft and the length that projects out of the adapter. The length that goes in the clutch depends on the length of the key that couples these two components, which eventually depends on the shear strength of the key. Using the shear

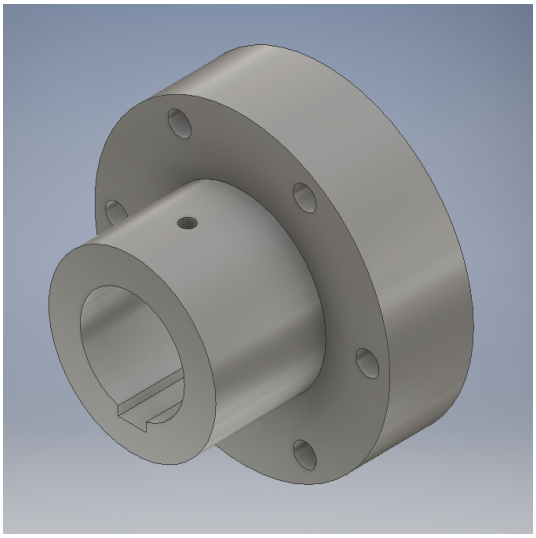

Figure 4.12: Clutch adapter. Reprinted Figure 9 from [16] with permission from ASME publications.

strength criteria for designing, the minimum length calculated was small. As such, the shaft will be simply supported between this adapter and the constant velocity (C.V.) joint of the transmission system. Additionally, due to the sleeve which couples the shaft and C.V. joint, it was ideal to have the adapter face flush with the existing sleeve. Therefore, the length of the shaft that goes in the adapter was obtained to be 10.2 *cm* (4.02 *in*). The length of the shaft projecting out of the adapter based on the sleeve and the C.V. joint was obtained as 10.8 *cm* (4.25 *in*). Thus the total length of shaft required comes 21 cm (8.27 *in*). The required key was also designed for the shaft and adapter assembly. The assembly is shown in Figure 4.13.

The rotational speed of this shaft would be low since the translational speed of the carriage was 2 *mph*. Since the shaft is simply supported with no load along the span other than the self weight. Thus the deflection of the beam would be very small. In fact, even for larger deflection, the critical speed won't be as low as the rotational speed at which the shaft would be running. The shaft was analyzed for bending, torsion, and shear using the standard bending and torsion formulas and they were determined to be well within the

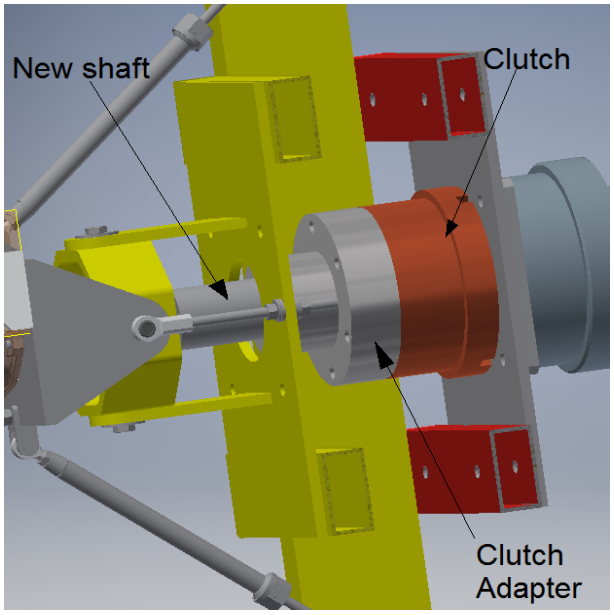

Figure 4.13: Assembly of clutch, adapter and the new shaft. Reprinted Figure 10 from [16] with permission from ASME publications.

acceptable limits for carbon steel materials. The next important task was the selection of exact material for the adapter and the shaft. The clutch that has been procured is made out of chromium based 40Cr with 0.4 % carbon and 1 % chromium heat treated alloy steel. The hardness of the material is 25−28 HRC after the heat treatment. Thus an equally strong but softer material of construction had to be selected for the shaft and adapter. Looking from the cost point of view, stainless steel would be costly. Further, the application of this shaft and adapter isn't in one of those under high temperature or chemical application. Thus, AISI 4140 alloy steel was selected for the shaft and adapter, since it has a similar chemical composition and it is of almost equal strength but softer than the clutch material of 40Cr.

The assembly is such that all the load of the clutch, its new adapter and the new shaft is to be supported by the output shaft of the gearbox. The dead weight of the clutch, adapter and the shaft are 295 N, 150 N, and 70 N respectively. The total load of 515 N acts at a center of gravity of 140 mm from the root of the clutch shaft as shown in Figure 4.14.

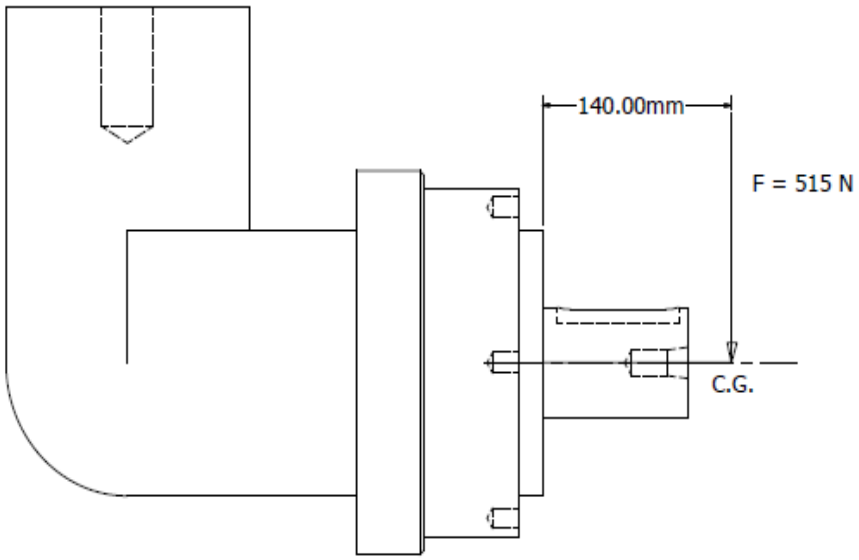

Figure 4.14: Dead weight on the output shaft of the gearbox.

In order to check the allowable load, the manufacturer of the gearbox 'Apex Dynamics' provided a chart for allowable radial and axial load at various output shaft speed. The maximum rotational speed of the output shaft is when the tire is suspended in the air for calibration and warm−up stage of the testing. The speed at that moment is 20 *rpm*. For the gearbox model **AER−235**, the maximum permitted radial load at the center of the output shaft is 8700 *N* for speed upto 100 *rpm*. However, the load in our case is not acting at the center of the output shaft but at 140 *mm* as shown in Figure 4.14. As per the manufacturer's recommendation, a correction factor called the 'position load factor' is to be applied to the allowable load at distance other than the center of the output shaft. Based on their gearbox datasheet, the correction factor is 0.67 for load applied at 140 *mm*.. Thus, the allowable load at 140 *mm* from the root is calculated to be 5829 *N*. Whereas the total actual load at 140 *mm* is 515 *N*. This gives a factor of safety of 11.31. However, it is always desirable to have the system as simply supported as against overhanging load. An ideal solution for this is to have a support bearing at the other end of this new clutch system such that this arrangement

is supported between the gearbox shaft and the bearing support. Based on the available space between the old and the new mounting plate, the best location would be to use the old mounting plate to support the other end of the clutch system. A bearing with housing would not only be costly, but would also require machining work on the old mounting plate which is difficult since it is permanently welded to the frame. It was required to design the support frame using the existing holes on the old mounting plate. A cost effective solution was to use a deep groove ball bearing and design the housing for the bearing based on the existing mounting holes on the old mounting plate. The only portion that could be supported easily is the smaller diameter section of the clutch adapter. Consequently the load acting the bearing is 245 N in the radial direction and the load acting on the gearbox output shaft would be 270 N. This would lead to the transformation of the arrangement as shown in Figure 4.15.

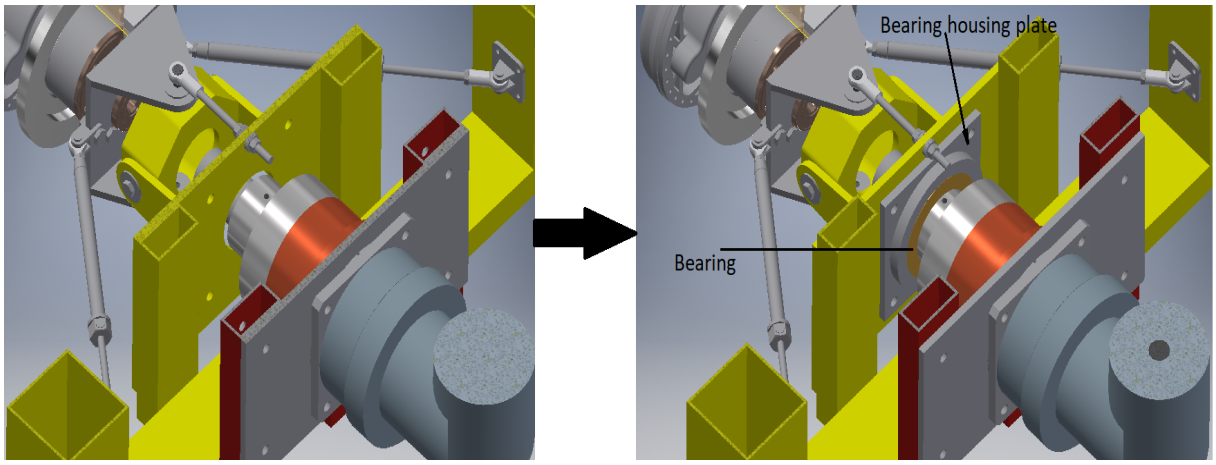

Figure 4.15: Bearing support for the clutch system.

The selection of a bearing depends on many factors such as available space, loads, speed of operation, operating temperature, level of contamination, lubrication, etc. Since the load, operating speed are considerably low as well the operating temperature would be normal atmospheric temperature for both the bearing rings, the main factor in the selection of bearing for the clutch system are:

- Available space
- Level of contamination

Based on the smaller diameter of little under 120 *mm* available on the clutch adapter, it was imperative use the next available standard bore size to work around the right fit and tolerance required. The next available size for standard bearing bore is 110 *mm*. We had to ensure that the width is least to avoid any kind of interference of the bearing housing with the clutch adapter. The second important factor was the level of contamination. The Terramechanics is used for testing of tires on soil as well as soft soil which contains fine soil particles. The preparation work for the test on soil involves shoveling and tilling which creates a lot of soil dust in the air. This kind of contamination level on a regular basis will damage the gear to a great extent. It was imperative to have a perfectly sealed bearing. Bearings are available as open, shielded (single and both sides), non−contact sealing (single and both sides), contact type seals. The best option is to have double sided rubber sealed bearing. *SKF* is the source of bearings with widest range of options. Based on our requirement of bore size of 110 *mm* and double sided rubber sealed, the cost effective option available on *SKF Bearings* is the bearing number **6022−2RS1** as shown in Figure 4.16.

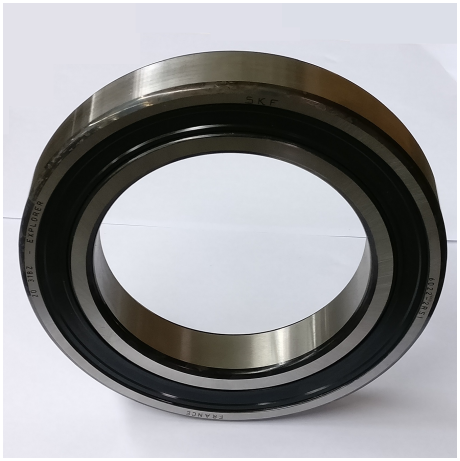

Figure 4.16: SKF Bearing number 6022−2RS1 : as received.

This bearing had a bore size of 110 *mm*, outer diameter of 170 *mm* and a lateral width of 28 *mm*. The bearing seals are rubber and contact type on both sides. Further, using the calculator available with *SKF Bearing*, the life of the bearing was considerably high for the radial load of the 245 *N*. Due to the presence of a contact type seal, there is a resistance moment of the seal. Based on the calculation tool of SKF, the resistance moment by the seal is equivalent to 1.095 *Nm*. The next task was to design the housing for the bearing. Since the load is on the inner ring of the bearing and it is the inner ring that is rotating, the ideal required fit to have a press fit on the inner ring and a loose fit for the housing and the outer ring of the bearing. Taking into account a housing and cover plate was designed as shown in Figure 4.17. The minimum and maximum sizes for the steps and shoulder within the housing were based on the recommended values from the product datasheet.

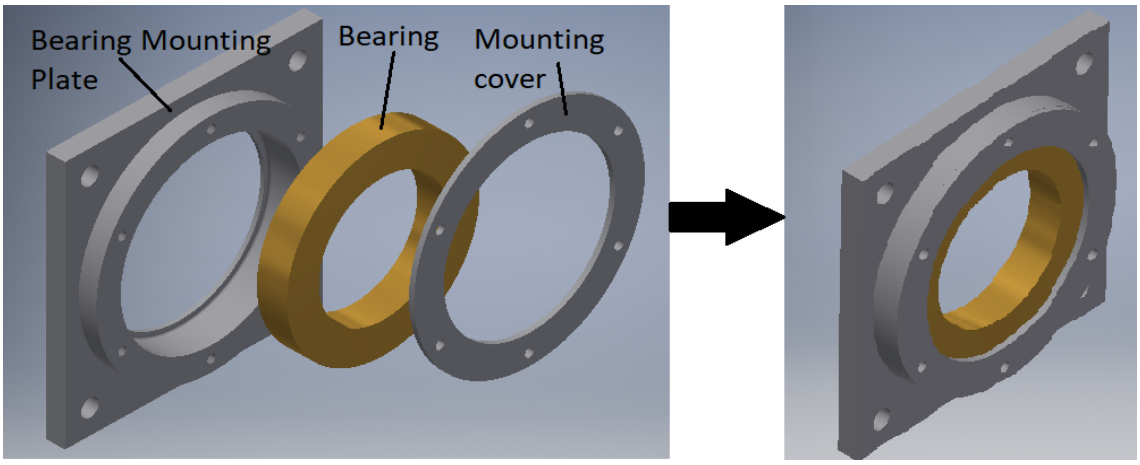

Figure 4.17: Bearing housing plate and cover.

The fit selection was to be determined based on the datasheet of the bearing. Since the load and operating speed was low, the recommended values of tolerance to achieve press fit for inner ring and loose fit for the outer ring was used. The bearing was procured and the housing plate and cover were fabricated at the machine shop.

The pneumatic clutch received has a hub for mounting onto the 75 *mm* output shaft

of the gearbox. The gearbox has a key with a width of 20 *mm* whereas the manufacturer of the clutch had supplied the clutch with a keyway width of 22 *mm*. In order to solve this problem, a non−standard customized stepped key had to be designed that couples the 20 *mm* keyway of the gearbox shaft and the 22 *mm* keyway of the clutch hub. Since the output shaft of the gearbox has a round end key way slot, the only way the key could be customized is as shown Figure 4.18.

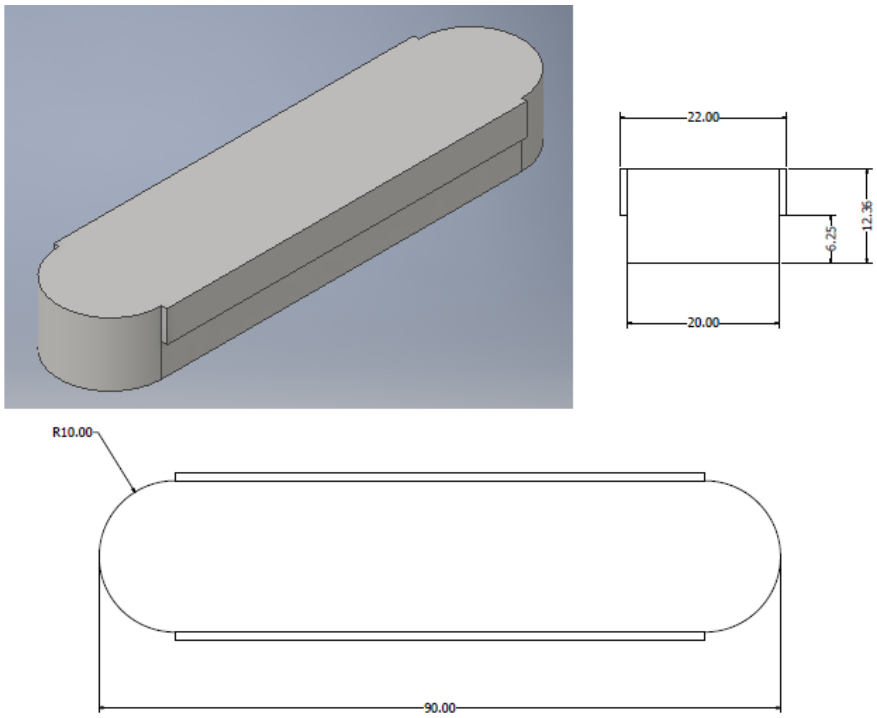

Figure 4.18: Custom stepped key.

The stress analysis of the key is based on the following resisting areas of the key as depicted in Figure 4.19. The force (F) considering maximum torque (T_{max}) of 1900 Nm and shaft diameter(D) of 75 mm is calculated as 50.67 kN. The shear area considering the smaller width is calculated as 1714.6 mm^2. Thus, the shear stress developed is 29.55 MPa. The bearing or crushing area is different for the clutch and shaft portion respectively. The area for clutch portion and the shaft portion are 438.06 mm^2 and 630 mm^2 respectively. The

maximum bearing or crushing stress comes out to be 115.66 *MPa* in the clutch portion.

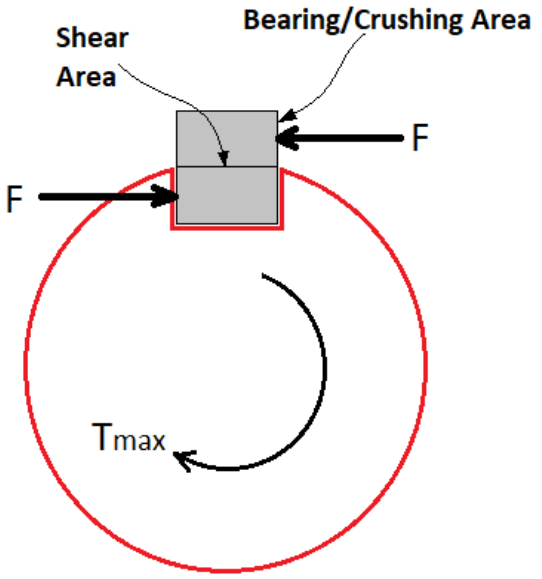

Figure 4.19: Load resisting areas of a key.

The existing key is made of 1018 steel which is of equal strength as the shaft but softer than 416 stainless steel. Thus, the same 1018 steel was chosen as the material for the key. This gives a factor of safety of 7.2 in shear and 3.2 in crushing. Considering an element at the interface of the two widths and the cross section. The 2D state of stress is a compressive stress of a compressive stress (σ_y) and a shear stress (τ_{xy}). The resultant von Mises stress is calculated to as per Eq. (4.1).

$$\sigma_{vm} = \sqrt{\sigma_y^2 + 3\tau_{xy}^2} \tag{4.1}$$

For the maximum bearing stress and shear stress at the interface of the step, the equivalent von Mises stress is calculated to be 126.5 *MPa* (18345 *psi*). This gives a factor of safety of 3. The major components of the clutch system to be fabricated and machined included the clutch adapter, the new gearbox mounting plate, box channels for mounting

this new plate, a new shaft for the clutch adapter, clutch support bracket, a customized key for the new shaft and a customized stepped key for the gearbox. We enquired for a quote on the fabrication of the major components which includes the clutch adapter, the new shaft, the customized key along with few other components for the brake system. We received quotation from 3 companies viz. AMG Inc., MPI, MPC. The quotation from M/s. AMG Inc., M/s. MPI, and M/s. MPT was $5430, $2326 and $2625 respectively, inclusive of the material cost. For getting the parts fabricated in the machine shop at Virginia Tech, we enquired the cost of the raw materials which includes the above components and the rest of the raw materials for the clutch mounting frame discussed in the previous sections, i.e., mounting plate, box channels, support plates, etc. The total cost of the raw material was $755 and the cost of some specific cutting tools such as drill bit of the required size and a carbide milling tool required by the machine shop was $402. Thus, the total cost for the fabrication of these parts in the machine shop at Virginia Tech was $1157. In the above scenario, the cost effective option was to procure the raw materials and get the clutch adapter, shaft, key and all other components fabricated in the machine shop at Virginia Tech. The raw materials and the cutting tools were procured. The final drawings for fabrication was given to the machine for fabrication. The finished clutch support bracket is shown in Figure 4.20. It is fabricated out of 1018 steel. This part supports the clutch as well as locks the rotation of the static part. The clutch adapter, as discussed above, is fabricated out of 4140 steel. The finished clutch adapter is shown in Figure 4.21. The shaft is made of 4140 steel while the key has been fabricated out of 1018 steel. As discussed previously, a customized stepped key was fabricated to couple the clutch and the gearbox output shaft. The finished stepped key is shown in Figure 4.22.

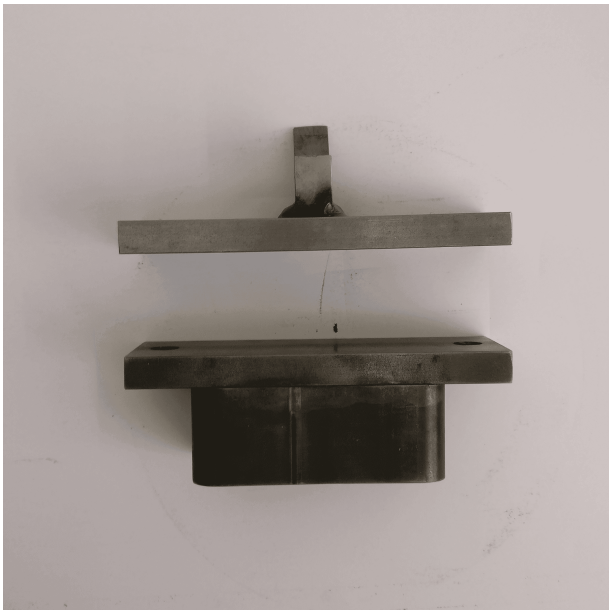

Figure 4.20: Finished clutch support.

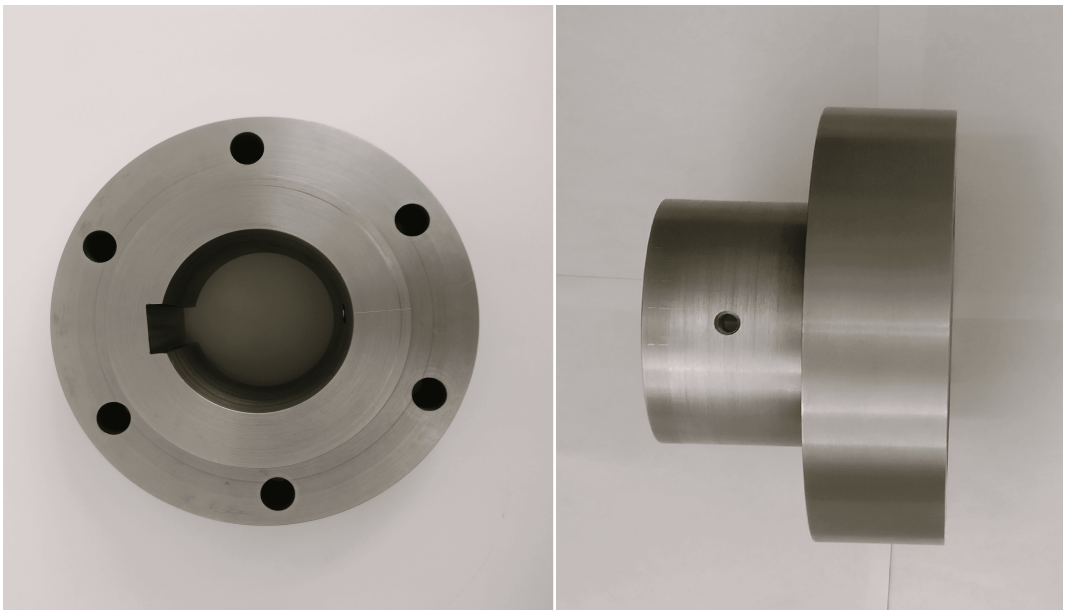

Figure 4.21: Finished clutch adapter.

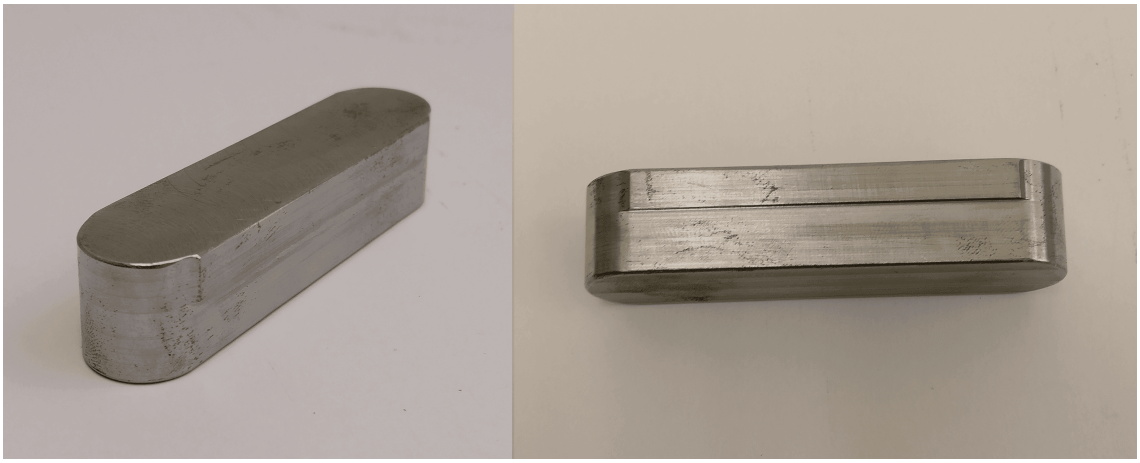

Figure 4.22: Finished stepped key.

4.5 Operation Mechanism

The operating pressure for the clutch is around 0.6 MPa (87 psi).The actuation system will include a pressure regulator, exhaust valves, solenoid valves, and pneumatic hoses and fitting. The general arrangement drawing of the actuation system is depicted in Figure 4.23.

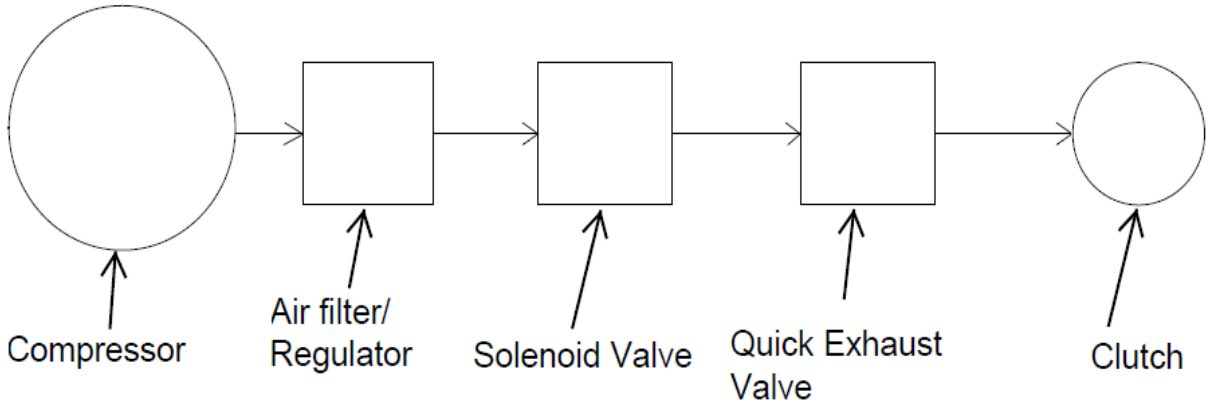

Figure 4.23: General arrangement drawing of the actuation system of clutch

The compressor supply at AVDL has a pressure of 0.69 MPa (100 psi). A filter must be used to avoid damage to the clutch due to dirt particles. Additionally, a pressure regulator is needed to reduce the pressure to 0.6 MPa (87 psi). Disengaging the power to

the wheel using the clutch will be an intermittent operation done based on different projects requirements. In general, the compressed air should be supplied to the clutch for most of the time. Thus, a normally open 3−port and 2−position as shown in Figure 4.24 solenoid valve can serve the purpose of remotely controlling the on−off mechanism of the clutch.

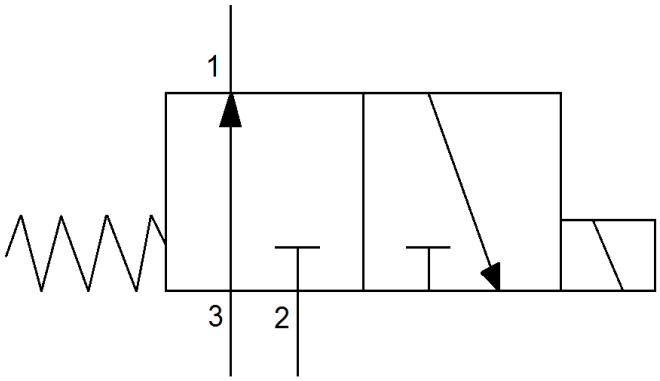

Figure 4.24: Symbolic representation of a 3/2 solenoid valve.

The valve is designed for two positions; a default open position and a closed position when it is energized. There are 3 ports in this type of solenoid valve. The port 3 as shown in Figure 4.24 is connected to supply. Port 1 is the outlet of the solenoid valve which is connected to the clutch. Port 3 serves as an exhaust port. In the de−energized or the normal operating state, the default position is as shown in Figure 4.24, which is called Normally Open(NO) position. Port 1 and 3 are connected while port 2 is blocked. This allows the compressed air to the clutch. When the solenoid is energized from an electric source, it goes into the closed position against a spring force. This allows a connection between port 1 and 2 while port 3 is blocked. This would relieve the pressure acting on the clutch thereby disengaging it. Further, when the clutch has to be engaged again, the power to the solenoid is cut, and the valve returns to its default position due to the spring force. In order to avoid any dirt particles to enter the pneumatic system through the exhaust port 3 in Figure 4.24, a muffler or silencer of the appropriate sized is to be connected to port 3. The inlet size of

the pneumatic line for the clutch is 3/8 *in* female NPT (Nominal Pipe Thread) (9.5 *mm*), so all the hardware, hoses, and valves must be of this size. Based on the requirement, a solenoid valve (**9574K3001W**) was ordered from *ROSS Controls* was ordered. The details of the valve are tabulated in Table 4.2. This sums up the components required for the clutch actuation system.

Table 4.2: Technical Specification: Solenoid Valve by ROSS Controls.

Type	3/2 Single Acting
Default Position	Normally Open (NO)
Inlet Port Size	9.52 *mm* (3/8 *in*)
Outlet Port Size	9.52 *mm* (3/8 *in*)
Actuation	Solenoid Controlled
Inlet Pressure Range	$1.5 - 10$ *bar*
Voltage	24 VDC

The operation of the clutch depends on the test that is conducted on the tire. In general, for any tire mounted on the rig, the first task will be to measure the free rolling radius of the tire for the required normal load. This test will additionally represent a test for 0 % longitudinal slip. For the measurement of the rolling radius of the free rolling tire, the clutch has to be disengaged. Actuating the solenoid valve will lead to cutting of the supply of the compressed air to the clutch. Switching off the solenoid valve will lead to engaging the clutch again. This concludes the design of the clutch system for the Terramechanics rig. With the clutch system in place, the next task was to design and implement a brake system for the rig. The following chapter discusses the concept generation and the detailed design of the brake system.

Chapter 5

Design of Brake System

Part of this chapter has been published in paper [16] by Khan, A. and Sandu, C. with permission from ASME publications.

5.1 Concept Generation

The drive system of Terramechanics rig at AVDL has two motors: one driving the carriage and the other driving the wheel. The linear motion control system enables pre−setting a desired slip ratio between the tire and the test surface. The negative slip in a way mimics the brake action. However, there is a need of fully locking the wheel to study the braking performance of tires on surfaces such as ice. Theoretically, negative slip of 100 % is achievable in this configuration by creating an equal and opposing torque in the wheel motor compared to the carriage. The rig had has been used to test only upto 80 % slip both positive and negative on surface such as ice which has low coefficient of friction. As against any other slip ratio, at 100 % negative slip (locked wheel condition), the motor of the wheel has to resist the entire brake torque, i.e., the gears in the gearbox and the stepper motor. The

fully locked condition (100 % negative slip) achieved through adjusting the torque in the motor may actually damage the motor and the gearbox especially when tested on surface with higher coefficient of friction such as soil. Thus, it was essential to come up with a more robust and reliable solution to achieve the fully locked wheel condition. For this various options for mechanical and other form of brake system were explored for the test rig. The biggest challenge that posed was the location of the brake system and the space constraint. Similar to the clutch system, the goal was to design and implement the brake system for the test rig with minimum modifications.

5.1.1 Location

The first task was to explore the location for the installation of the brake system. Since the space behind the old mounting plate was now completely occupied by the clutch system, a suitable location in front of the old mounting plate was to be explored. As discussed previously, the series of components and parts that existed in front of the mounting plate are as follows. Firstly, a constant velocity (C.V.) joint followed by the small knuckle, followed by the big knuckle which imparts a toe angle to the wheel, then a *Jeep* hub, mounting adapter for a wheel force measurement system, i.e., *Kistler* system [6], followed by the *Kistler* system and finally the wheel. Of all these components and parts, the most critical is the *Kistler* system, both in terms of its importance and criticality. The modification of the rig to add the brake system should not hinder or affect the measuring capacity of the *Kistler* system. The idea is to install the brake system as close to the wheel as possible. The work started off by inspecting the outermost component before the wheel. Adding anything in front of the *Kistler* system would be very difficult to lack of availability of any kind of rigid surface structure to support the brake system. The space between the small knuckle and the big knuckle is too less to install any kind of additional system since most of the space is taken

up the CV joint. Furthermore, removing the *Jeep* hub and installing anything between the big knuckle and the *Jeep* hub would require lot of modification since the output of the CV joint has been customized to suit the *Jeep* hub. Adding anything between this would mean, replacing the CV joint or the *Jeep* hub. Further, its practically inefficient to include anything between the *Kistler* adapter and the *Kistler* system itself. Thus, the only option left is to include the brake system between the *Jeep* hub and the *Kistler* adapter.

5.1.2 Selection of Brake System

Having selected the location for the brake system, the selection of the brake system is going to be greatly influenced by the factors that are critical to this particular test rig. There are many factors that would affect the selection of a brake system in case of an automobile. However, in case of the Terramechanics rig at AVDL, the major factors are as follows:

- Speed of the carriage
- Space available
- Maximum torque to be resisted
- Frequency of the brake operation

The carriage is designed to run at a maximum speed of 2 *mph*. At this low speed, the thermal heat generated due to the braking action would be very less. The thermal heat generated at the frictional surface of the braking system is directly proportional to the speed of the vehicle [11, 9]. Thus the thermal analysis wouldn't play a major role in the selection of the brake system. Unlike the regular automobiles, the Terramechanics rig will not require high frequency of the brake application. Thus, even a simple hand operated mechanical

brake that can produce the required braking torque will be sufficient. The braking torque generated would depend on the type of braking system, the coefficient of friction between the tire and the terrain, the coefficient of friction between the brake pads and the resisting surface and the normal load on the tire [11, 9]. The major factor that governs the selection of the brake system for Terramechanics rig is the space constraint. Since the space available is very limited, a large drum brake system is eliminated at the outset. Apart from this technical requirement, we also had the cost constraint. Compared to a simple drum or disc brake system, an electromagnetic brake system would be bulky and expensive. In the current configuration of the test rig, the best solution is to install a manually operated hydraulic disc brake system.

5.2 Selection and Customization of Brake Components

A disc brake system primarily comprises of a brake rotor which rotates with the wheel and brake caliper which is mounted on a fixed surface relative to the wheel. The caliper has brake pads which come in contact with the brake rotor to create a frictional torque [11]. This frictional torque is the braking torque that slows down and finally stops a vehicle in a finite amount of time if the right value of brake torque is generated [11, 9]. For the Terramechanics rig, the location for installing this brake system is finalized as between the *Jeep* hub and the *Kistler* adapter as shown in Figure 5.1.

The assembly of *Jeep* hub, *Kistler* adpater and the *Kistler* system is mounted on the Big knuckle of the Terramechanics rig as shown in Figure 5.2. Brake rotors come with or without an offset. A rotor with no offset will ideally cater to the specified requirement. However, there are chances that the caliper of that rotor might interfere with the *Kistler* system.

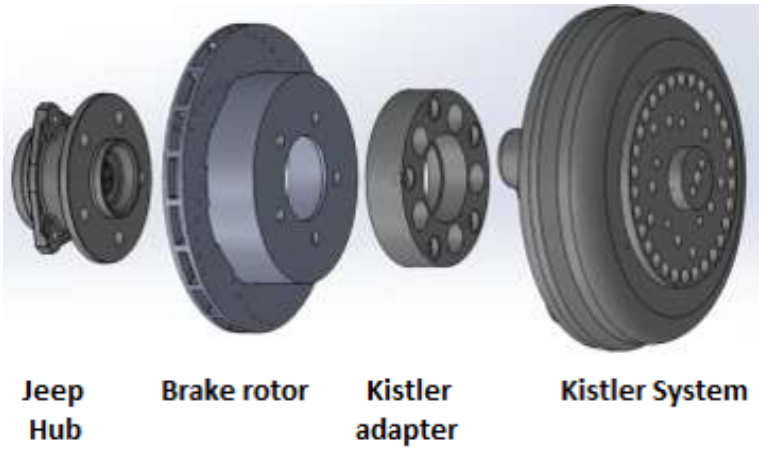

Figure 5.1: Location of brake rotor with reference to the *Jeep* hub, *Kistler* adapter and the *Kistler* system. Reprinted Figure 11 from [16] with permission from ASME publications.

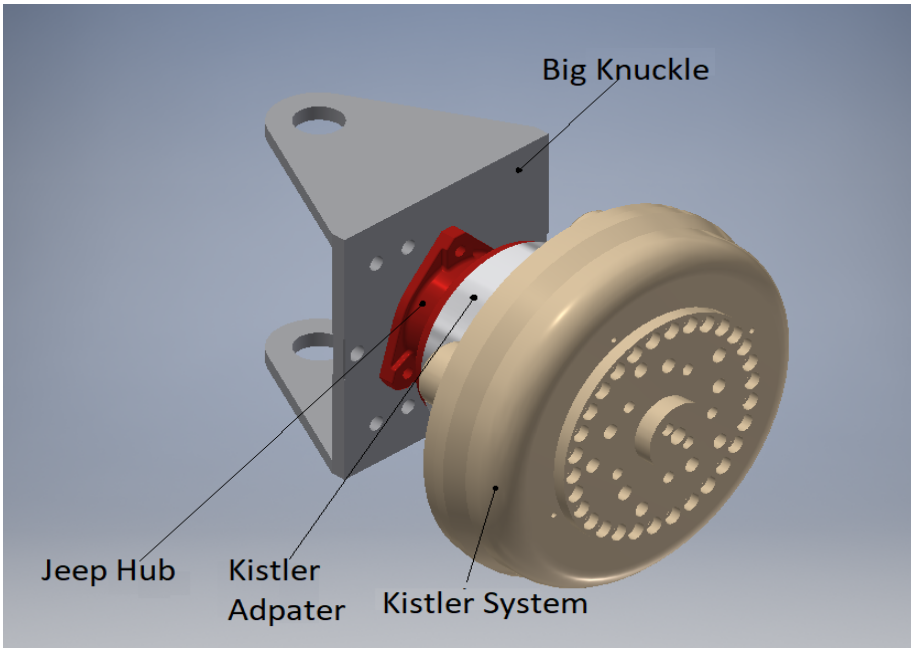

Figure 5.2: Existing assembly of the big knuckle, Jeep Hub, *Kistler* adapter and the *Kistler* system.

In the case of the Terramechanics rig, the space available to fulfill the offset or enable non-hindering assembly of the caliper is only 5.4 cm (2.13 in) as shown in Figure 5.3. It would difficult to design or fit a mounting bracket for the caliper in this space.

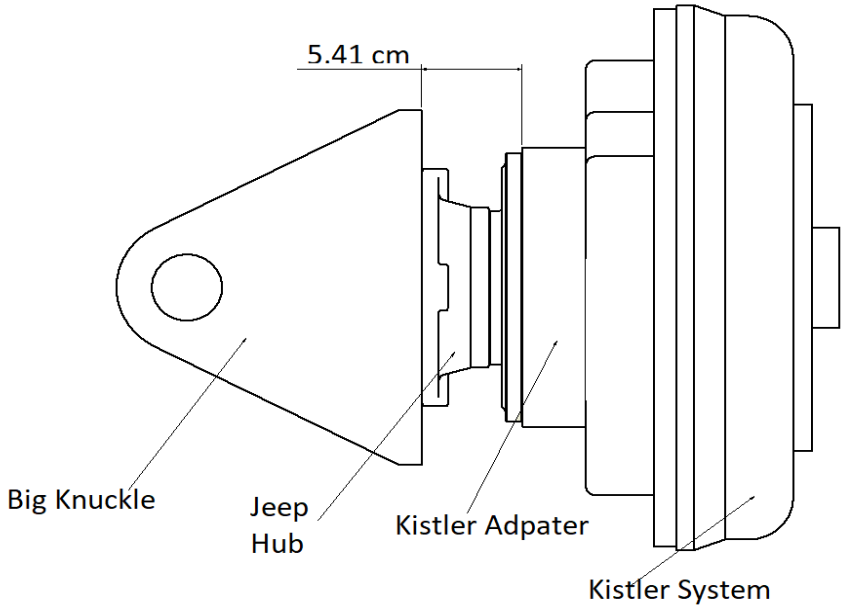

Figure 5.3: Top view : Existing assembly of the big knuckle, Jeep Hub, *Kistler* adapter and the *Kistler* system.

5.2.1 Selection of Rotor and Caliper

The selection of rotor and caliper is mutually dependent. There were many physical constraints when it came to the selection of the rotor and the caliper for the Terramechanics rig. The selection itself became an iterative process. If the rotor was selected as per the constraints that the rig mounting location offered, the corresponding caliper for that rotor would interfere with the big knuckle or other component in the vicinity and vice versa. The final selection and the modifications that were made in order to incorporate the brake rotor and the brake caliper at the finalized location is explained in the subsequent sections.

Rotor

Initially, the plan was to select a standard available rotor to suit our requirements. Some of the most important parameters based on which the selection is made are the rotor

thickness, diameter, and the type. Rotor thickness is dependent on the heat generated during the braking action. For the Terramechanics rig, the heat generated would be minimal. It was decided to select a standard rotor that would fit the required bolt pattern (5 on 4.5 *in* bolt circle). However the major constraint in the selection of the brake rotor is the brake diameter. A larger diameter brake rotor generates greater braking torque for the given value of applied pedal effort [11]. However in the case of Terramechanics rig, the maximum diameter is restricted by a some of the components of the *Kistler* system and the size of the big knuckle. The big knuckle is the the rigid surface in the vicinity which will be used to fix the brake caliper mounting bracket to. Due to the size of the big knuckle, it would be difficult to design a mounting bracket or support the brake caliper of a larger diameter rotor. Further, the *Kistler* system has Data Acquisition Module (DAQ) which is a non contact type wheel electronics system made of two parts − a rotor (ring antenna) which is connected and fixed onto the *Kistler* system and a stator (data transmitter) which is supported from a nearby rigid body. In this case, the big knuckle supports the stator of the wheel electronics system of the *Kistler* system shown in Figure 5.4.

The brake rotor should be of the diameter that would not interfere with the supporting rod of the stator. Additionally, there should be adequate clearance between the outer diameter of the brake rotor and supporting rod. As per the current arrangement, the distance from the tire axis to the under surface of the supporting rod is approximately 13.97 *cm* (5.5 *in*). This would mean that the brake rotor has to have a diameter less than 27.9 *cm* (11 *in*). This created a problem in finding the right sized rotor and caliper combination. The nearest available combination was a 29.85 *cm* (11.75 *in*) diameter rotor with 2.26 *cm* (0.89 *in*) thickness. This required a minor modification of the supporting rod for the wheel electronics system's stator. For the procurement, we looked into various brake components vendors. Amongst them 'Wilwood Disc Brakes' was the one with a wide range and bolt pat-

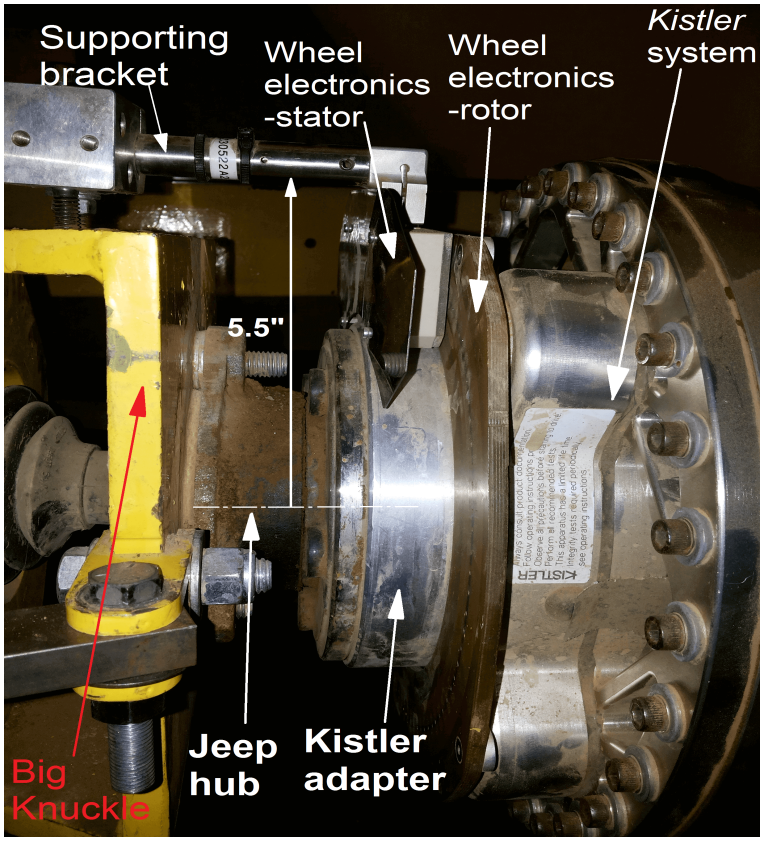

Figure 5.4: Kistler Wheel Electronics systems : rotor(wheel antenna) and stator(data transmitter). Reprinted Figure 12 from [16] with permission from ASME publications.

tern. The customization and the final selection of brake rotor is discussed in the following subsections.

Selection of Caliper

The selection of caliper for the Terramechanics rig was largely dependent on the customized rotor, the availability of space and the fluid pressure at which it is rated. In general, for this application, it was both time and cost effective to explore the market available caliper for automobiles. From the geometric aspect, a caliper meant for 2.26 *cm* (0.89 *in*) thick and 29.85 *cm* (11.75 *in*) diameter brake rotor is the ideal requirement. The major aspect to be looked over was the overall dimensions of the calipers and the distance between its 2 mount-

ing points. There was a need of a caliper that had a shorter lateral length and a shorter mounting length. The available lateral space of 5.4 *cm* (2.13 *in*) as shown in Figure 5.3 is insufficient to incorporate any caliper meant for 2.26 *cm* (0.89 *in*) thick rotor.

The customization of the brake rotor and the creation of lateral space through few modifications is described in the following subsection. The other major task to look into was the mounting point distance. This is important because it would become difficult to support a large caliper from the big knuckle. The front dimension of the big knuckle is just 20.32 *cm* x 20.32 *cm* (8 *in* x 8 *in*). Additionally, the *Jeep* hub occupies most of the frontal face and leaves very little room for mounting any other component. Therefore, it was essential to procure a caliper for the selected rotor with the least distance between the mount centers. After looking into various catalogs, model **120−11873−BK** from *Wilwood Disc Brakes* was finalized as shown in Figure 5.5. The dimensional and other technical details of the caliper is as mentioned in Table 5.1.

Figure 5.5: Procured brake caliper model 120-11873 by Wilwood Disc Brakes.

The mount center of 13.87 *cm* (5.46 *in*) was still a difficult challenge in the design of the mounting bracket. However this being smaller than the edge length of 20.32 *cm* (8 *in*) of the big knuckle, designing a mounting bracket for the same would be feasible. The lateral

Table 5.1: Wilwood Brake Caliper − 120−11873−BK

Type	Floating Single Piston
Mount center	13.87 *cm* (5.46 *in*)
Lateral width	12.62 *cm* (4.97 *in*)
Max. rotor diameter	30.96 *cm* (12.19 *in*)
Max rotor width	20.57 *mm* (0.81 *in*)

width of 12.62 *cm* (4.97 *in*) was a major concern. The brake rotor required customization to accommodate this lateral width.

5.2.2 Customization of Rotor

The small space of 5.4 *cm* (2.13 *in*) that was available as shown in Figure 5.3 had to be increased to make space for the brake rotor and caliper such that there is no interference. The rotor final location is between the *Jeep* hub and the *Kistler* mounting adapter. The only place where anything could be placed so as to increase the offset or create space was this same location. The best way to increase this space was to include wheel spacers at this location. A minimum of 7.62 *cm* (3 *in*) space would be sufficient for no interference after assembly. It had to be ensured that the bolts for the wheel toe angle assembly doesn't interfere. Spacers are a standard component easily available and with various width option. The specification we required was 7.62 *cm* (3 *in*) thick and bolt pattern of 5 on 114.3 *mm* (4.5 *in*) . In order to allow for a minor adjustment later, it was decided to have two spacers of 3.8 *cm* (1.5 *in*) thick instead of just one 7.6 *cm* (3 *in*) spacer. The spacer available in came with a pre−installed studs of a specific length. The available brake rotor came with an offset suiting to a particular automobile model. None of these off set matched the rigs requirements. Therefore, a plain rotor without the mounting section and a customized rotor hat were the best solution. A rotor hat with an offset of 0.64 *cm* (0.25 *in*) is required based on the available space. Getting

a hat with the required offset posed a big challenge. Since it was a very specific offset,the other option was to fabricate a custom rotor hat meeting out requirements. Since, heat dissipation and other thermal aspects weren't a major concern, a simple rotor meeting the desired dimensions was sufficient. **Ultra lite vane rotor model−160−0471** from *Wilwood Disc Brakes* was a simple vane rotor which met our dimensional requirement and was cost efficient. The procured rotor is shown in Figure 5.6.

Figure 5.6: Procured brake rotor model 160−0471 by Wilwood Disc Brakes.

This rotor had a rotor bolt pattern of 8 holes on a 17.78 *cm* (7 *in*) bolt circle and a mounting hole size of 8.22 *mm* (0.326 *in*). *Coleman Racing* was a manufacturing firm dealing with custom components of automobiles. The requirements for the rotor hat was communicated to the firm and was requested for a draft drawing. customized rotor hat was ordered from *Coleman Racing* that met our dimensional requirement. The dimensions of the procured vane rotor was also supplied to *Coleman Racing*.

The drawing received from the vendor was verified with respect to the dimensions and the order was placed. The final product received from *Coleman Racing* is shown in

Figure 5.7. The nuts and bolts to fix the plain rotor to the customized rotor were also ordered from *Coleman Racing*. The brake rotor and the custom hat received were assembled as shown in Figure 5.8.

Figure 5.7: Customized Brake Rotor Ha.t

The next task was to procure the wheel spacers for the brake system. The requirement was of a wheel spacer for a bolt pattern of 5 on 114.3 mm (4.5 in) bolt circle, bolt size of $1.27cm$ (1/2 in) and width of $4.45cm$ (1.5 in). The idea was that the first wheel spacer would be mounted directly on the *Jeep* hub and then the second spacer would be mounted on the first spacer. Then the brake rotor would be placed followed by the *Kistler* adapter onto this second spacer. All these spacers come with a preinstalled studs of a specified length. This length is sufficient for automobile application where only the wheel is supposed to be mounted. In the case of the Terramechanics rig, the components that take up the length of the stud are as follows: thickness of 6.35 mm (0.25 in) by the rotor hat, additional length of 7.2 mm (0.283 in) taken up by the *Kistler* adapter and finally the rest of the length would be taken up by the nut for this stud. Its a general practice to leave $2-3$ threads points out

Figure 5.8: Assembly of brake rotor and rotor hat. Reprinted Figure 13 from [16] with permission from ASME publications.

after the assembly has been tightened. Taking all of this consideration, a minimum of 40 mm (1.55 in) length pointing out from the spacer was required. Since the *Kistler* adapter flushes with the *Kistler* system, the total length of the stud pointing out can't be greater than the sum of the width of the adapter (38.1 mm) and the face thickness of the rotor (6.35mm), i.e., the length of the stud point out can't be more than 44.45 mm (1.5 in). Further, taking into account the length of bolt that will be used up in the spacer for press−fitting it, the maximum and minimum limit on the stud length was imposed. It was difficult to find a wheel spacer that had pre−installed studs which were within the acceptable range. A decision was made to procure a spacer with the available length and additionally procure a set of wheel studs of the required length range or longer. The idea was to remove the pre−installed studs from the spacer, counter−bore it if required and, then press fit the procured studs. Various catalogs of wheel spacer vendors were reviewed and *50 Caliber Racing* was decided upon as the vendor for the wheel spacer. The studs that came pre−installed had a threaded length less than the minimum required value. It was difficult to find set of studs that matched the

serrated diameter, stud size of 1/2 *in* and, the required length. Eventually, a set of studs from *ARP* was available which had the serrated/knurl diameter of 1.44 *cm* (0.568 *in*), stud size of 1.27 *cm* (1/2 *in*) and under head length of 7.54 *cm* (2.97 *in*). For a value within the acceptable range, the stud had to be cut from 7.54 *cm* (2.97 *in*) to 5.84 *cm* (2.3 *in*). A drawing for the machining work was drafted and released depicting the work to be done as shown in Figure 5.9.

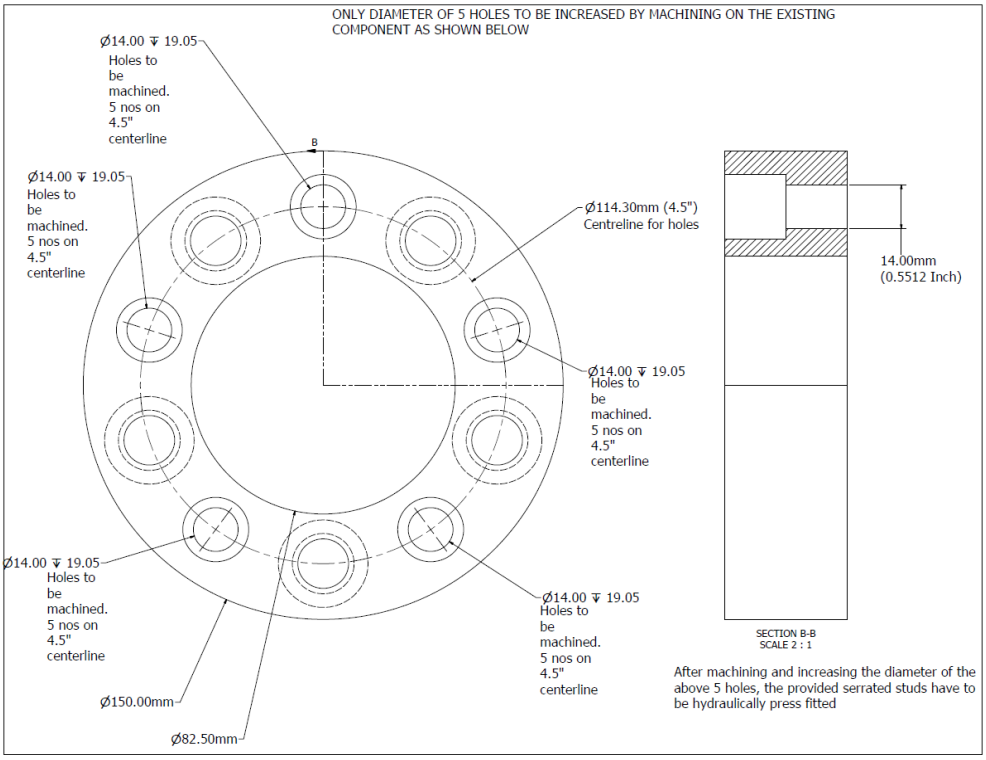

Figure 5.9: Drawing of post procurement machining work of Wheel Spacer.

The machining involved removal of the existing studs, machining the holes to 14 *mm* (0.5511 *in*), cutting the new studs to the under head length of 5.84 *cm* (2.3 *in*) and finally press fitting the new studs. The final machined and installed spacer is as shown in Figure 5.10. With this, the task of creating lateral space for installing brake rotor and brake caliper without causing interference was achieved. The next task at hand was designing the mounting bracket for the brake caliper which is described in the following section.

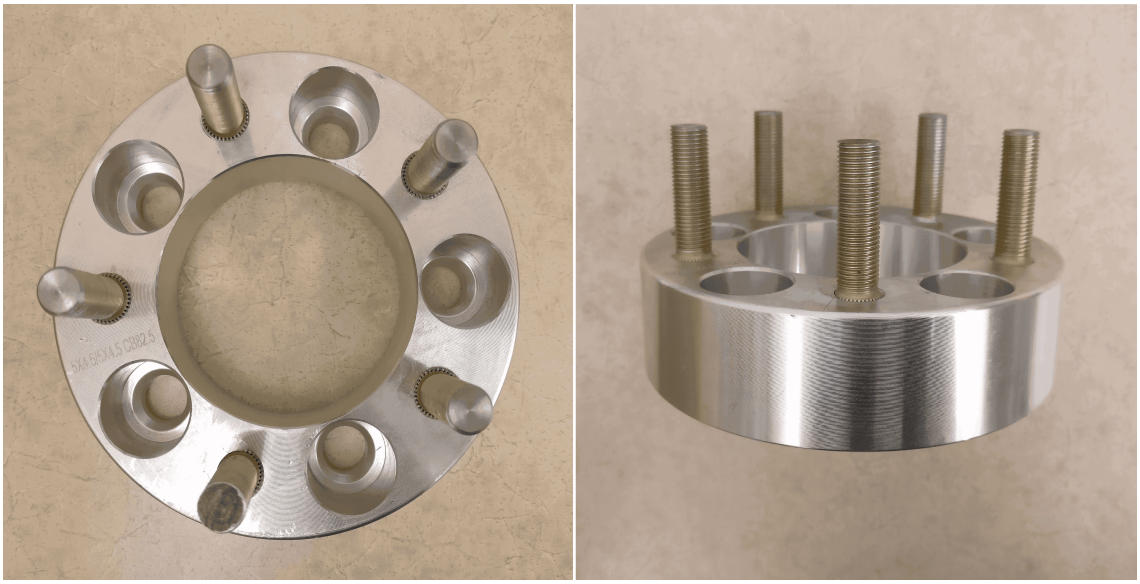

Figure 5.10: Wheel Spacer with new studs installed. Reprinted Figure 14 from [16] with permission from ASME publications.

5.3 Design of Brake Caliper Mounting Bracket

The first task in the design of the brake caliper mounting bracket is to decide the exact location of the caliper with respect to the circumference of the brake rotor. Ideally the caliper can be placed at any position around the 360 degrees of the rotor. However, there are carious factors that can limit the location in case of an automobile. However, in case of the Terramechanics rig, the main factors that limit the location of the caliper with respect to the rotor are as follows:

- Availability of rigid surface for the caliper bracket
- Space available
- Easy maintenance
- Bleed points of the caliper to be pointing up

Considering a sample location drawing as shown in Figure 5.11, there are 4 locations where the caliper can be mounted. Location 1 as shown in Figure 5.11 cannot be used since the cables of the *Kistler* Electronics and its support are mounted on the top.

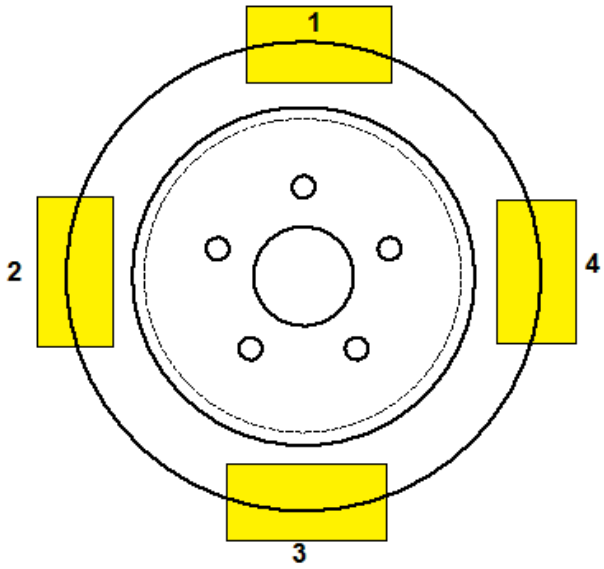

Figure 5.11: Sample locations for caliper around the brake rotor.

It would be difficult to design a mounting bracket for locations 2 and 4 as the wheel's toe angle setup is mounted there. At location 3, both the bleed point will point down and plus from the maintenance and accessibility point of view, location 3 is not the ideal location. Now these locations were primarily front, rear, top and bottom location which turned out to be undesirable locations in the case of the rig. Considering another sample location drawing as shown in Figure 5.12, the other available locations are A, B, C and D.

Locations C and D would cause problem with maintenance and accessibility. In this scenario, locations A and B were the best locations to mount the brake caliper. Hence, location A was initially selected as the caliper location. The next task was to evaluate the assembly and then design an appropriate mounting bracket for the same. The assembly with the caliper and brake rotor mounted on the big knuckle is shown in Figure 5.13.

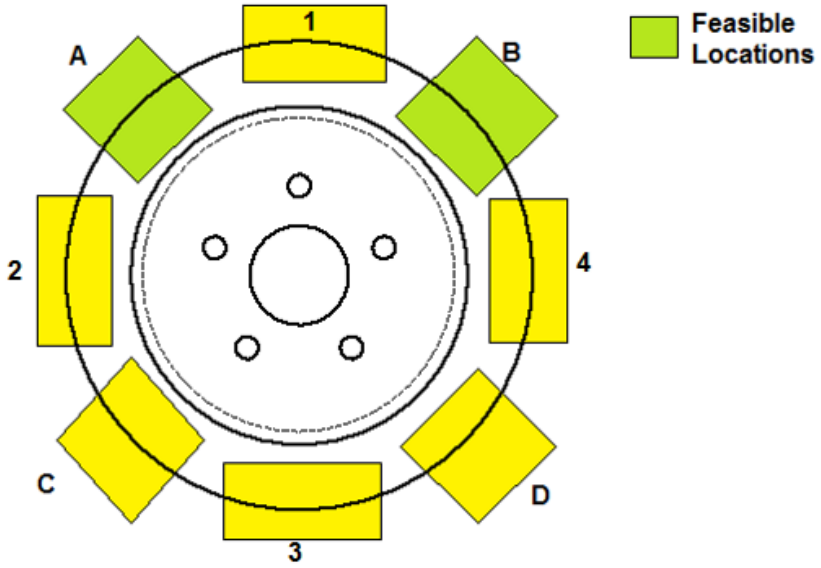

Figure 5.12: Feasible locations for caliper around the brake rotor. Reprinted Figure 15 from [16] with permission from ASME publications.

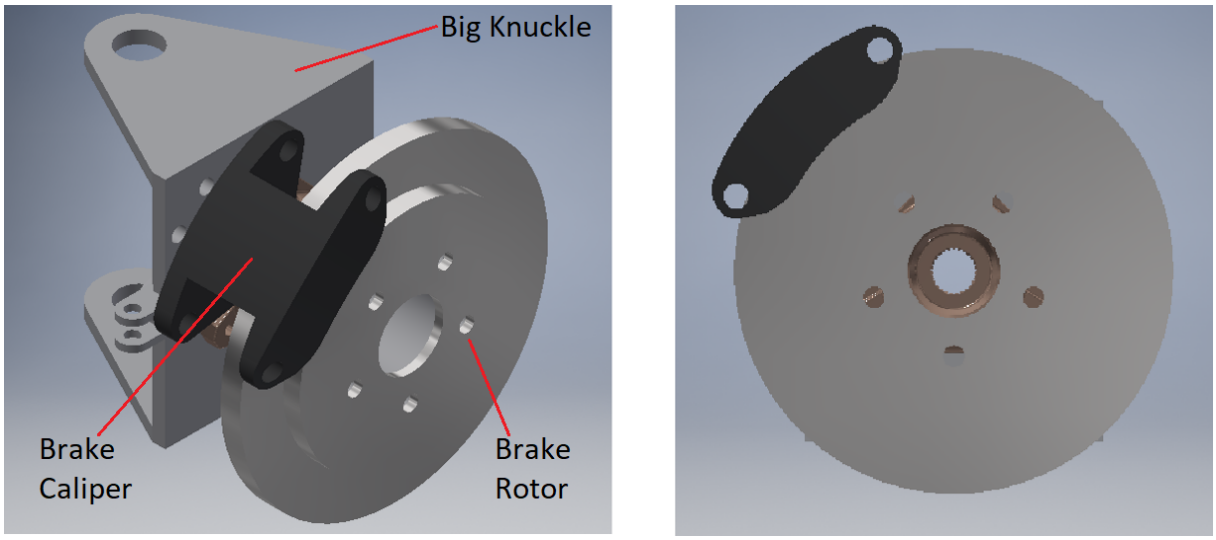

Figure 5.13: Initial assembly of caliper and brake rotor w.r.t. feasible location

Looking at the rear side of the assembly as shown in Figure 5.14, it is seen that there is a section where there is very less clearance between the outer surface of the wheel spacers and the lowest point of the brake caliper. This was an additional constraint in the design of the mounting bracket.

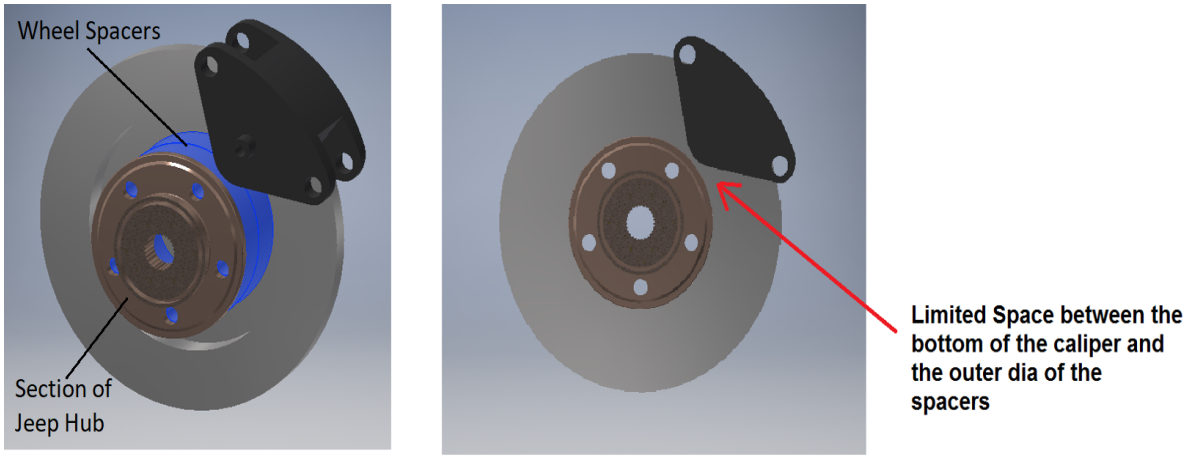

Figure 5.14: Small clearance between outer surface of wheel spacer and the bottom of brake caliper.

The designing of the caliper mounting brackets required multiple iterations. The initial concepts included a two part design to enable minor adjustments, if any, during the actual assembly. This initial two part design is shown in Figure 5.15. The assembly of this bracket is shown in Figure 5.16.

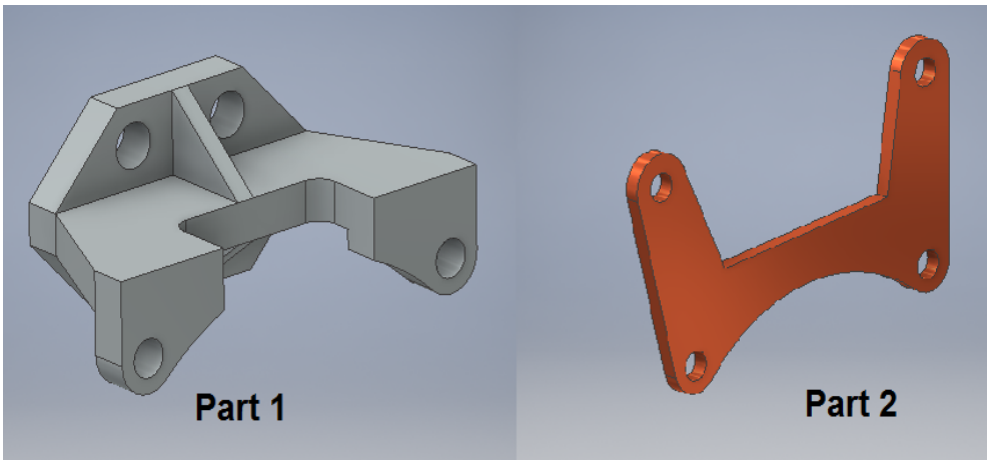

Figure 5.15: Initial design of caliper bracket – two part design.

However, this initial two part designed posed a big challenge from the actual assembly point of view. There was very small clearance to install the hardware to join the two parts. Even if it is assembled initially, for any kind of maintenance work, it would become imperative

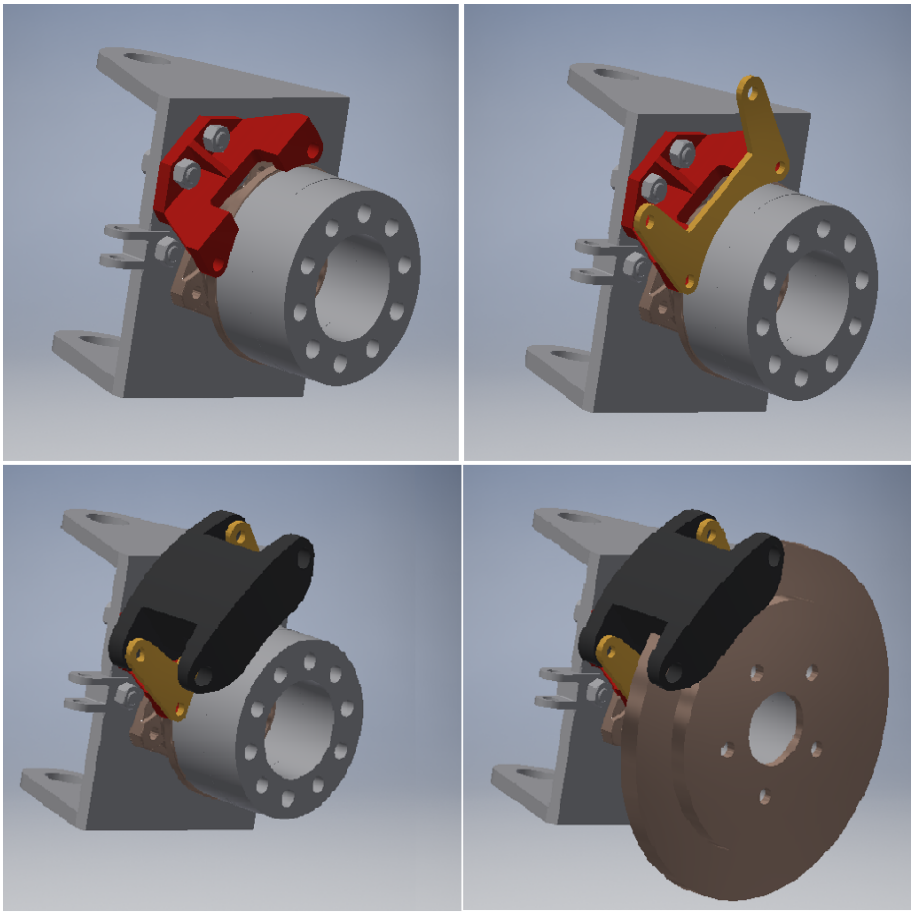

Figure 5.16: Assembly of Initial design of caliper bracket − two part design.

to remove the rotor first. Removing the rotor would be tedious since it involves removal of the *Kistler* system first. Additionally, *Kistler* system would require recalibration every time it is dismounted. Thus in the interest of better accessibility during maintenance, it was needed to modify this design to one part. The next design iteration was a custom single part bracket taking into consideration all the space and assembly constraints. The design is as shown in Figure 5.17.

It is very similar to the first two part design. It has the same base for mounting it onto the big knuckle. The portion where the brake caliper is mounted has been modified since part 2 of the previous design is eliminated. The bracket is more sturdier than the

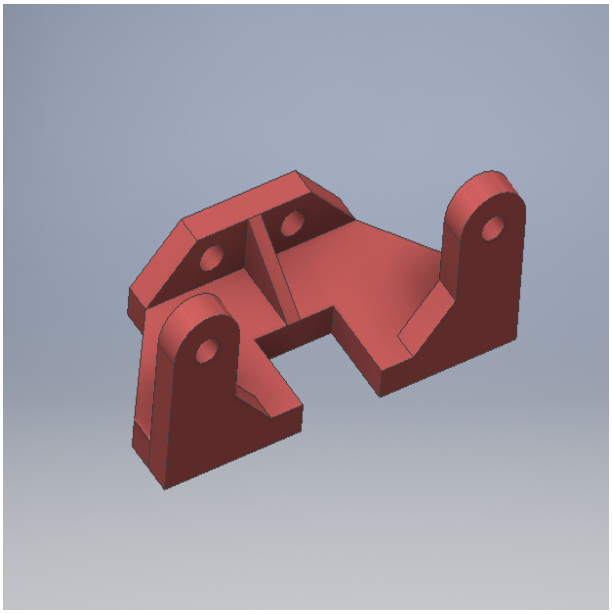

Figure 5.17: Initial design of caliper bracket – one part design.

previous two part design. The assembly using this design of bracket is shown in Figure 5.18.

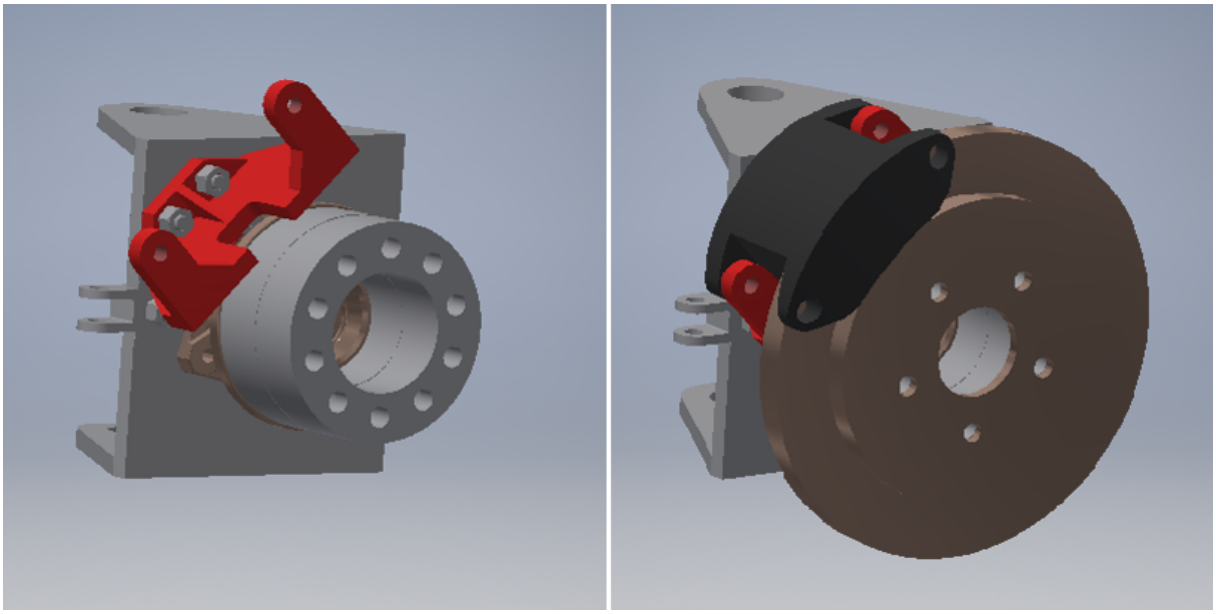

Figure 5.18: Assembly of initial design of caliper bracket – one part design. Reprinted Figure 16 from [16] with permission from ASME publications.

The next task was to analyze the design to sustain the loads and to modify the design

if necessary. The loads that act on the bracket are the braking torque and the dead weight of caliper. Both of the above loads will be transmitted by the caliper mounting pins to the pinholes on the caliper. The load is eventually transmitted to the entire big knuckle through the bolted joint of the bracket. The braking torque that the caliper generates and is eventually resisted by the mounting bracket primarily depends on the following parameters [11]:

- Normal load
- Tire radius
- Coefficient of friction for the tire−terrain interface
- Rotor size
- Piston size of the caliper

For the calculation of the braking torque, locked condition of the wheel (100 % skidding) is considered. The procured caliper is rated at around a maximum of 8.2 MPa (1200 psi) of brake line pressure. The brakes in general have to resist the frictional force F generated [11] given by Eq. (5.1), where μ is the coefficient of friction between the tire and terrain interface and N is the normal load on the wheel.

$$F = \mu N \tag{5.1}$$

Equating the torque generated due to the frictional force at the wheel terrain interface to the torque at the brake rotor, we get Eq. (5.2) where F_x is the frictional force at the brake pad and rotor, R is the rolling radius of the wheel and r is the radius of the brake

rotor where the clamping force of the brake pad acts.

$$F_x = \frac{\mu N R}{r} \tag{5.2}$$

This is the force which the brake caliper and eventually the caliper mounting bracket has to resist. The terramechanics rig is meant for testing tires of various sizes up to 37 *in* [6]. The brake rotor size is fixed and limited by the physical constraints of the rig. Thus, the maximum normal load N that can be tested for different tire−terrain interface will vary depending upon the size of the tire. The braking torque would be generated due to the clamping force of the brake caliper which is given by Eq. (5.3).

$$F_{clamp} = \frac{F_x}{\mu_{pad}} \tag{5.3}$$

where μ_{pad} is the coefficient of friction between the brake pad and the brake rotor. The force exerted on one side of the brake caliper piston is given by Eq. (5.4)

$$F_{piston} = \frac{F_{clamp}}{B.F.} \tag{5.4}$$

where $B.F.$ is the brake factor which is 2 in case of disc brake [11]. This piston force is generated by the brake fluid pressure as shown in Eq. (5.5)

$$P_l = \frac{F_{piston}}{A_{piston}} \tag{5.5}$$

where P_l is the brake fluid pressure, A_{piston} is the cross−sectional area of the brake caliper piston. Mechanical effort through the master cylinder given by Eq. (5.6) generates

the fluid pressure.

$$P_l = \frac{F_{manual} L.R.}{A_{m.c.}} \tag{5.6}$$

where F_{manual} is the manual effort to be applied and $L.R.$ is the lever ratio of the brake pedal or hand lever and, $A_{m.c.}$ is the cross−sectional area of the master cylinder. Considering equations Eq. (5.1) to Eq. (5.6), the maximum normal load that can be applied during testing at the Terramechanics rig for various tire−terrain interface is as shown in Table . For these calculations, the maximum size of the wheel which can be tested, i.e., 94 *cm* (37 *in*) is considered and a maximum manual effort of 25 *kg*, i.e., around 55 *lbf*. The maximum normal load that has been tested previously in the Terramechanics rig is $8kN$ and is considered as the upper limit in the calculations. *Wilwood Disc brakes* provided the coefficient of friction(μ_{pad}) of 0.46 between the brake pad and the brake rotor. The values of coefficient of friction [5] for the various tire−terrain interface is also tabulated in Table 5.2.

Table 5.2: Maximum normal load that can be tested considering peak brake coefficeient for various tire−terrain interface [5] at the AVDL Terramechanics rig. Reprinted Table 1 from [16] with permission from ASME publications.

Tire/Terrain Surface [5]	Peak brake coefficient [5] (μ_p)	Theoretical Max. Normal Load (kN)	Actual Normal load that can be applied (kN)
Asphalt/Concrete(dry)	0.9	5.8	5.8
Concrete(wet)	0.8	6.5	6.5
Asphalt(wet)	0.7	7.5	7.5
Gravel	0.6	8.7	8
Earth road(dry)	0.68	7.7	7.7
Earth road(wet)	0.55	9.5	8
Snow(hard-packed)	0.2	26.1	8
Ice	0.1	52.2	8

In order to carry out the stress analysis of the caliper mounting bracket, we consider

the worst case scenario of the maximum load. Considering a coefficient of friction of 1 for the tire−terrain interface, maximum tire size of 94 cm (37 in), i.e., to consider approximately 47 cm (18.5 in) of rolling radius of the tire, the effective rotor radius (where the clamping force acts) of 12.7 cm (5 in) and maximum manual effort of 25 kg (55 lbf), the maximum torque was calculated using equations Eq. (5.1) to Eq. (5.6). The maximum torque value that the brake caliper bracket had to be designed for was to resist a torque of 2452 Nm (1809 $lbf.ft$). The mounting hole of the brake calipers is 13.99 cm (5.505 in) and the distance between the two mounting pins is 13.84 cm (5.45 in). This translates to a mounting radius of 15.62 cm (6.15 in). The force acting on each mounting pin of the brake caliper is calculated to be4.8 kN (1766 lbf). The model was analyzed using finite element software tool Abaqus. the part was tested for the load of 4.8 kN (1766 lbf) on each of the mounting hole in the tangential directions keeping the bolted holes as fixed. The material for the caliper was decided to be carbon steel 1018 whose yield strength is around 310 MPa (53 $kpsi$). The stress analysis of the the initial bracket (Figure 5.18), showed a Von Mises stress of 840 MPa (121.8 $kpsi$). This is shown in Figure 5.19 (in psi).

Due to this high von Mises stress, the design had to be modified. This started an iterative process of modifying the design and performing the stress analysis. The next design iteration and its stress analysis are shown in Figure 5.20 and Figure 5.21 respectively.

The maximum von Mises stress in this iteration was little under the yield strength of the 1018 steel. However, given the functional requirement of the bracket, a factor of safety of atleast 1.5 is desirable. Further, this variation of the design involved lot of webs and reinforcements which would have increased the machining cost of the component. The next iteration resulted in a design as shown in Figure 5.22 and its stress analysis as shown in Figure 5.23.

This design developed a maximum Von Mises stress of 248.2 MPa (36 $kpsi$), which

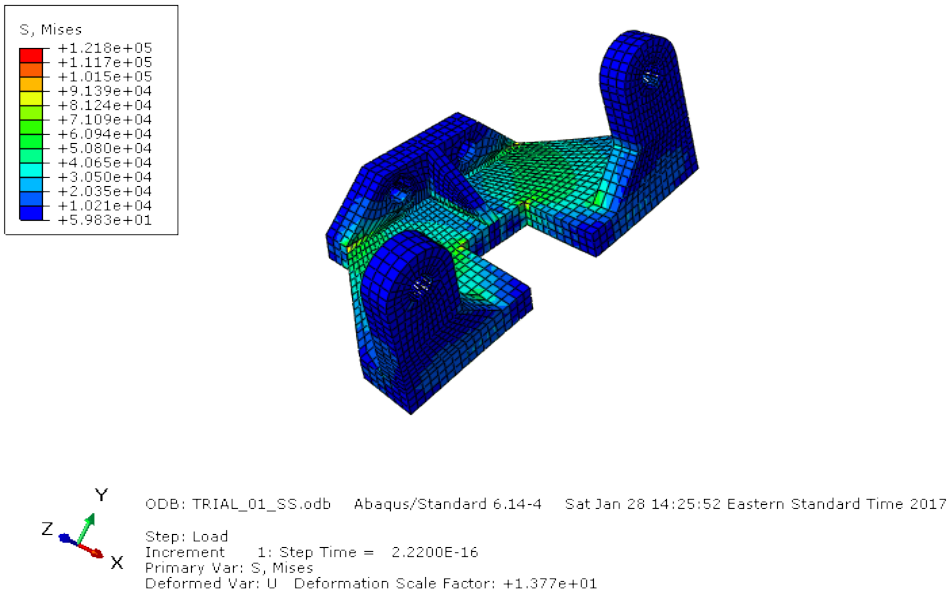

Figure 5.19: Stress analysis of initial design of caliper bracket − one part design. Reprinted Figure 17 from [16] with permission from ASME publications.

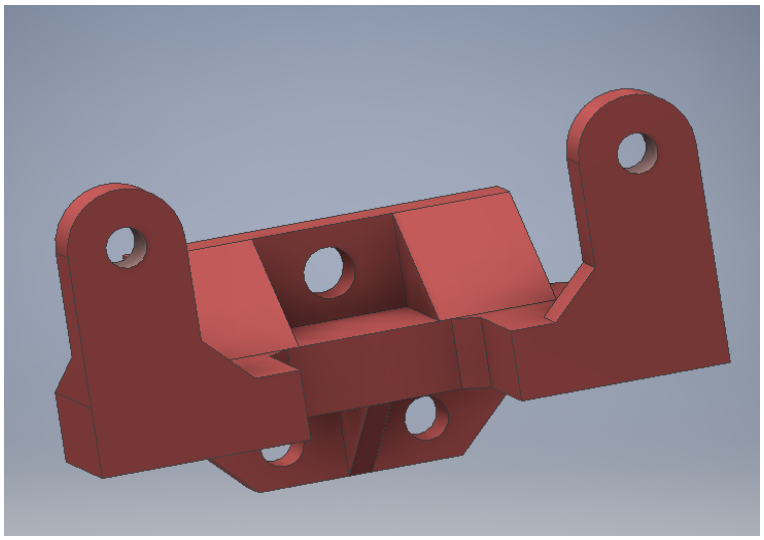

Figure 5.20: Variation 1 : Design of caliper bracket − one part design

gives a factor of safety of around 1.4. However, this design is bit complex from machining point of view. Additionally, there were high chances that this design may not be feasible when it came to the assembly stage. The bolting location would have accessibility issues during fixing it to the big knuckle. It was concluded that the basic reason for this high stress

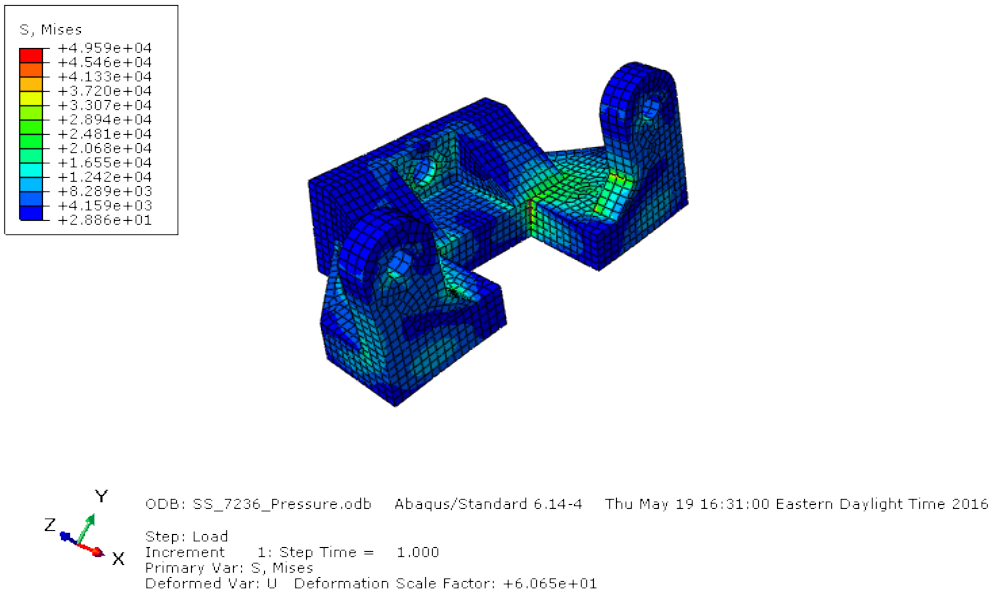

Figure 5.21: Stress analysis of variation 1 : Design of caliper bracket − one part design. Reprinted Figure 18 from [16] with permission from ASME publications.

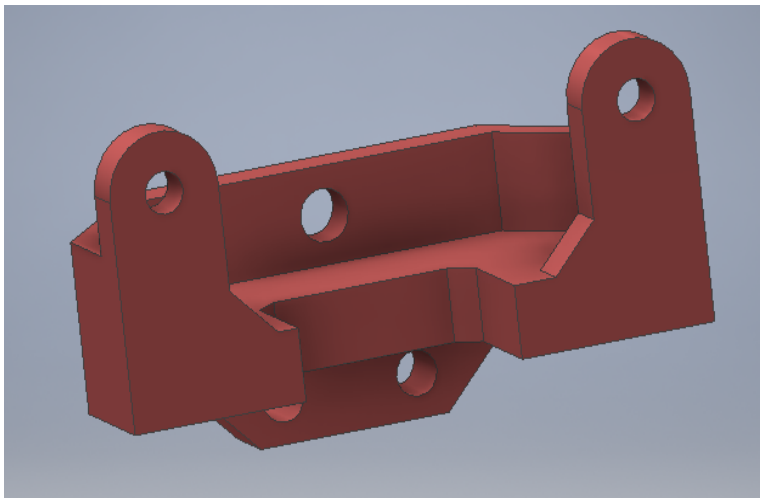

Figure 5.22: Variation 2 : Design of caliper bracket − one part design

is due to the fact that the fixed end of the bracket which supports the bracket is a small area. It acts like a cantilever with an increasing cross−sectional area and a load applied at the free end. There was a need to reconsider the location of the brake caliper around the brake rotor. As shown previously in Figure 5.11, locations 2 and 4 were eliminated only due

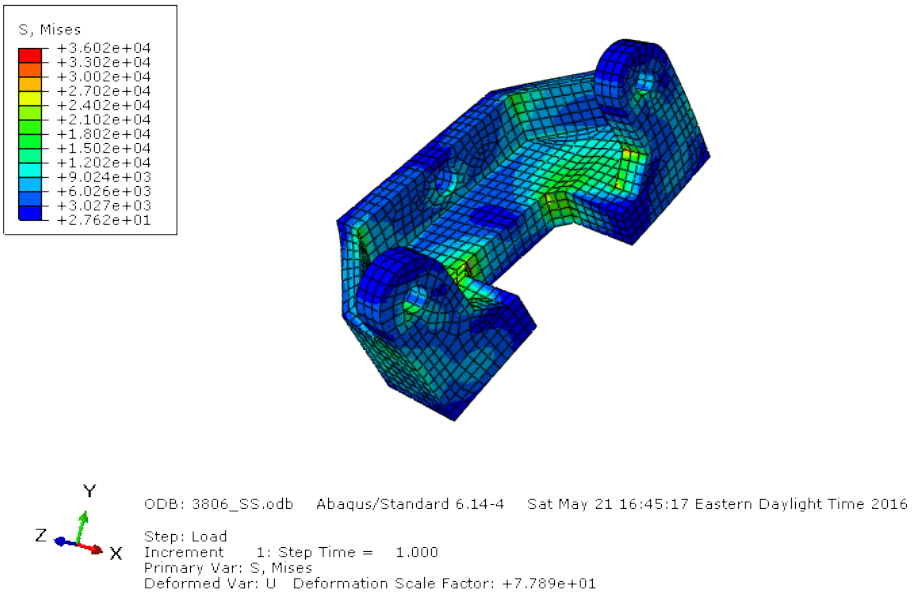

Figure 5.23: Stress analysis of variation 2 : Design of caliper bracket − one part design. Reprinted Figure 19 from [16] with permission from ASME publications.

to the possibility that the caliper or its mounting could interfere with the toe angle setup of the test rig. However, when the locations 2 and 4 were reviewed with respect to the caliper, it was found that the caliper would not interfere in anyway with the toe angle setup, due to the offset created by the wheel spacers. The *Jeep* hub which is fixed on the big knuckle is made of two parts − the static/fixed part and the mobile part. Considering location 2 from Figure 5.11, the available space to fix the base of the caliper mounting bracket is shown in Figure 5.24.

The area shaded in yellow is the only feasible region from where the caliper can be supported so that the base of the bracket doesn't interfere with either the fixed part of the *Jeep* hub or the toe angle setup of the test rig. Additionally, the mobile part of the *Jeep* hub has a larger exterior dimension as compared to the static part as shown in Figure 5.25 and this had to be considered while designing the mounting bracket for the caliper to be placed at location 2 as per Figure 5.11.

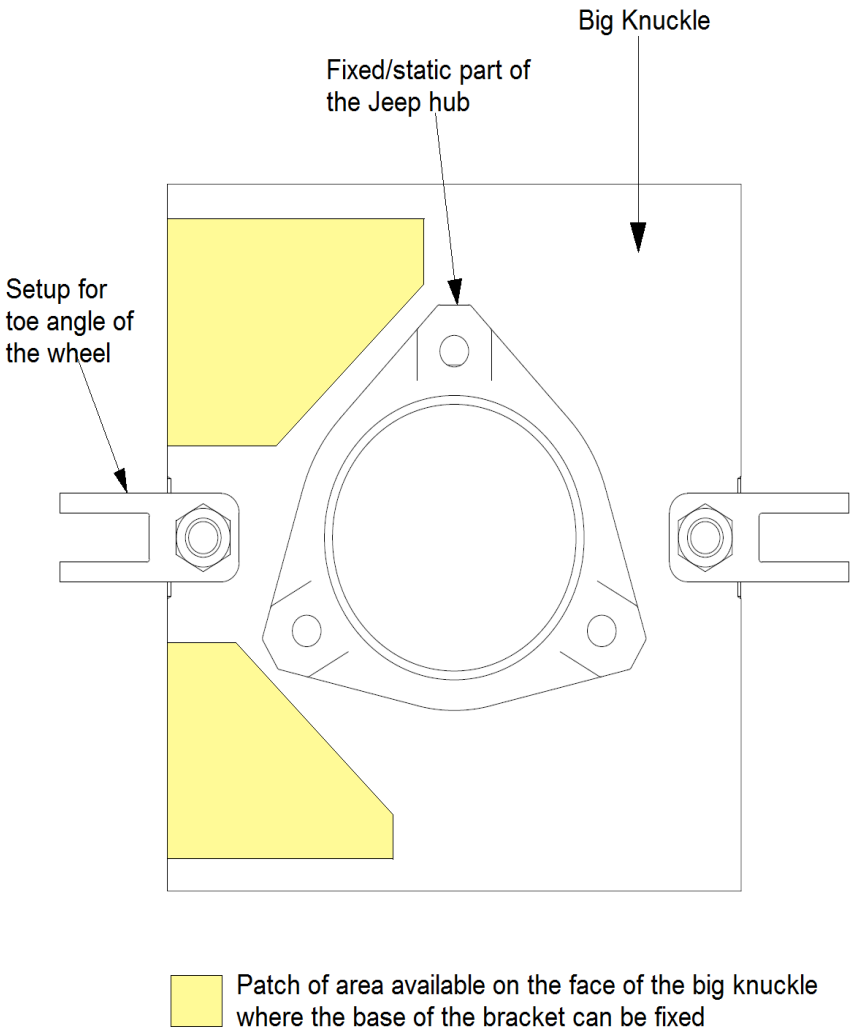

Figure 5.24: Face area of big knuckle available for the base of the brake caliper bracket. Reprinted Figure 20 from [16] with permission from ASME publications.

It was concluded that a one part bracket is difficult to design in this scenario. After multiple iterations, a two part mounting bracket was designed for the brake caliper that satisfied all the physical constraints. The new mounting brackets as shown in Figure 5.26 are mirror image of each other and shall be placed symmetrically.

This design satisfies all the physical constraints and there is no interference with any

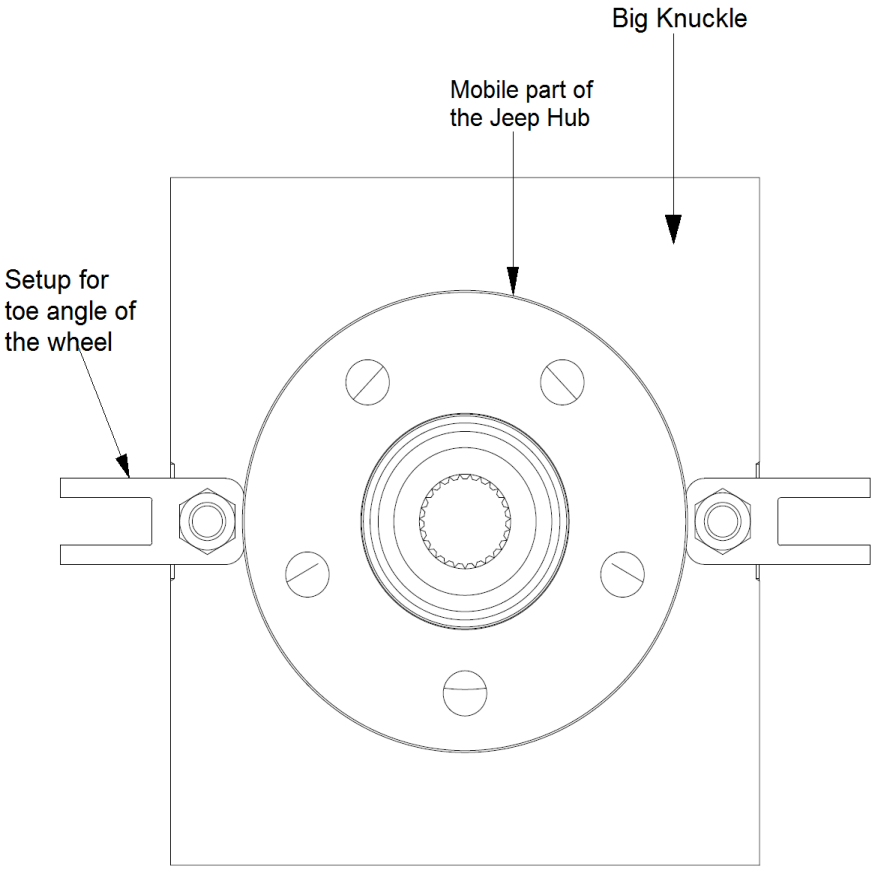

Figure 5.25: Big knuckle and *Jeep* hub with its mobile part

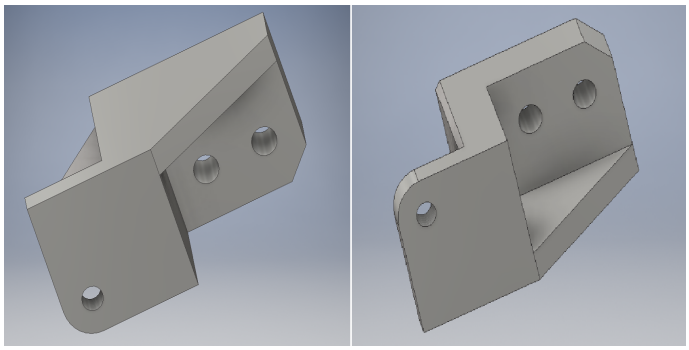

Figure 5.26: Final design − Brake caliper mounting bracket. Reprinted Figure 21 from [16] with permission from ASME publications.

of the other components mounted on the big knuckle. The stress analysis as carried out in Abaqus software. The maximum Von Mises stress induced in the two parts were 186.2

MPa (27 *kpsi*) and 179 *MPa* (26 *kpsi*) for the bottom and top parts respectively as shown in Figure 5.27. This gave a factor of safety of around 1.9 which is above the desirable value of 1.5. This concluded the design phase of the brake components. The fabrication of the brackets was done in the machine shop at Virginia Tech and the finished caliper mounting brackets is shown in Figure 5.28.

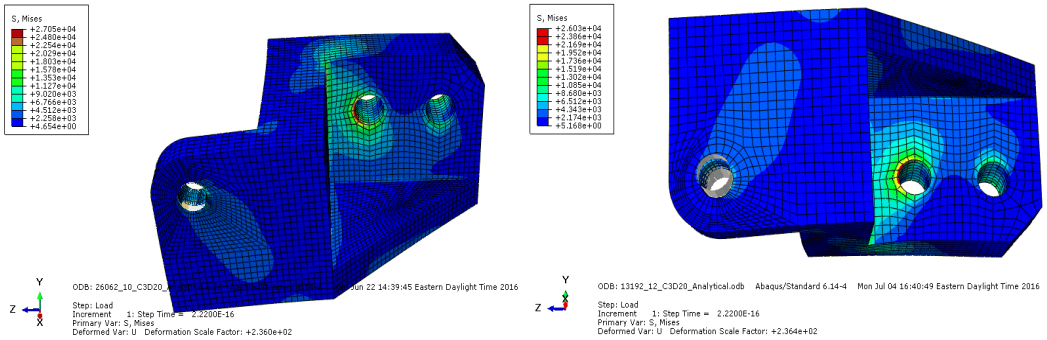

Figure 5.27: Stress analysis of bottom and top part of the mounting bracket. Reprinted Figure 22 from [16] with permission from ASME publications.

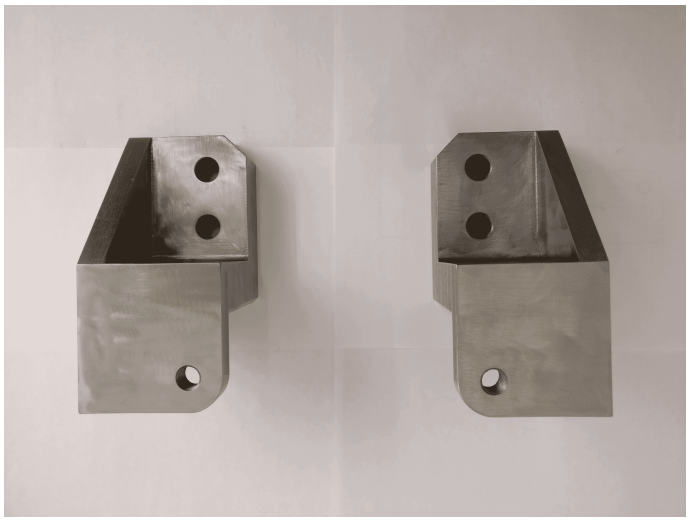

Figure 5.28: Finished brake caliper mounting brackets.

5.4 Operation Mechanism

The disc brake designed works using hydraulic fluid pressure. The major components for hydraulic actuation system comprises of a master cylinder, brake fluid reservoir, pedal or hand lever arrangement, brake fluid hose, and hose fittings. The fittings required are based on the inlet and outlet port of the master cylinder, and the inlet port of the brake caliper. Based on the space available, it was ideal to use a banjo fitting and a banjo bolt. The banjo fittings and its connection on the caliper is as shown in Figure 5.29. A handbrake with master cylinder was in the inventory and it was cost effective to use it for this application. The other components included steel braided hose and the fittings to connect to the master cylinder and the banjo fitting. This concluded the list of the components for the brake actuation system.

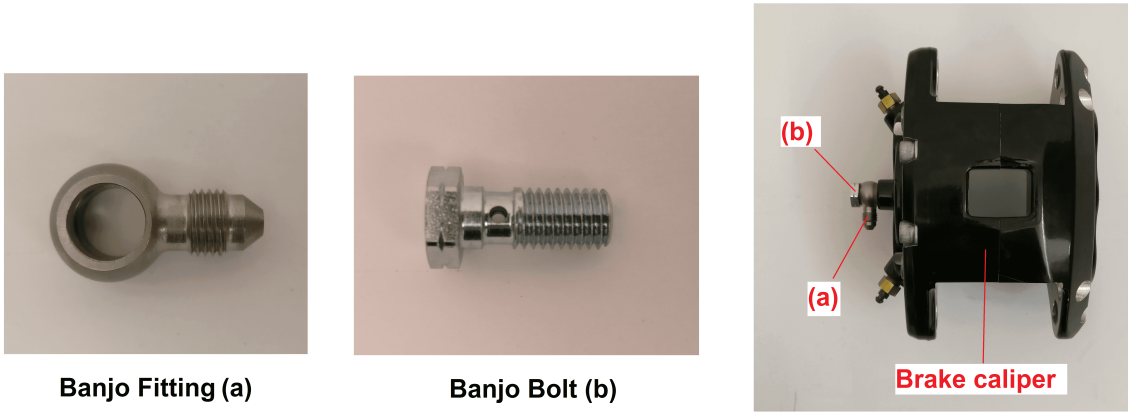

Figure 5.29: Banjo fitting, banjo bolt and its assembly on the brake caliper

The mechanism is similar to the brake application in case of an automobile. The application of manual effort will lead to pressure building in the master cylinder and consequently the movement of the caliper pistons outward. For the Terramechanics rig, the velocity of the carriage will remain constant throughout the braking test. For every test run, the clutch is to be actuated first, i.e., the supply of the compressed air to the clutch

will be cut off. This will lead to the tire to free roll and the next step will be to apply the manual effort to the brake lever. Depending on the manual effort, a corresponding amount of brake torque will act on the tire leading to its braking. With the longitudinal velocity and a constant brake torque will lead to a constant negative slip ratio. The brake torque can be increased to achieve locked wheel condition thereby allowing to skid with a 100 % negative slip. This concludes the design of the brake system for the Terramechanics rig.

Chapter 6

Assembly and Calibration

6.1 Challenges

The biggest challenge in this work was to adapt and design the two systems for the existing rig structure. In case of an automobiles, these systems are standardized for various models. Incorporating these systems in a unique indoor testing facility, required a lot of customization. Right from the design and customization of the various components to the assembly of these components depended a lot on the current state of the mating components on the rig. The hindrance created by the other support structures made the design process challenging. Selecting the right type of clutch and brake system in a way that ensures coupling the existing components on the rig. The design of all the components had to specific to their function as well as adapted to be mounted on the rig without interference. The clutch system's biggest challenges were the selection of the right clutch and the design the mounting frame. The mounting frame had to be designed in a way that it supports the clutch and that it could be easily mounted on the existing structure. Similarly, for the brake system, the biggest challenge was to work around the space available. The selection of the

brake rotor and brake caliper was dictated on the lateral space that could be created and eventually whether a bracket could be designed within the space created. The presence of nuts and bolts for the various toe angle and camber angle arrangement around the vicinity of the caliper and bracket posed a challenge. The design and fabrication of few components had to be kept on hold until the existing components are disassembled inorder to get the correct measurements.

With all the parts fabricated and procured, the next step was to assemble the clutch and brake system on to the tire test frame of the carriage. The tire test frame is designed to move on vertical linear guides. The linear rails are bolted on the carriage and the corresponding bearings are fixed on the tire frame as shown in Figure 6.1.

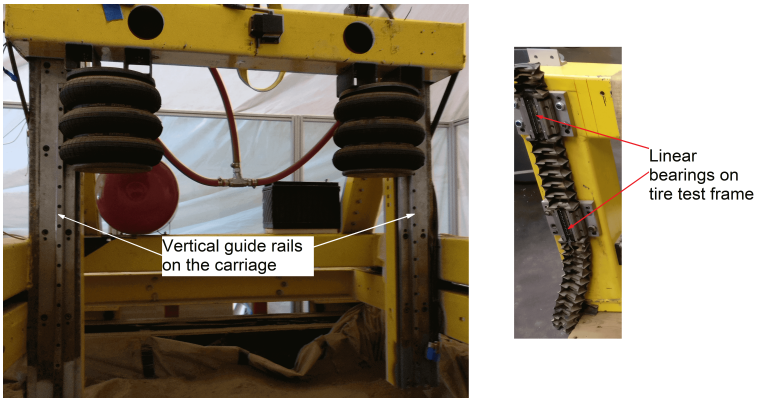

Figure 6.1: Vertical guide rails on carriage and corresponding linear bearings on the tire test frame

The tire frame is lifted using a manual winch arrangement on the carriage which allows to suspend the tire frame. In order to carry out any kind of modification work to the tire test frame, it had to removed from the carriage. With the available lifting−shifting facilities, the only feasible way to remove the tire frame was to lower it down completely on to the bottommost surface of the soil vane. This required the removal of the U−channels that create a false bottom. In order to access the false bottom, the soil from one section of the soil vane had to be moved to another section as shown in Figure 6.2.

Figure 6.2: U−channels of the false bottom

With the false bottom removed, the carriage was moved to this end. With the help of the mechanical winch and the overhead crane, the tire frame was lowered on to a pallet. The tire frame was fastened and secured onto the pallet as shown in Figure 6.3.

In order to move the pallet, the soil vane door had to be opened. This required creating access for the door to swing open and for the forklift to lift the pallet as shown in Figure 6.4. The pallet was loaded onto a truck and brought to the Mechanical Engineering department's machine shop to continue with the assembly work.

6.2 Assembly of the Clutch System

The assembly of the clutch system involves removal of the gearbox first. The assembly of the gearbox upto the *Jeep* hub included the motor, gearbox, adapter sleeve and the CV joint. The disassembled gearbox and motor, sleeve is shown in Figure 6.5.

The task of assembling the clutch system involves welding of the new box channels

Figure 6.3: Test tire frame secured on a pallet

Figure 6.4: Access created for the forklift

to the tire frame and the assembly of the new mounting plate along with the gearbox and the clutch system to be bolted on top these two box channels. In order to ensure that the assembly is correct without misalignment, it was best to get the bolting assembly first as

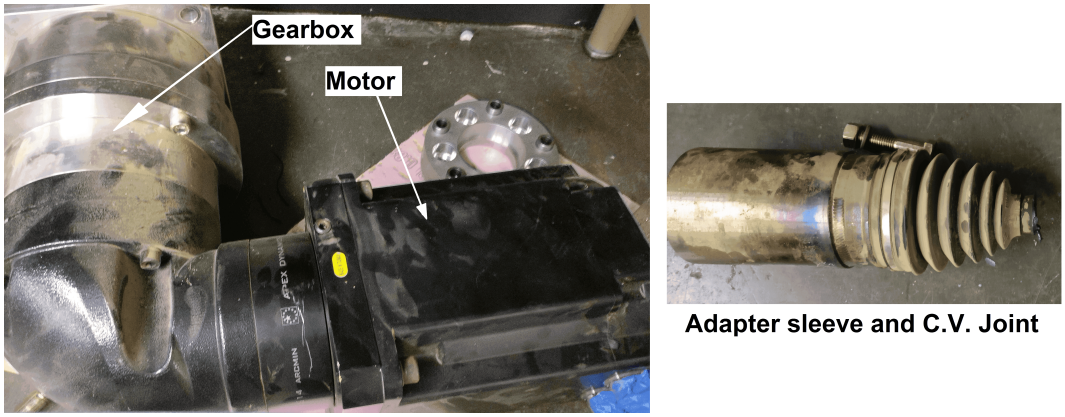

Figure 6.5: Disassembled gearbox & motor, adapter sleeve and C.V. joint

shown in Figure 6.6 and then weld this bigger assembly to the test tire frame as shown in Figure 6.7.

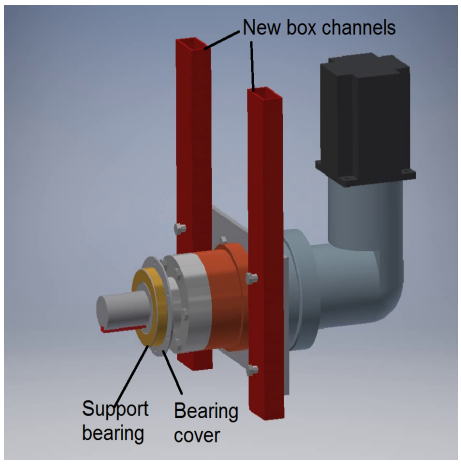

Figure 6.6: Assembly 1 – Bolted assembly of gearbox, clutch system and new mounting plate on the new box channels

6.3 Assembly of the Brake System

The brake system has been designed to be placed between the *Jeep* hub and the adapter for the *Kistler* system. The brake caliper brackets were to be supported by the Big Knuckle. The first task in the assembly of the brake system involved disassembly of the force

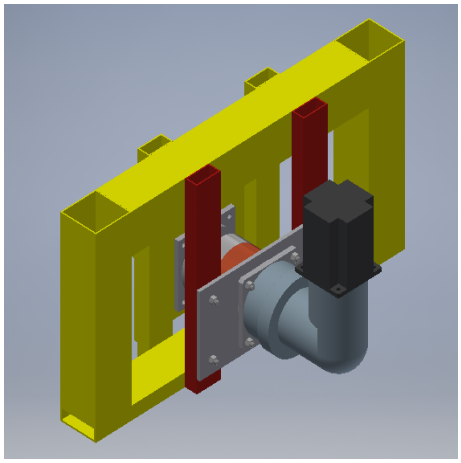

Figure 6.7: Assembly 2 – Welding of assembly 1 on tire test frame

hub (*Kistler* system). The outermost cover of the *Kistler* system is its Universal Adapter which allows for mounting of tires with different bolt patterns. The disassembled *Kistler's* Universal Adapter is shown in Figure 6.8.

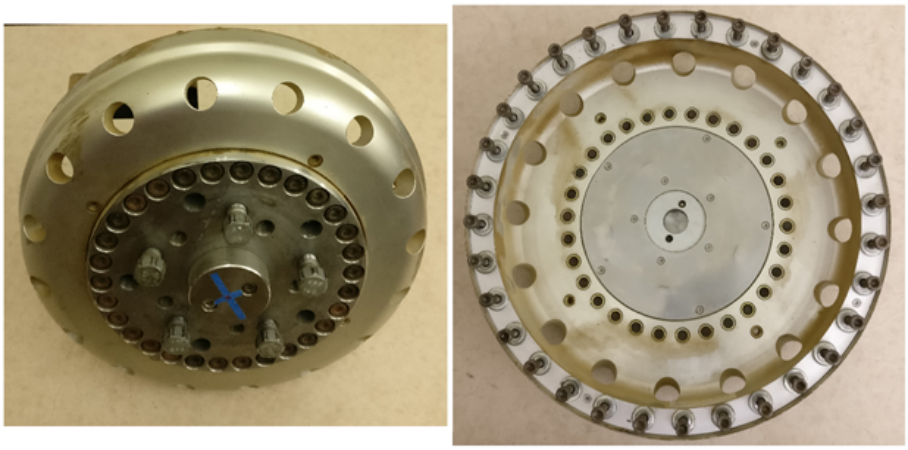

Figure 6.8: Disassembled *Kistler* system – Universal adapter

Once the Universal Adapter was disassembled, the next task was to remove the actual force hub of the system. The *Kistler* force hub is mounted on the *Jeep* hub through an adapter. This adapter is press fitted on to the force hub. Due to the critical nature of this component, the manufacturer of the force hub were contacted. They suggested to use bottle jack or a similar jack and apply lateral force on the outer ring of the force. Thus, we

decided to use a jack screw turnbuckle to apply lateral force on the rim of the force hub. Two turnbuckle were placed diametrically opposite between the outer rim and the existing gear box mounting plate as shown in Figure 6.9.

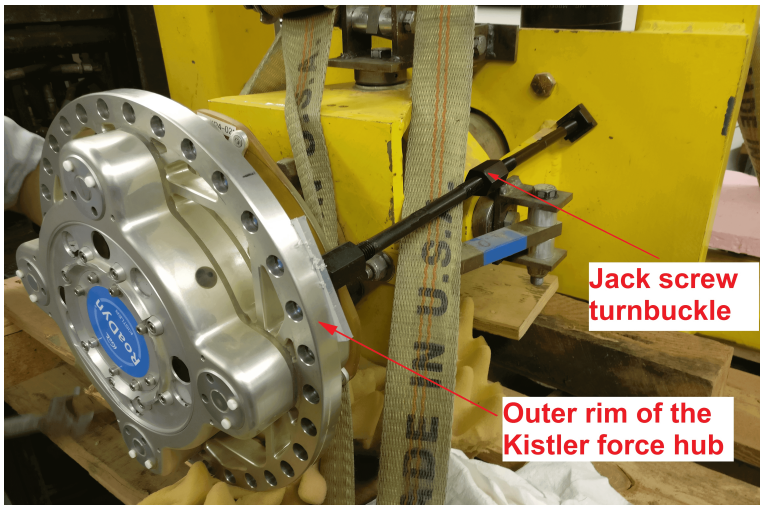

Figure 6.9: Use of jack screw turnbuckle to remove the force hub

The following tasks included the removal of the adapter of the force hub, the *Jeep* hub and finally the big knuckle. The mounting brackets for the caliper had to be bolted on the big knuckle. Thus, the necessary holes had to be drilled on the big knuckle. With the holes drilled, the assembly of the brake system includes bolting the brackets on the big knuckle followed by remounting the *Jeep* hub on the big knuckle; mounting the two new wheel spacers on the *Jeep* hub, followed by the brake rotor and the brake caliper, and finally remounting the force hub.

6.4 Calibration and Validation

With the completion of the assembly of the clutch and brake system, the next step is to calibrate the Terramechanics rig with these two new systems in place. The first task would involve the alignment and the calibration of the force hub, i.e., the *Kistler* system.

The next task would involve calibration of the drive system of the carriage and the wheel assembly.

6.4.1 Alignment and Recalibration of the Force Hub

The assembly of the *Kistler* system requires it to be press fitted on the adapter. Thus, it is essential that the *Kistler* system is properly aligned with reference to the big knuckle and the tire so that it reads the right values. There are more than one way in which the *Kistler* system can be set to be aligned and calibrated as per the requirement.

Alignment

It is necessary that the *Kistler* system is parallel to the big knuckle. This will be ensured if the components between the big knuckle and *Kistler* system are aligned properly. The first task will be to check the alignment of the brake rotor with respect to the big knuckle. This can be done using a distance measuring laser. The sensor has to be placed on the big knuckle such that it projects the beam on the rotor face as shown in figure 6.10.

Since the clutch is installed, the rotor is free to rotate on the *Jeep* hub. The rotor is to be manually rotated and the reading in the laser sensor has to be observed. Based on the observation, the required mounting studs of the *Jeep* hub has to be tightened or loosened accordingly. If there is still some error, then the tension in the relevant mounting nuts of the brake rotor needs to be adjusted. Once the rotor is perfectly aligned, the next step will be to ensure that the alignment of the force hub is right. Since the outer diameter of the force hub is greater than the outer diameter of the brake rotor, the laser distance measurement method can be used as shown in figure 6.11.

The sensor has to be placed on a support such that the laser beam can be projected

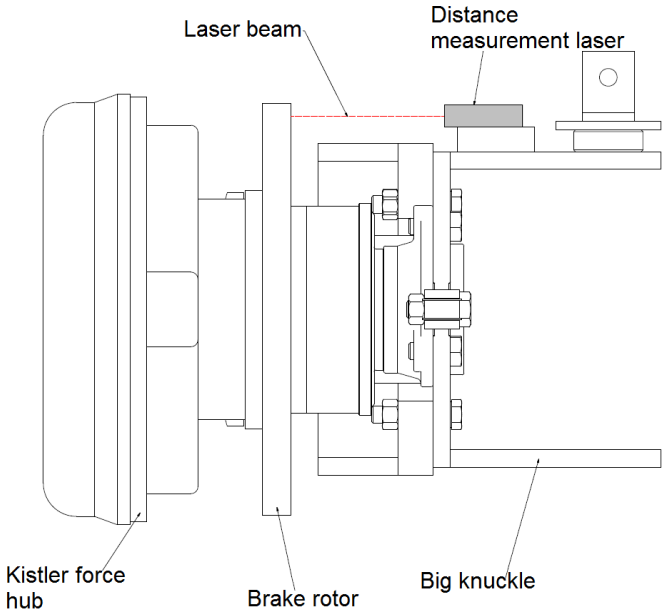

Figure 6.10: Alignment of the brake rotor with respect to the big knuckle.

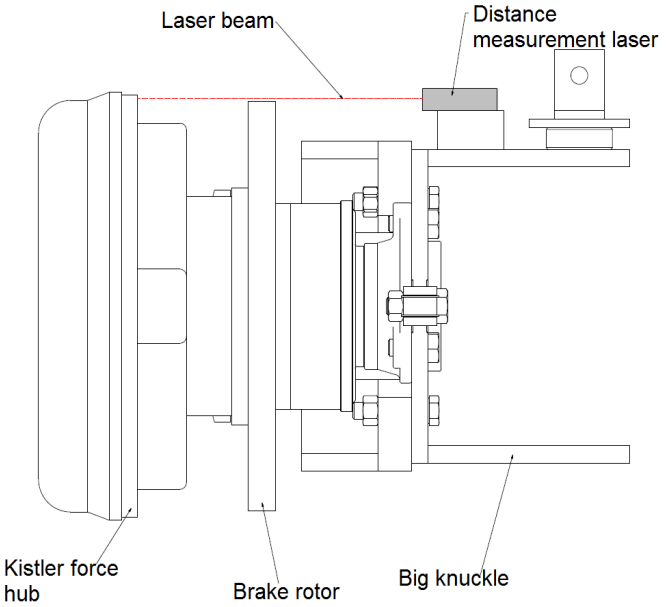

Figure 6.11: Alignment of the force hub (*Kistler* system) with respect to the big knuckle.

on the outer rim of the force hub. A process similar to the brake rotor alignment is to be used for the force hub as well.

Recalibration

Once the alignment of the force hub is done correctly, it should essentially perform in the same manner as it used to before it was dismounted. Calibration in case of the force hub is to check that the force hub reads the right value of loads and moments. Ideally, the force hub calibration is done by the manufacturer. However, the calibration of the force hub can be checked by simple tests. A quick and easy method would be to suspend or apply known loads on the *Kistler* system and then observe the measured value of the forces in all the three directions. If the load is placed vertically down and the face of the *Kistler* system is perpendicular to the ground and parallel to the big knuckle, the *Kistler* system should read the value of the load in the normal direction only with no value in the other two directions. Similarly, the *Kistler* can be recalibrated in the lateral direction by applying a known load in the lateral direction and longitudinally by applying a known pull force in the longitudinal direction. Another method can include using the normal load application mechanism of the rig to apply the desired load and then verify it by using a *TekScan* pressure mat. The alignment check using the laser distance measurement system needs to be performed again in concurrence to checking the calibration. If the alignment is evaluated to be correct then any significant difference in the applied and measured value can be attributed to the internal calibration of the force hub. This will require getting the force hub recalibrated by the manufacturer

6.4.2 Recalibration of the Drive System

The addition of the clutch system in the drive system for the wheel will require the recalibration of the control system of the wheel motor. A master−slave configuration is used to control the motor−gearbox arrangement of both the drive system. A PicPro ladder

program is used to control the master−slave arrangement. The modifications made to the rig are such that the control for the longitudinal motion controller remains unchanged. The PicPro code uses "ladder units per minute"*(*LU/min) for setting the speed. Thus, the units for the velocity has to be converted to Ladder Units for the speed of the carriage and the angular speed of the wheel. The existing conversion factor is 34515.9285 *(*LU/min) represents the translational velocity of 1 *cm/s* for the carriage drive system and 572957.7684 *(*LU/min) represents the angular velocity of 1 *rad/s* for the wheel drive system [17]. As mentioned previously, the ladder conversion unit for the translational speed for the carriage will remain unchanged. The task is to find the new conversion factor for 1 *rad/s* for the wheel drive system. A trial and error method has to be used to find the value of the ladder units corresponding to 1 *rad/s*. This can be done in the warm up stage where the ladder program is set to run the wheel at 2 *rad/s*. With the clutch system in place, the original setting for 2 *rad/s* might actually result in a speed which is less than 2 *rad/s*. An average measured value has to be determined for the angular velocity in the warm stage by repeating the warm up step. Considering this average measured value of the angular speed as ω_1 and the ladder unit already present in the code for the warm up run as LU_1, the ratio of LU_1/ω_1 will now represent the *LU/min* conversion factor for the wheel drive system. A simple validation can be done for this new conversion factor of the ladder units for the wheel drive system by using different value of angular speed in small steps of 0.01 starting from 0.1 *rad/s* during the warm up stage. At the end of this calibration step, the default value for the warm stage should be kept corresponding to 2 *rad/s* using the new conversion factor. For the measurement of the angular speed during the recalibration, the data from the *Kistler* system can be used. A quicker way to measure the rotational speed will be to use a low−rpm tachometer. The data in revolutions per minute (rpm) can be easily converted to *rad/s*.

6.4.3 Validation of Free−Rolling and Braking Capabilities

The main task of this work involved enabling the tire to free−roll. With the clutch system in place, the tire will now free−roll. However, the validation will involve measuring the rolling resistance of the tire on surfaces whose coefficient of rolling resistance is known. The rolling resistance will be denoted by the quantity measured as F_x by the *Kistler* system. The resistance offered by the support bearing for the clutch will not affect the measurement of F_x by the *Kistler* system due to the working principle of the *Kistler* system. The torque resistance by the rotating components and bearing will show up in the M_y measurement by the *Kistler* system. As mentioned previously, the moment resistance of the seals of the support bearing will contribute to 1.095 Nm in the reading of M_y. Further, coefficient of rolling resistance obtained by free−rolling the tire can be compared to the known values of coefficient of rolling resistance from literature. Additionally, the F_x value can be compared to the previously obtained F_x corresponding to 0 % slip condition.

The effectiveness of the clutch in engaged position for a traction test has to be validated as well. The validation procedure has to be done on ice or soil surface by repeating previously performed set of experiments for which the data is available. The validation has to be done by using design of experiments for different set of normal loads, slip ratios, and tire sizes. In the current configuration of the installed braking system, controlling the negative slip is not automated. A combination of manual effort, normal load, and the coefficient of friction will lead to a particular negative slip. Thus, the braking test validation will involve testing the tire with a nominal value of manual effort and incrementing it in steps to achieve various negative slip ratios.

Chapter 7

Results and Conclusions

7.1 Summary of Accomplishments

This project was targeted at enhancing the testing capabilities of the Terramechanics rig. The main accomplishment of this project was the physical realization of the desired systems on the Terramechanics rig. In summary, the first work done in this project was a feasibility study for incorporating free rolling and braking capabilities into the rig. This involved a comprehensive overview of various in-house, portable or outdoor tire testing facility to understand their design with respect to their intended functional capabilities. This phase was followed by the understanding of the existing design of the Terramechanics rig and identifying the scope and the space for expansion. The second part of the work involved the design and the implementation of a clutch system to enable free rolling of the test tire. This required a detailed design methodology involving selection and detail engineering of the various components of this system. The third task in this project involved the detailed engineering in the design of a customized brake system for the rig. The following task included procurement and/or fabrication of the various components of the clutch and brake system

and finally the assembly of these systems.

7.2 Novel Contribution

With the installation of the clutch system, it was now possible to determine the free rolling radius of the tire. A more accurate knowledge of the free rolling radius of the tire will lead to an improvement in setting the predefined longitudinal slip ratios for tire traction studies. Additionally, this system will now help in studying rolling resistance on terrains such as sand and soft soil, which have a relatively high coefficient of rolling resistance.

The brake system will enable studying negative slip or skid of tires on off terrain surfaces specifically ice. With the brake system in function, it will be possible to attain fully locked wheel condition of the tire on various surfaces.

These two new systems have increased the testing capabilities of the Terramechanics rig substantially. The rig is suitable to study rolling resistance and braking performance apart from studying tractive performance of tires over off−road conditions, such as sand, ice, etc.

7.3 Recommendation for Future Improvements

The next step is to validate these two new systems which will include the validations as described previously. Having said this, there is room for improvement in these two systems. The clutch system can be automated and integrated in the main motion control of the motors. This will eliminate the manual control of the clutch operation. Similarly, the brake system can too be automated by eliminating the manual operation to operation through a

motor, which will ensure controlled application of the brake force. Currently, the negative slip achieved depends on the uniformity of the manual effort. Thus, automating this manual effort will result in a uniform braking force to be applied during the test.

Bibliography

[1] A. Yahya, M. Zohadie, D. Ahmad, A. K. Elwaleed, and A. F. Kheiralla. UPM indoor tyre traction testing facility. *Journal of Terramechanics*, 44(4):293–301, 2007.

[2] Brad Michael Hopkins. *Adaptive Rollover Control Algorithm Based on an Off-Road Tire Model*. PhD thesis, Virginia Tech, 2009.

[3] Thomas R Way. Three single wheel machines for traction and soil compaction research. *Agricultural Engineering International: CIGR Journal*, 2010.

[4] Yoshiyuki Kawase, Hiroshi Nakashima, and Akira Oida. An indoor traction measurement system for agricultural tires. *Journal of Terramechanics*, 43:317–327, 2006.

[5] Jo Yung Wong. *Theory of ground vehicles*. John Wiley & Sons, 2008.

[6] Corina Sandu, B Taylor, J Biggans, and M Ahmadian. Building an infrastructure for indoor terramechanics studies: the development of a terramechanics rig at virginia tech. In *Proceedings of 16th ISTVS international conference, Turin, Italy*, pages 177–185, 2008.

[7] Richard J Godwin, James L Brighton, Kim Blackburn, Terence E Richards, Dirk Ansorge, and Paul N Wheeler. Off-Road Dynamics Research at Cranfield University at Sil-

soe. In *Proceedings of ASABE Annual International Meeting, Portland, Oregon (9th12th July 2006)*, 2006.

[8] Karl Iagnemma, Hassan Shibly, and Steven Dubowsky. A laboratory single wheel testbed for studying planetary rover wheel-terrain interaction. *MIT field and space robotics laboratory technical report*, 1:5, 2005.

[9] Ray Shaver and S A E Clutch Standards Committee. *Manual transmission clutch systems*. Society of Automotive Engineers, Warrendale, PA :, 1997.

[10] William C Orthwein. *Clutches and brakes: design and selection*. CRC Press, 2004.

[11] Rudolf T A T T Limpert. *Brake design and safety*. Society of Automotive Engineers. Electronic publications.; Society of Automotive Engineers. Electronic publications. Society of Automotive Engineers,, 3rd ed. nv edition, 2011.

[12] Society of Automotive Engineers. Vehicle Dynamics Committee. *Vehicle Dynamics Terminology: SAE J670e*. Society of Automotive Engineers, 1978.

[13] S Naranjo. Experimental investigation of the tractive performance of an instrumented off road tire on a soft soil terrain. Master's thesis, Virginia Tech, Blacksburg, 2013.

[14] C. Sandu. Chapter 2. Severe Environmental Conditions and Situations. 2.1. Experimental and Modeling Terramechanics Studies. In M.V. Vantsevitch, V.V. and Blundell, editor, *Advanced Autonomous Vehicle Design for Severe Environments*, page 408. IOS Press BV, NATO ASI, Vol. 44 of NATO Science for Peace and Security Series - D: Information and Communication Security, 2015.

[15] Scott David Naranjo, Corina Sandu, Saied Taheri, and Shahyar Taheri. Experimental Testing of an Off-Road Instrumented Tire on Soft Soil. *Journal of Terramechanics*, 56:119–137, 2014.

[16] Aamir K. Khan and Corina Sandu. Design and manufacturing of a clutch and brake system for indoor tire testing. In *ASME 2017 International Design Engineering Technical Conferences and Computers and Information in Engineering Conference*. American Society of Mechanical Engineers, 2017.

[17] Benjamin Paul Taylor. Experimental evaluation and semi-empirical modeling of the tractive performance of rigid and flexible wheels on lunar soil simulant. Master's thesis, Virginia Tech, 2009.

Appendix A

Detail Drawings of Components

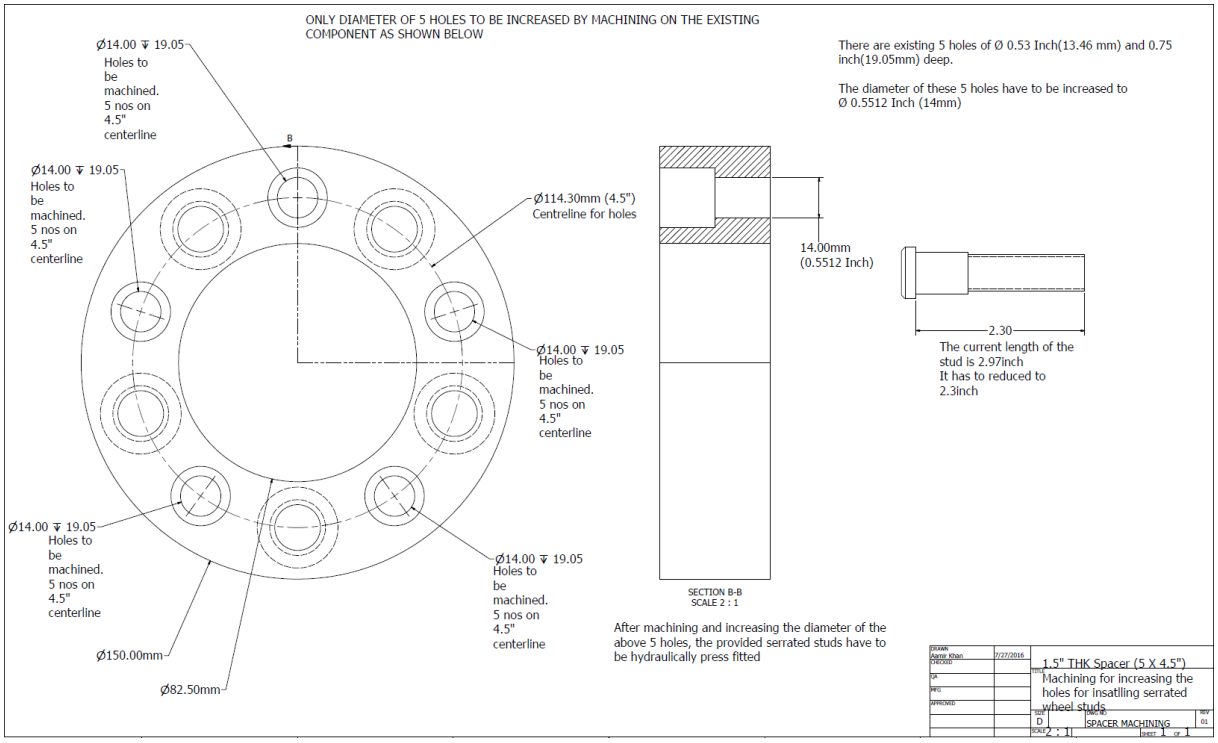

Figure A.1: Post procurement machining of wheel spacer and wheel stud.

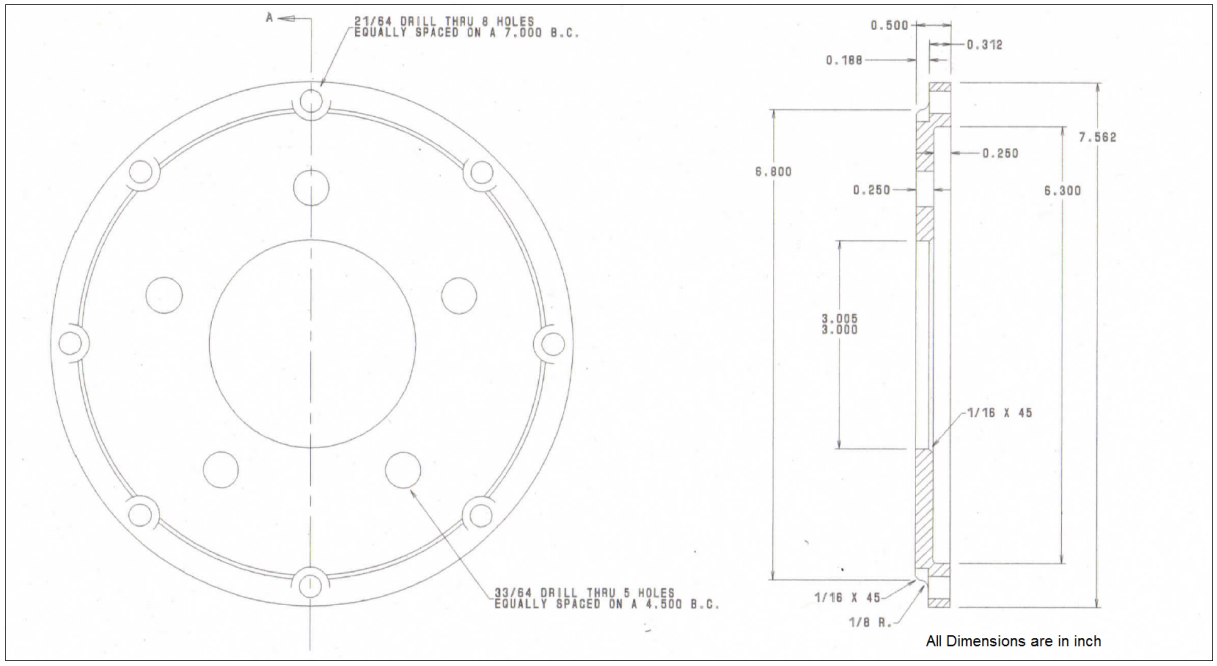

Figure A.2: Brake Rotor Hat - Courtesy Coleman Racing.

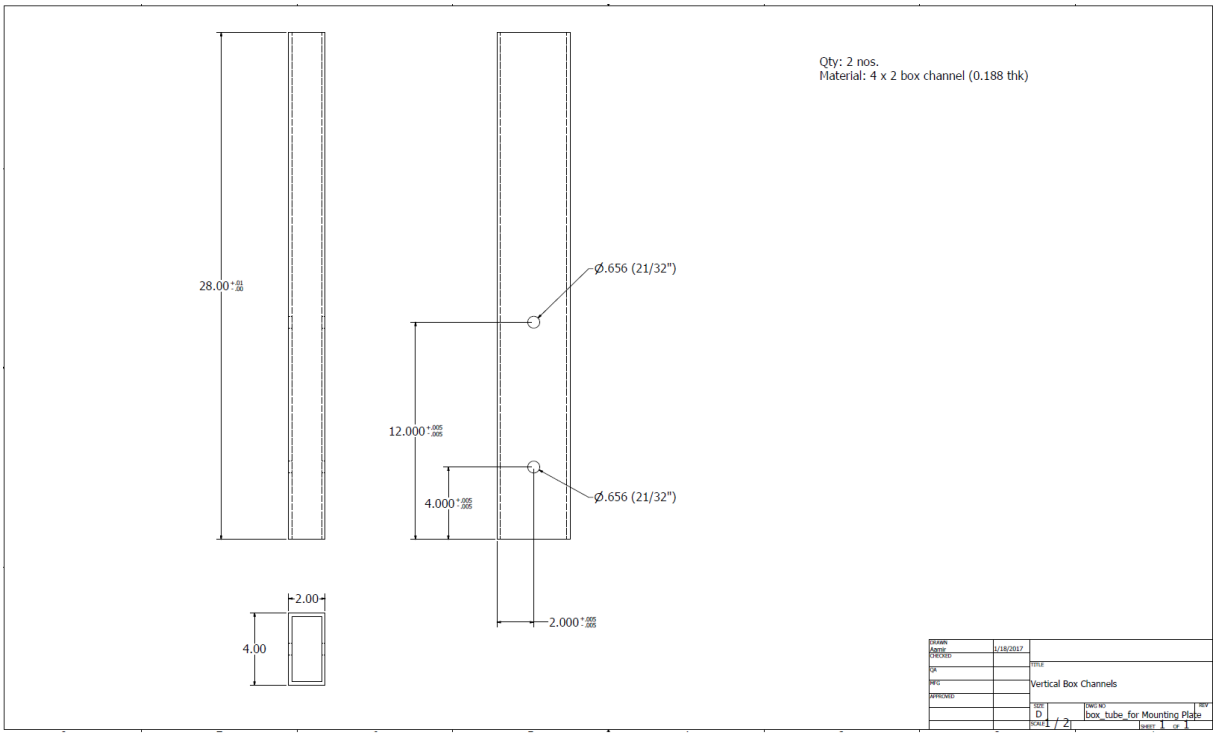

Figure A.3: Box channels for new mounting plate.

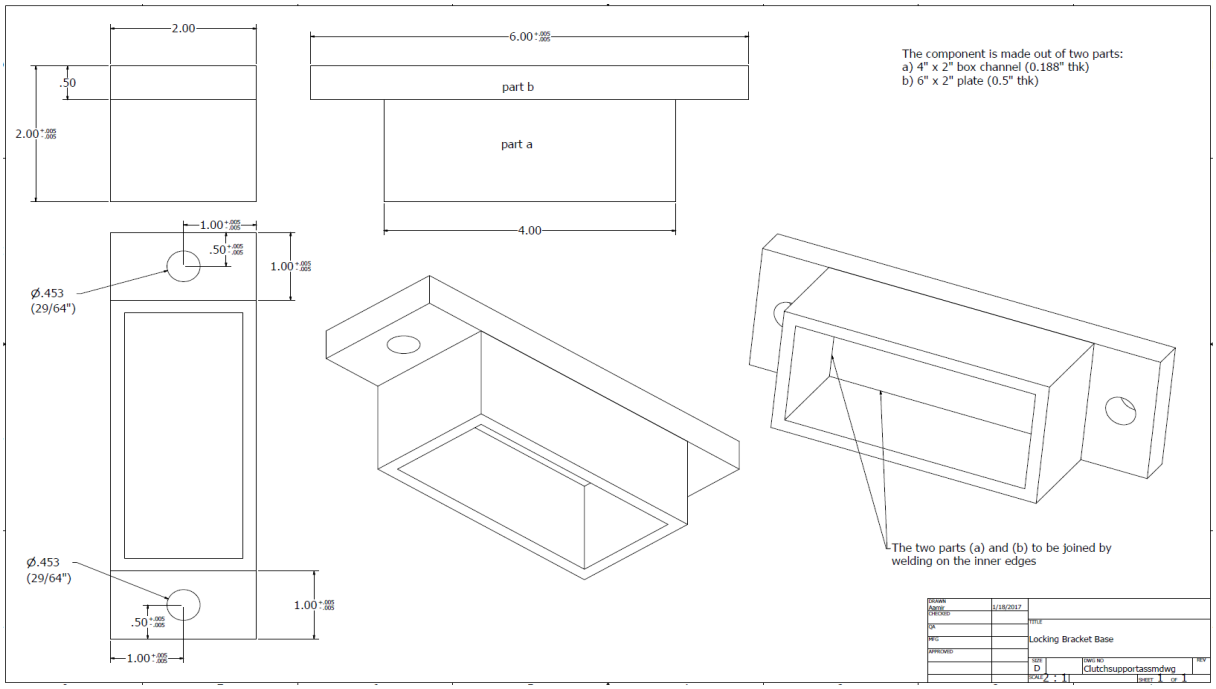

Figure A.4: Locking bracket for clutch - Part A.

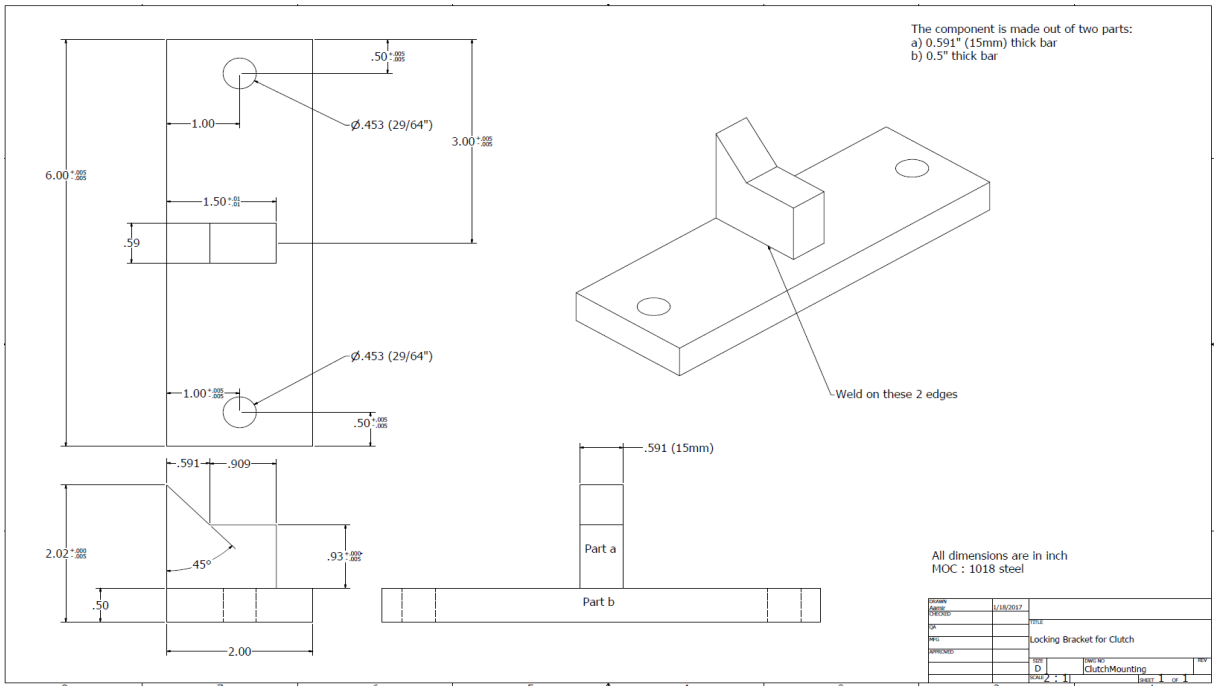

Figure A.5: Locking bracket for clutch - Part B.

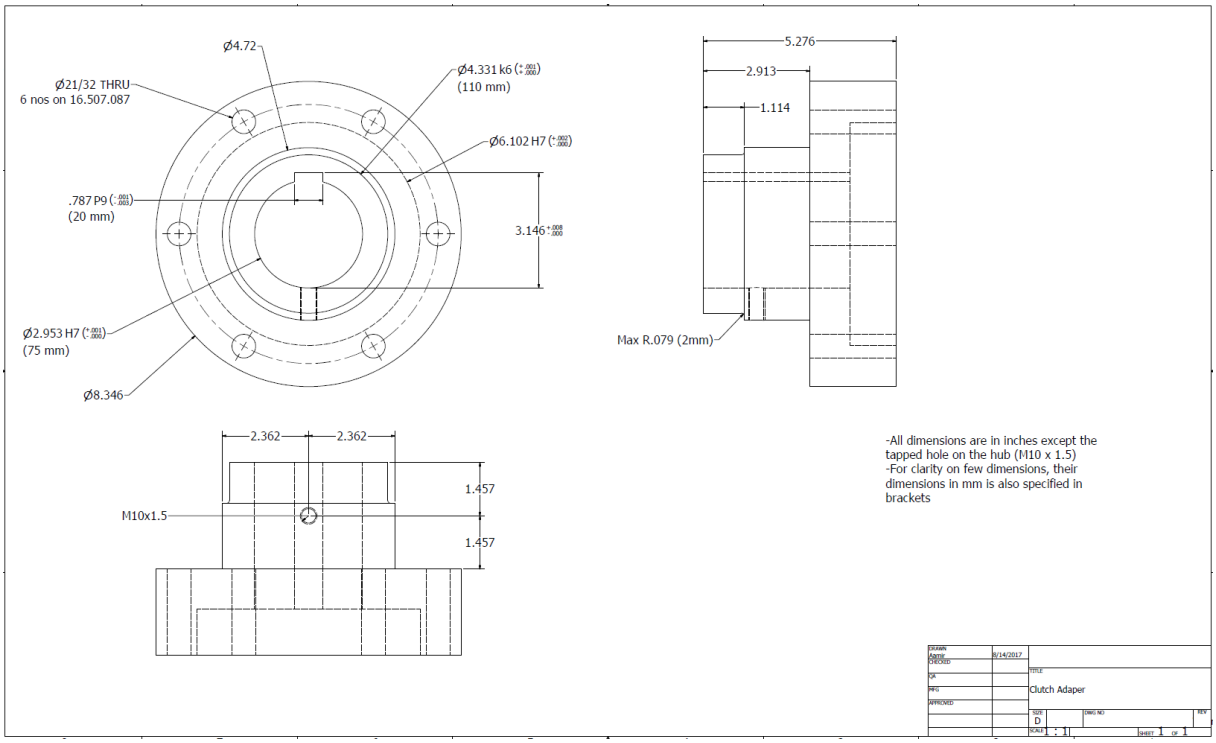

Figure A.6: Clutch adapter.

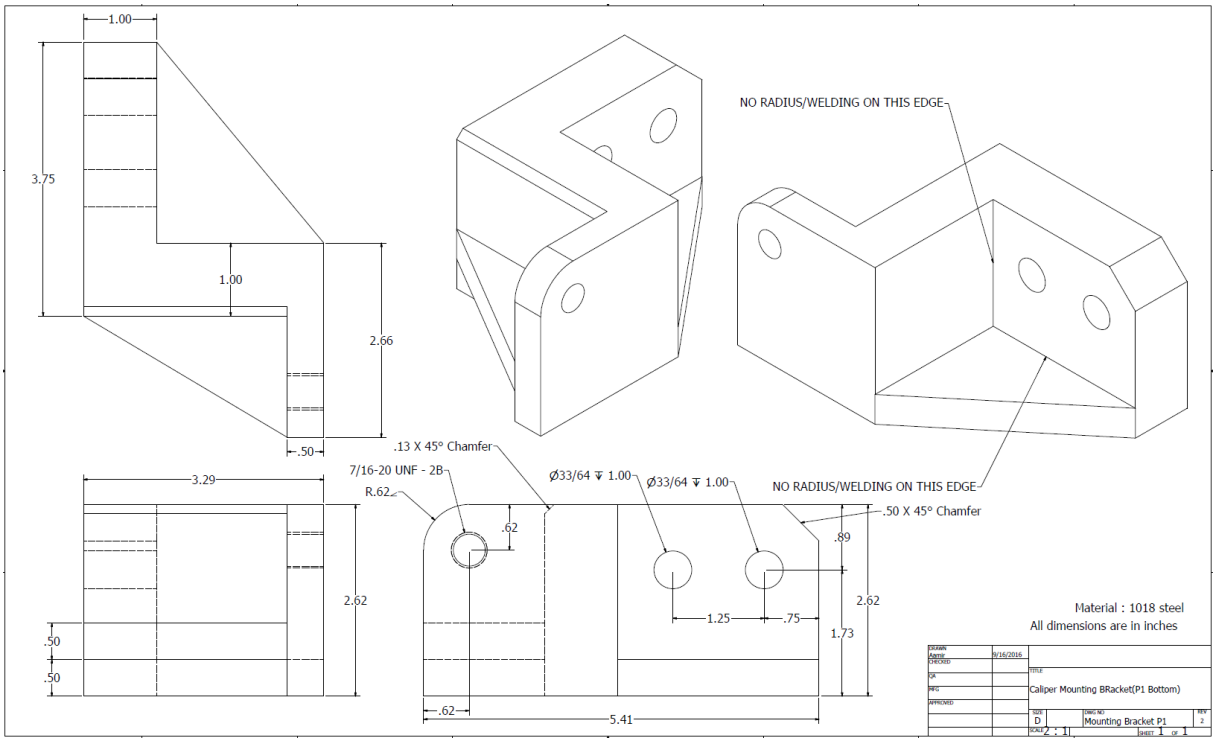

Figure A.7: Brake caliper bracket - Part 1.

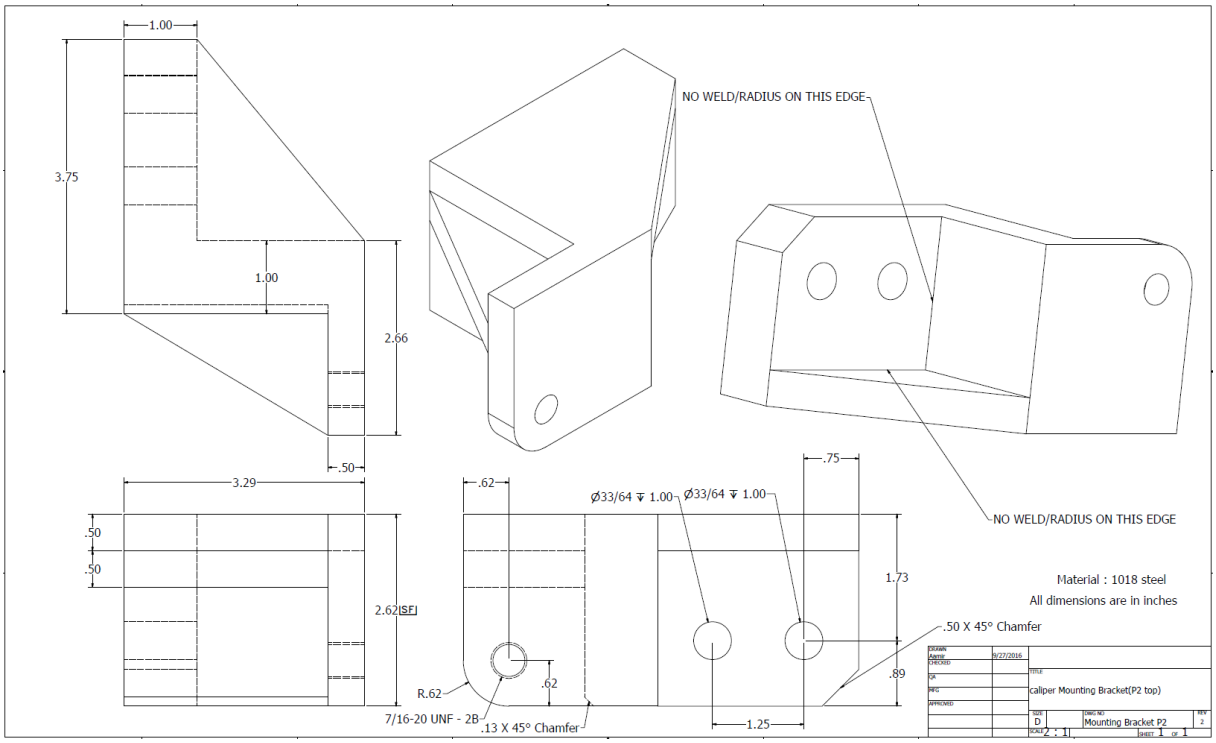

Figure A.8: Brake caliper bracket - Part 2.

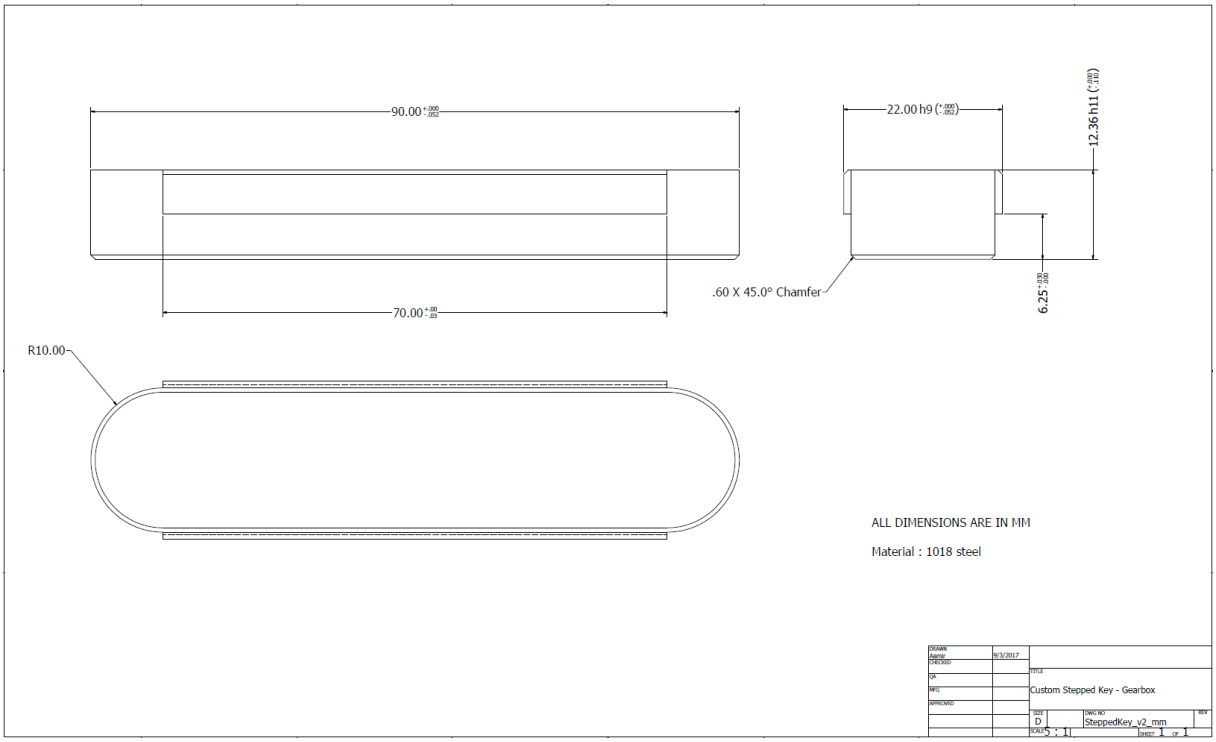

Figure A.9: Custom stepped key for gearbox shaft and clutch hub assembly.

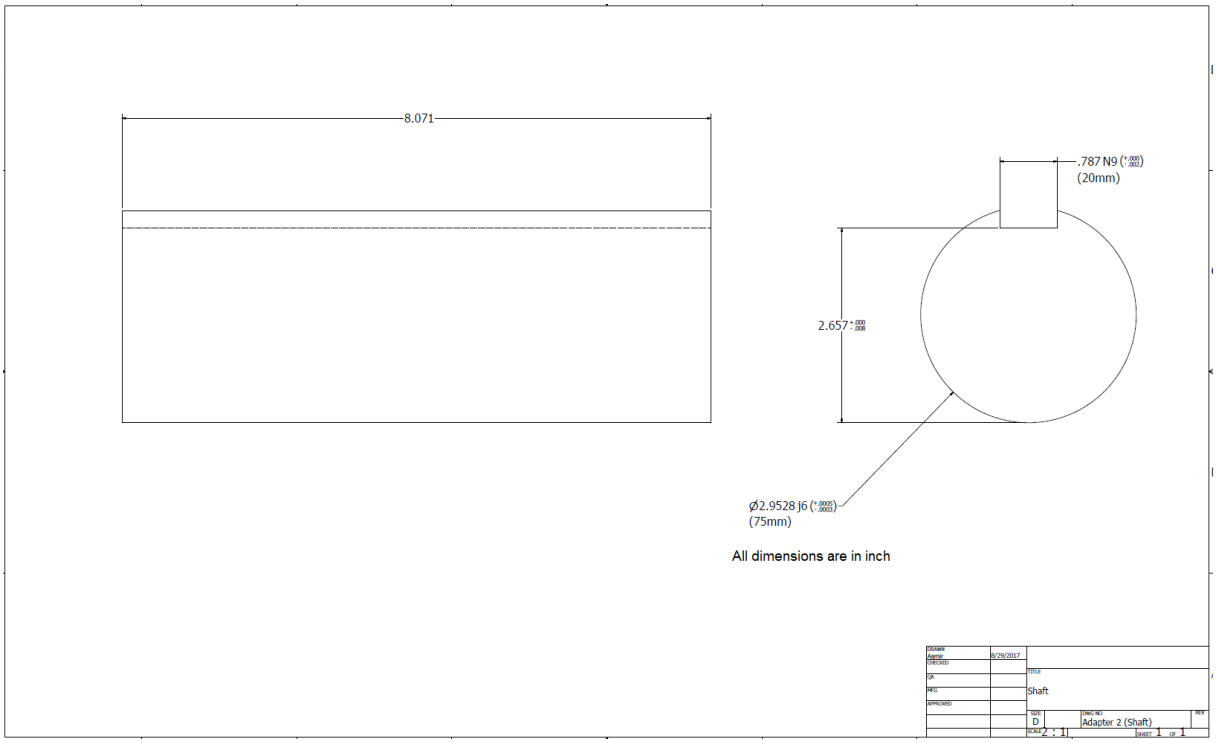

Figure A.10: New shaft to couple clutch adapter and C.V. joint.

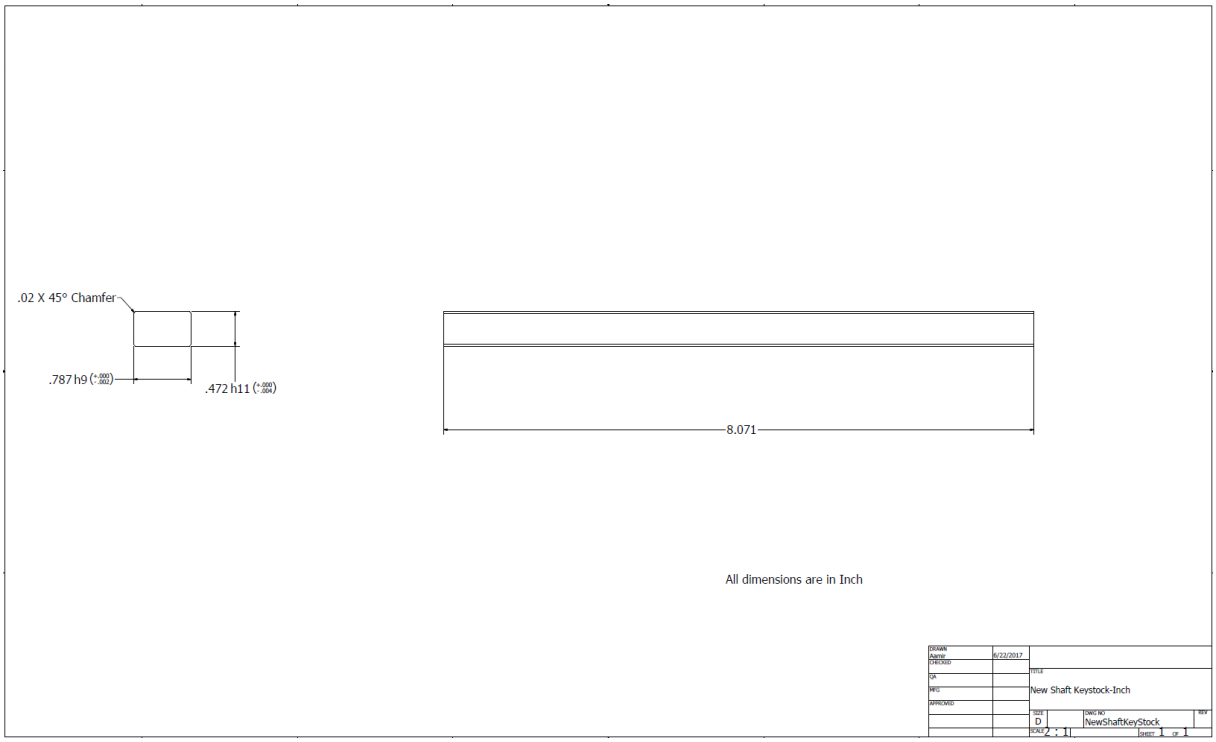

Figure A.11: Key to couple clutch adapter, new shaft and sleeve for C.V. joint.

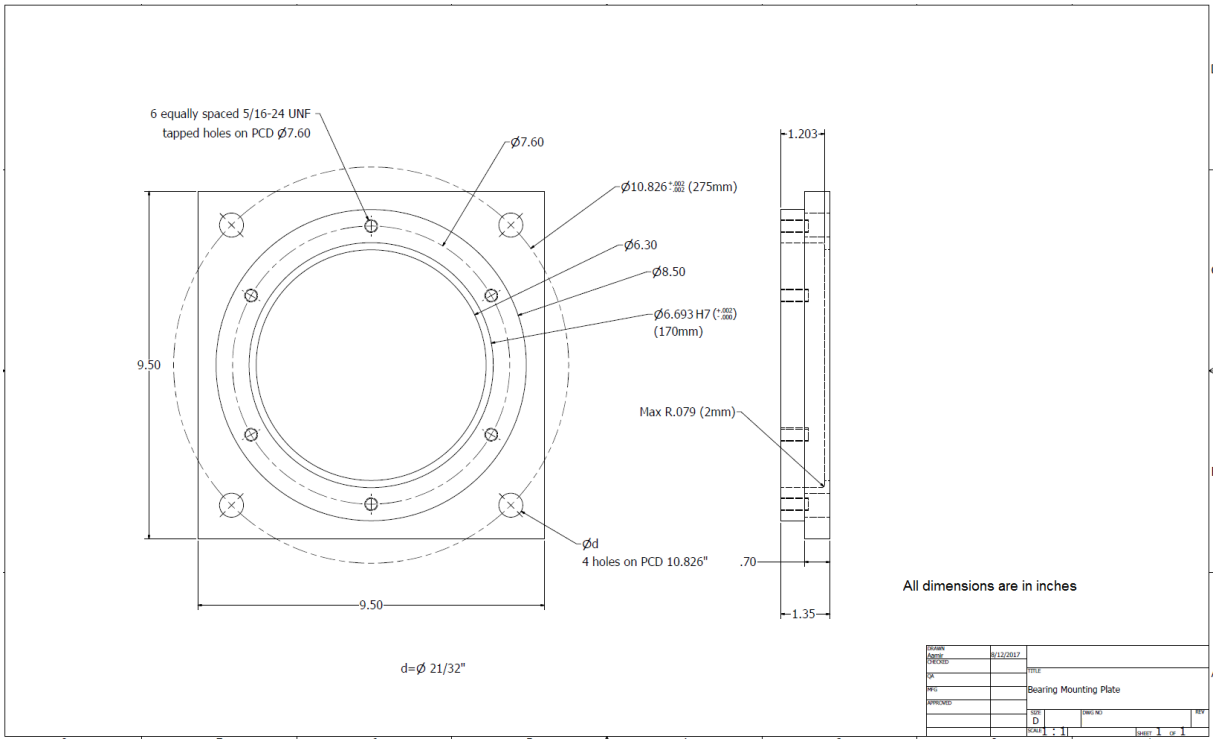

Figure A.12: Bearing housing.

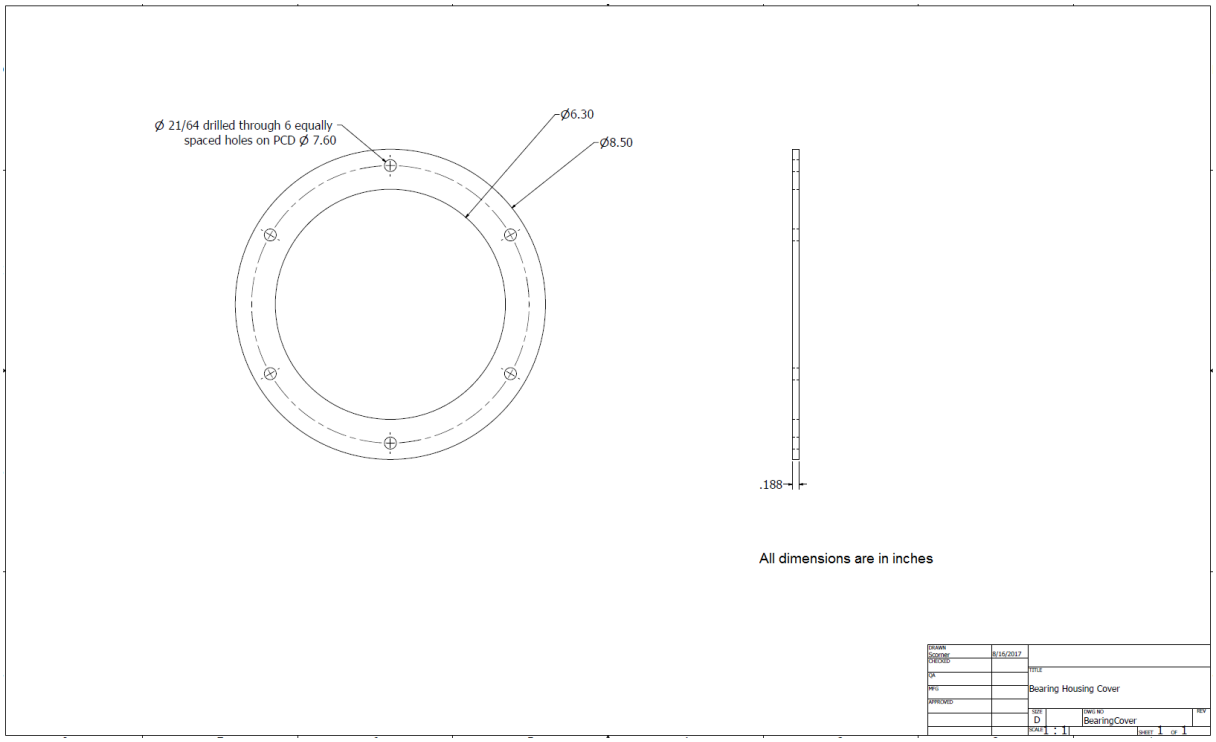

Figure A.13: Cover plate for bearing housing.

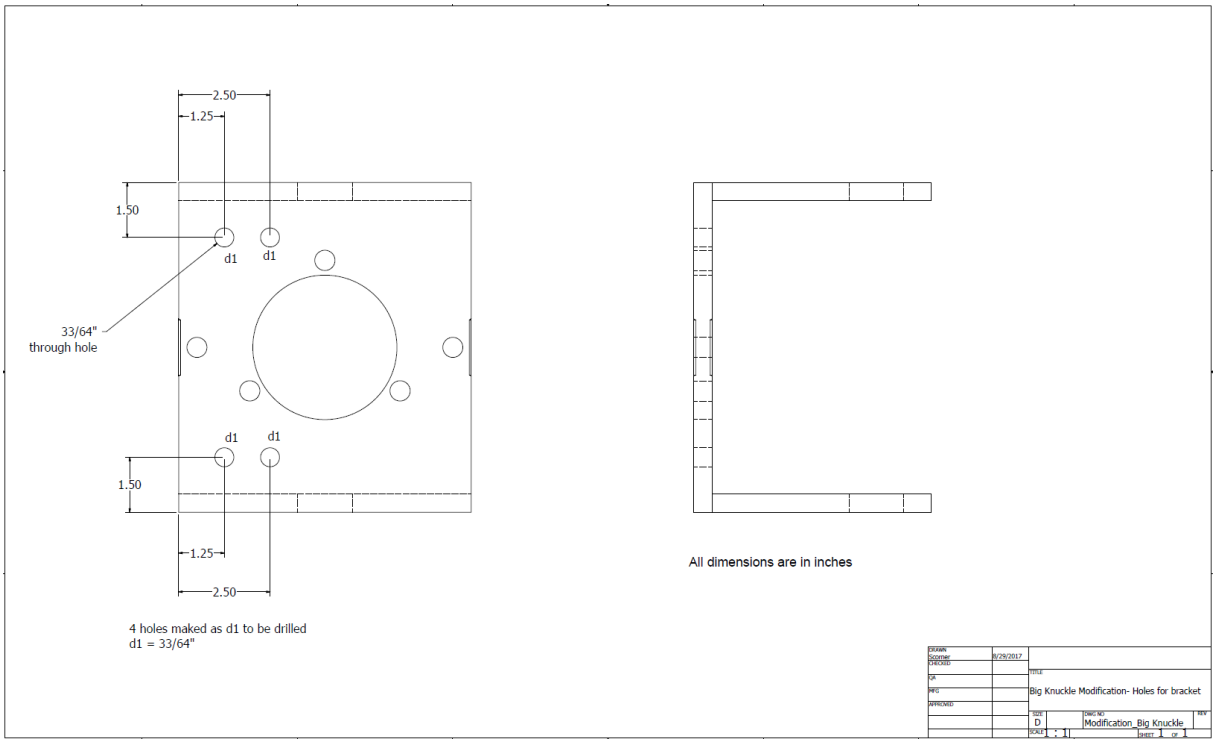

Figure A.14: Drilling of holes on big knuckle for mounting the brake caliper brackets.

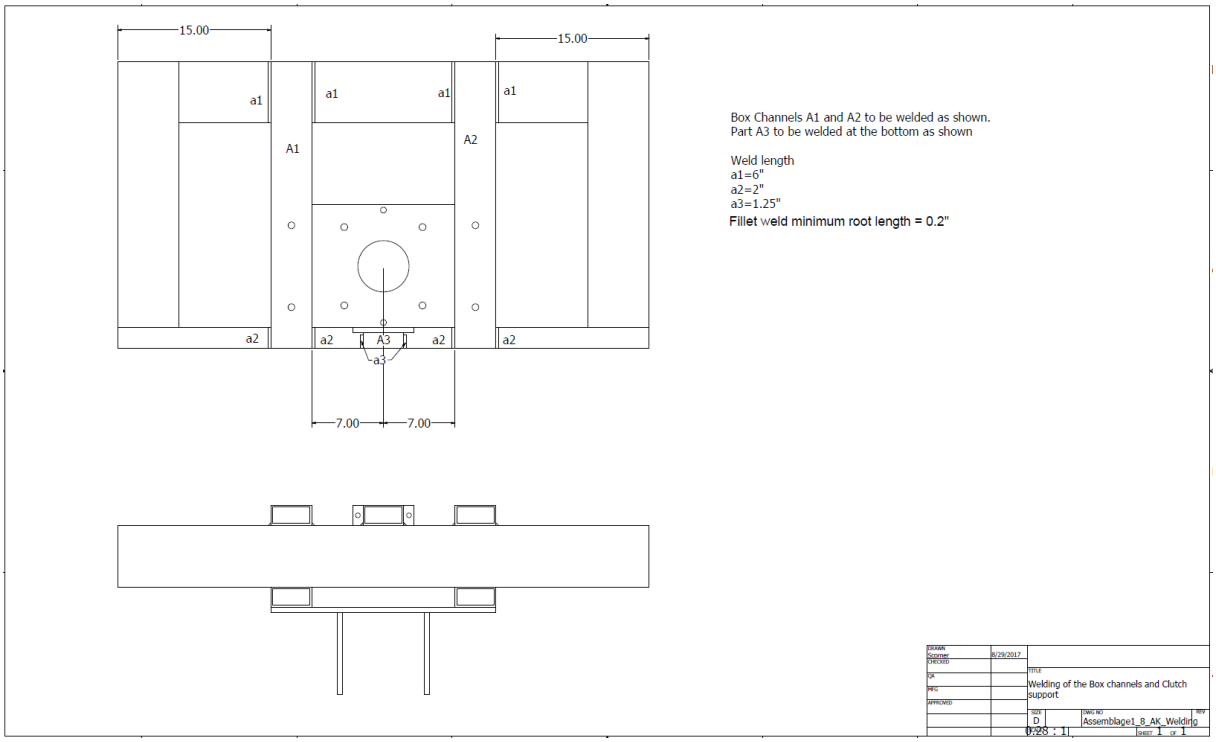

Figure A.15: Welding of box channels on the test tire frame.

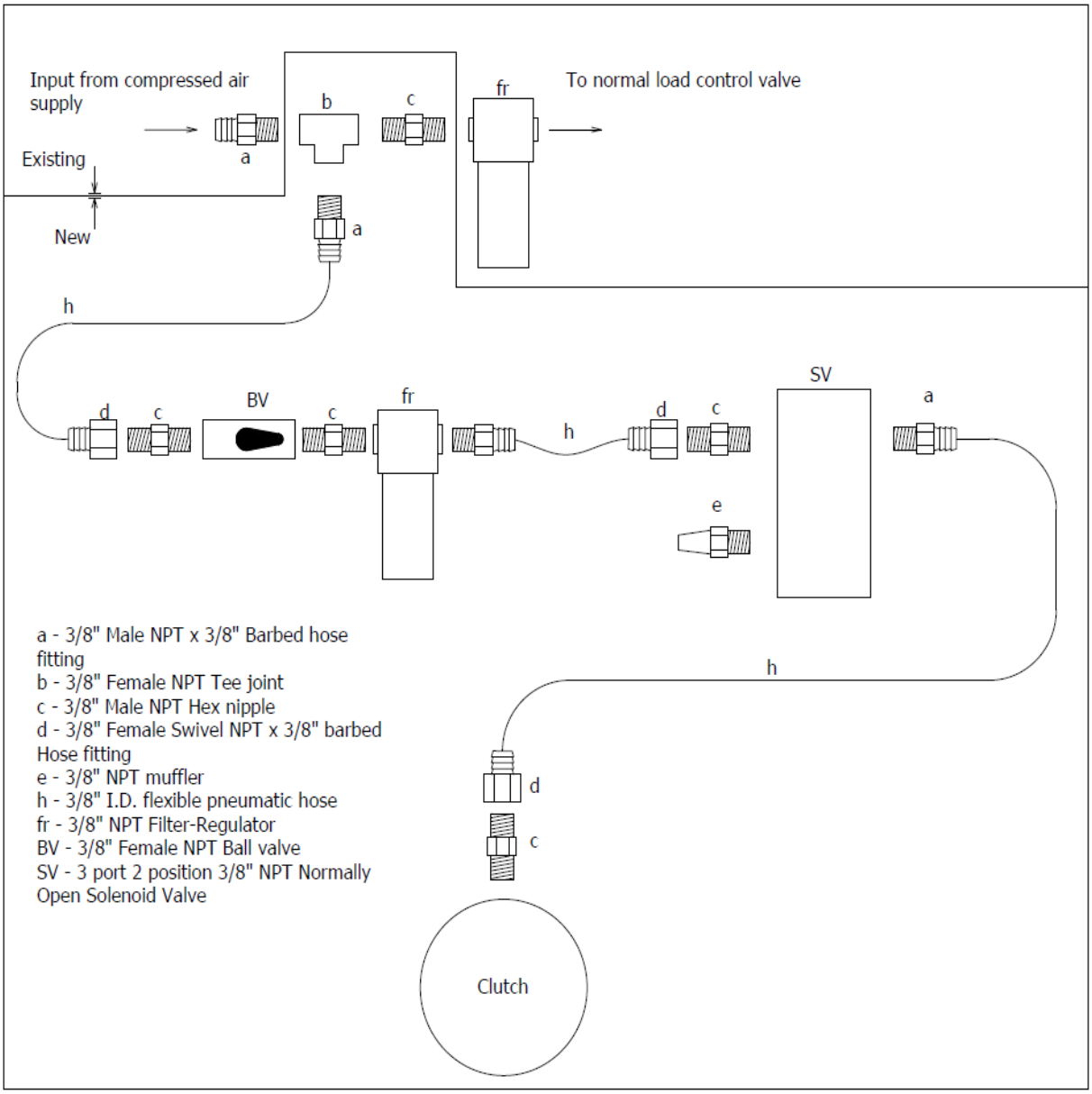

Figure A.16: Detailed drawing of the clutch actuation system.

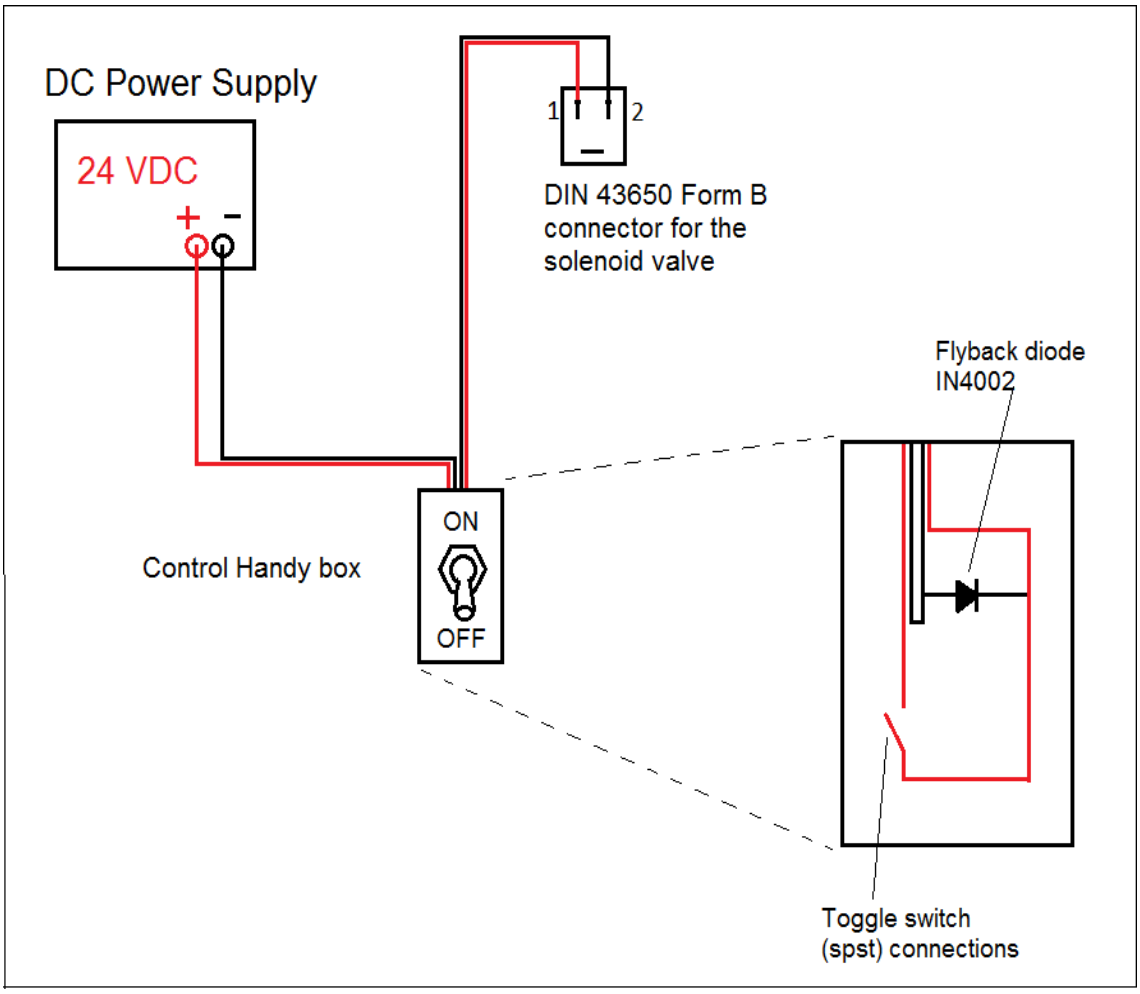

Figure A.17: Wiring diagram for solenoid valve for clutch actuation system.

Appendix B

Photos of Assembly Procedure of the Clutch and the Brake Systems

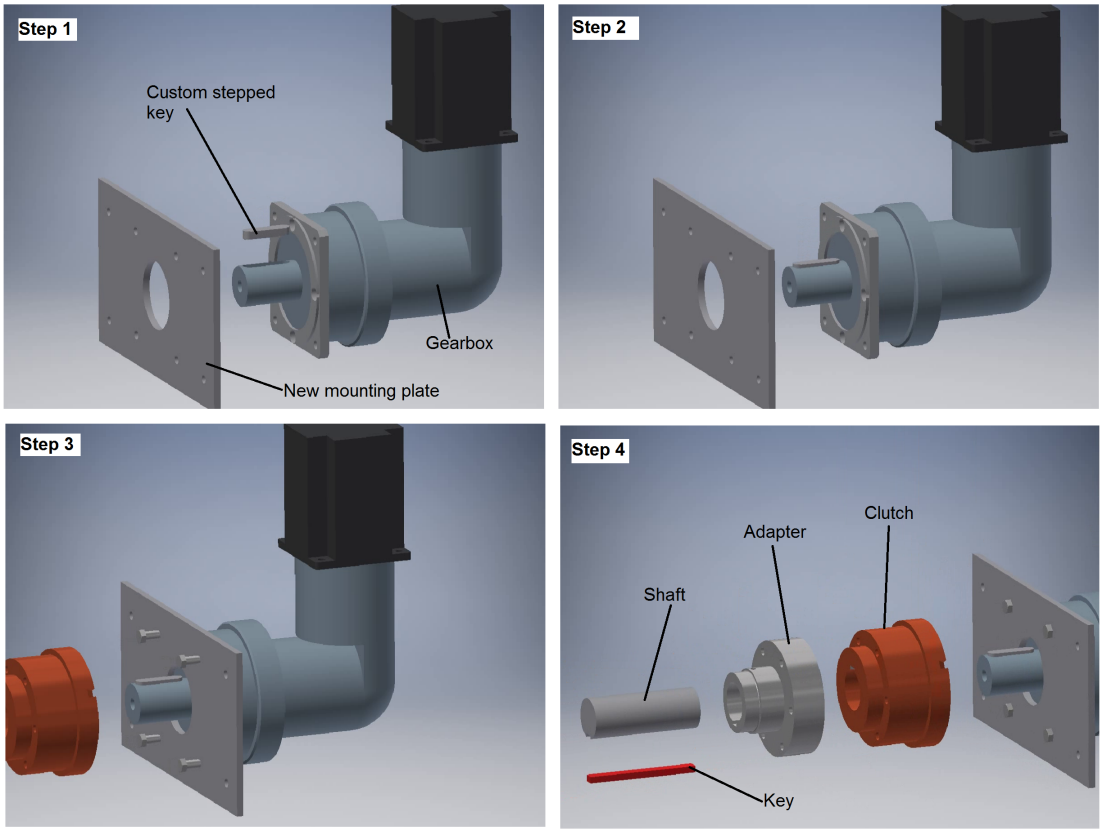

Figure B.1: Procedure for assembly-1 of the clutch system - bolting of gear box, clutch, adapter and new box channels - Step1 to Step4.

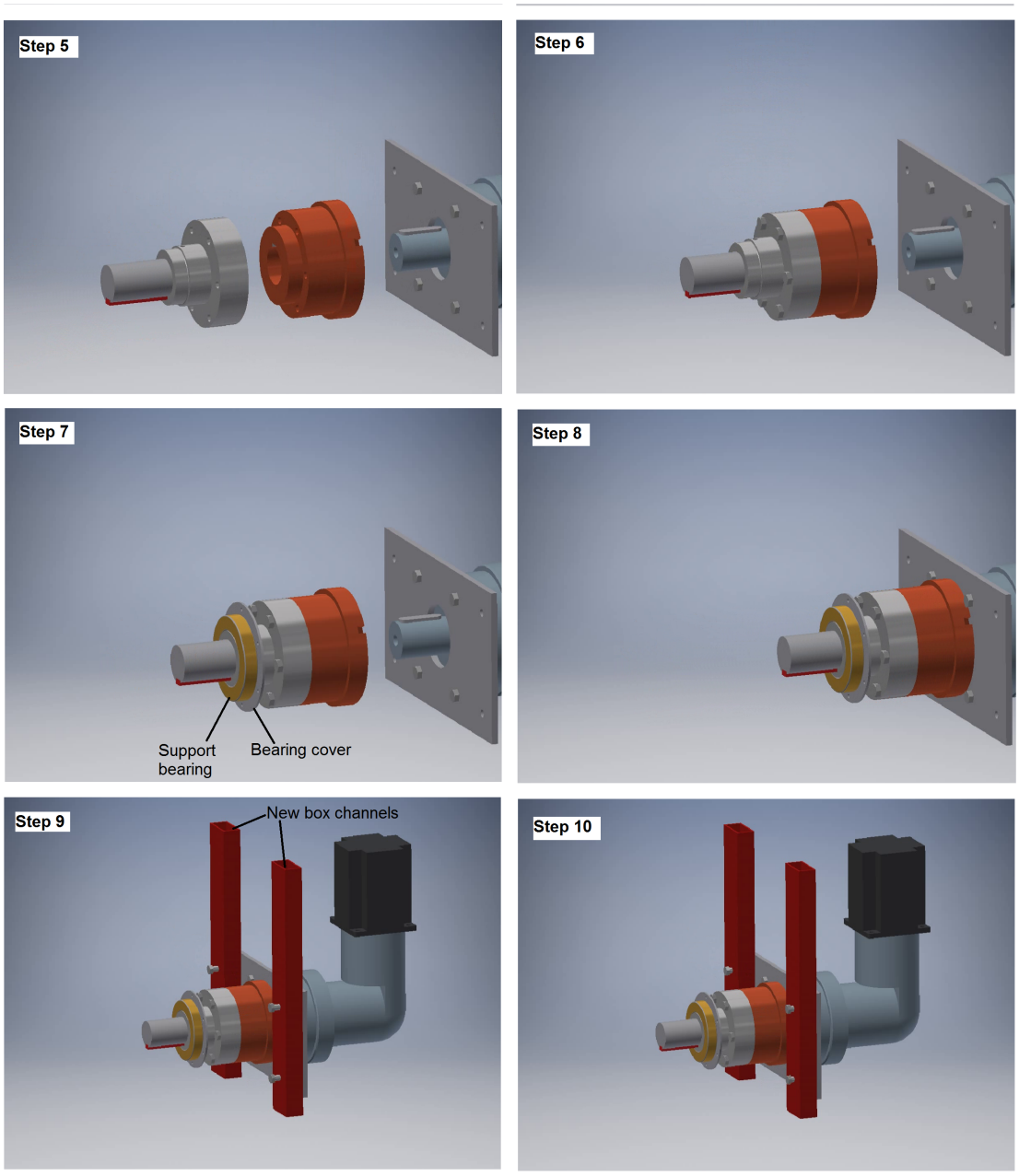

Figure B.2: Procedure for assembly-1 of the clutch system - bolting of gear box, clutch, adapter and new box channels - Step5 to Step10.

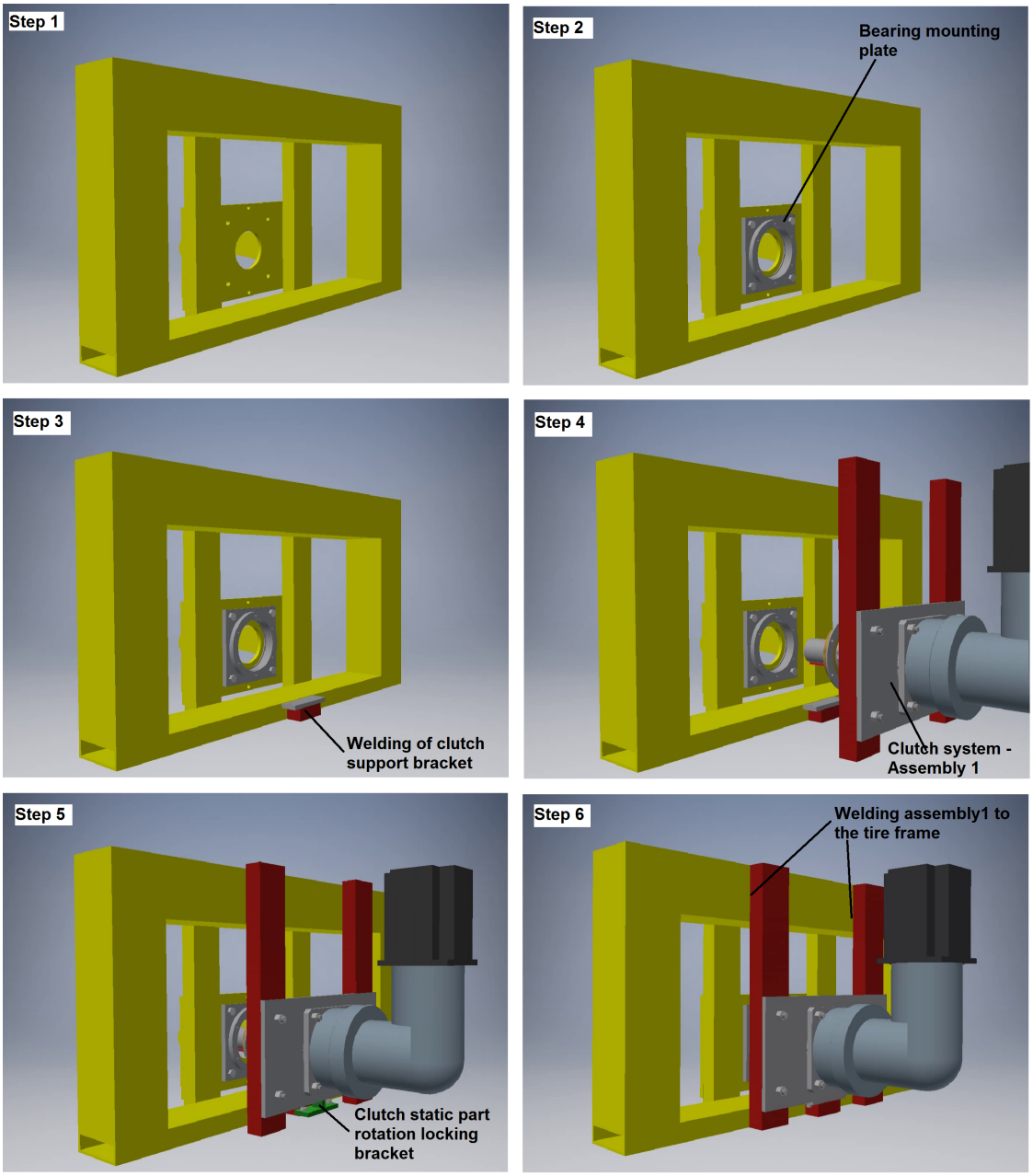

Figure B.3: Procedure for assembly-2 of the clutch system - welding of assembly 1 on the tire test frame.

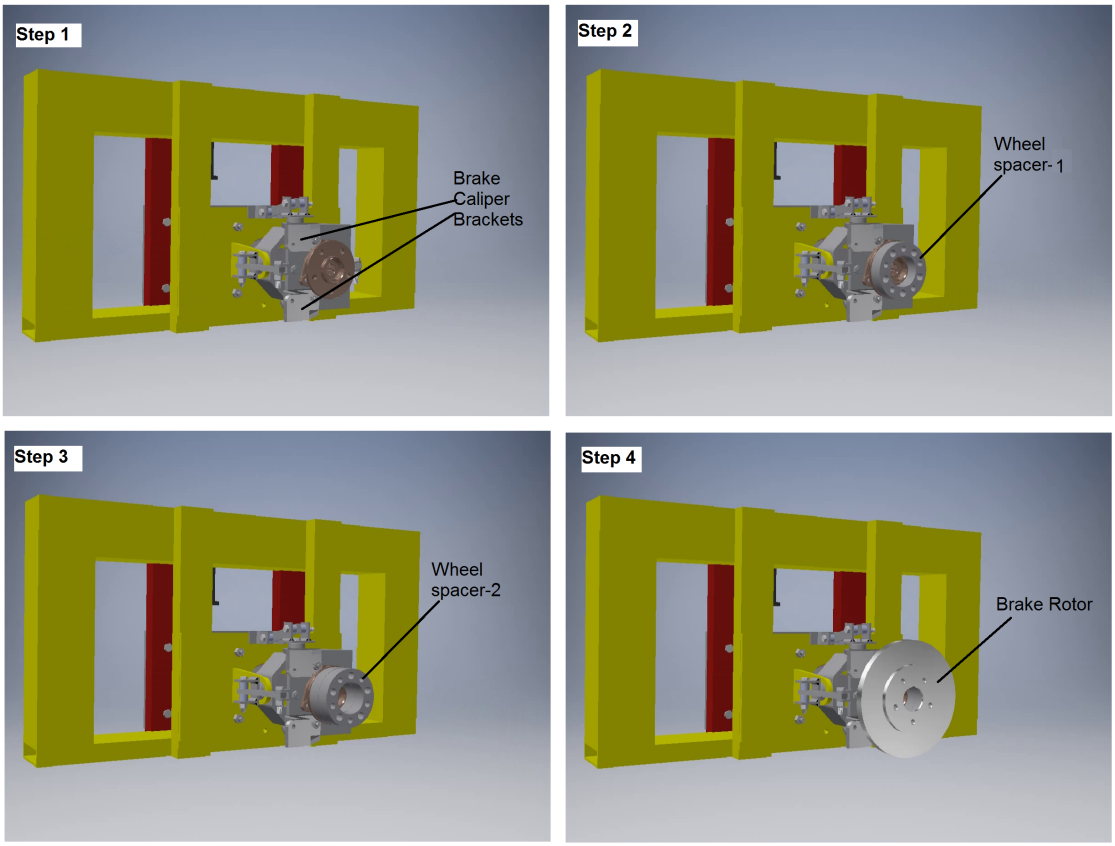

Figure B.4: Procedure for brake system assembly - Step1 to Step4.

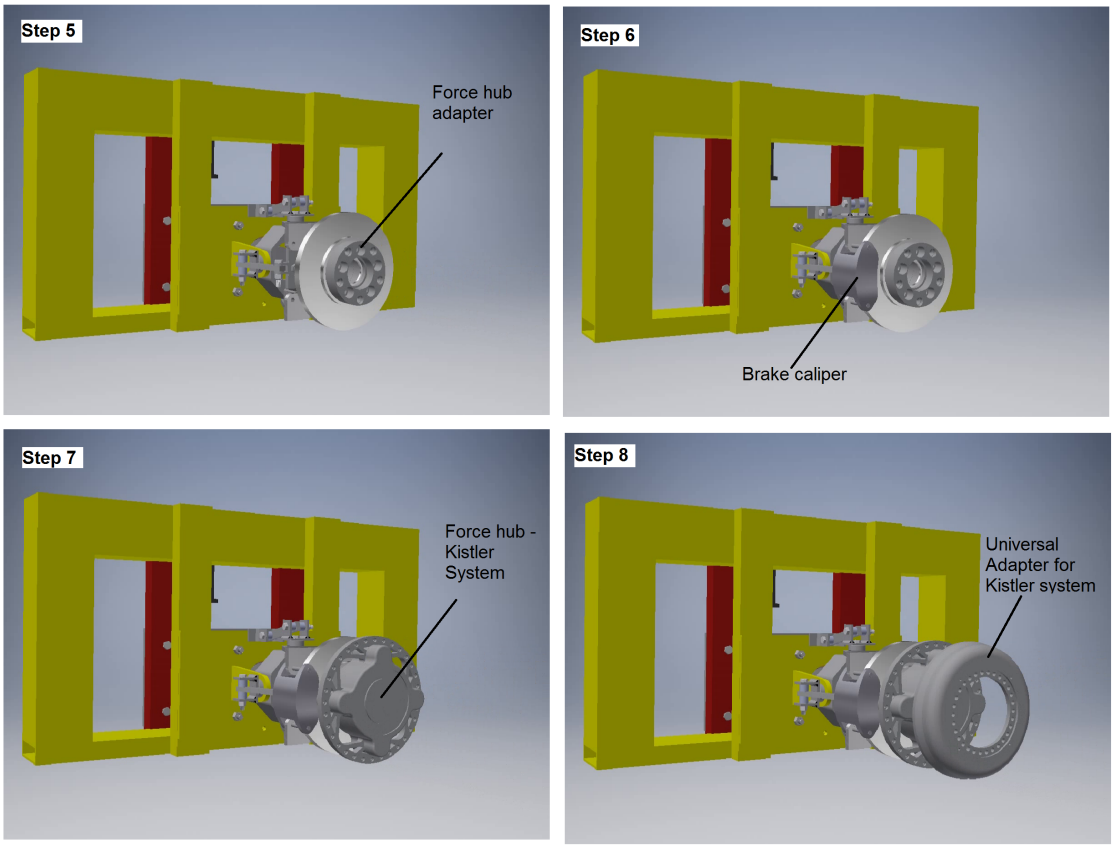

Figure B.5: Procedure for brake system assembly - Step5 to Step8.

Appendix C

Operation Procedure of the Clutch and the Brake System

This appendix documents a general operating procedure for the clutch and the brake system.

C.1 General Operating Procedure for the Clutch System

1. Turn ON the main valve on the compressed air line.
2. Turn ON the valve on the tapped compressed air line to the clutch.
3. Set/Check that the pressure regulator of the line to the clutch reads 0.6 MPa (87 psi) or little over it.
4. Always set the ON−OFF toggle switch on the handy box controller of the clutch to

the off position at the beginning.

5. For a traction test run, no further operation is required on the clutch system.

6. For a free rolling or a braking test run, the following steps are to be followed with the clutch system.

   There are two ways to control the the flow of the compressed air to the clutch. Either to use the ON-OFF ball valve placed right before the filter/regulator for the compressed air line to the clutch.

   (a) Turn OFF the ball valve placed right before the filter/regulator for the compressed air line to the clutch.

   (b) Open the drain knob on the filter/regulator for the compressed air line to the clutch to release the back pressure. With this the clutch will be diengaged.

   (c) Once a test is complete and the clutch has to be engaged again, close the drain knob on the regulator filter and then turn ON the ball valve of the clutch line.

   NOTE: Use the above method, if and only the complete test run requires the disengagement of the clutch. If the test run involves halfway traction and halfway braking or free−rolling, then use the next method involving the use of the solenoid valve.

   OR

   (a) Ensure that the toggle switch on the handy box of the clutch system is set in OFF position.

   (b) Turn ON the main switch of the DC−power supply.

   (c) Set/Check that the output voltage reads 24 V.

(d) Before application of the normal load to the frame, flip the switch of the handy box to the ON position. This will cut off the compressed air supply to the clutch and disengage it.

(e) Once the test is complete and the carriage reaches the end of the soil vane and the normal load is released from the frame, flip the switch of the handy box back to OFF position before sending the carriage back to the start position.

(f) The clutch can be disengaged anytime during the test run depending the test plan.

(g) Since the test run can accommodate 4 different slip ratios in a run. For those duration of the test which involves the disengagement of the clutch, the ladder unit of the wheel motor be set to a value that would correspond to 0 % longitudinal slip.

NOTE: Although the power from the wheel motor is isolated during a free−rolling or braking test, the linear motion controller still has to be fed with a ladder unit for the wheel motor during the test run. It is recommended that this ladder unit be set to a value that would correspond to 0 % longitudinal slip. This will have no effect on the test run, but will ensure that the *PicPro* code functions properly for the carriage motor.

C.2 General Operating Procedure for the Brake System

1. Before the test, manually check that the brake calipers are functioning when a manual effort is applied to the handbrake/pedal.

(a) Apply a set manual effort and observe whether the caliper pads move outwards. If yes, then continue with step 2.

(b) If the pads do not move outwards, or move out very less as against a set manual effort or if the manual effort is easy to apply (quick movement of the pedal/lever), this could indicate leakage or air in the system.

(c) In case of a leakage, detect the source and take necessary action of sealing or replacing.

(d) If there is no leakage, it may indicate air in the brake lines. Proceed with brake bleeding operation.

2. Next, follow the steps mentioned for the operation of clutch system during a free rolling or braking test.

3. After the application of the normal load to the tire, apply the set load on the brake lever.

4. Start with the test run.

5. Once the carriage reaches the end of the test, release the brake force and then release the normal load on the tire.

6. Flip the switch of the handy box of the clutch back to OFF position as described in the operating procedure of the clutch

Appendix D

Publications

Peer-Reviewed Conference Papers

1. He, R., Khan, A. , Guthrie, G., Sandu, C., and Els, S. "A Technical Survey on Terminology, Testing Methodologies, and Equipment used in Modeling and Parameterization of Soft Soil for Vehicular Applications", 9th International & 14th European-African Regional Conference of the ISTVS, Sept. 25-27, 2017, Budapest, Hungary.

2. Khan, A. and Sandu, C. "Design and Manufacturing of a Clutch and Brake System for Indoor Tire Testing", ASME International Design Engineering Technical Conferences & Computers and Information in Engineering Conference (IDETC/CIE 2017), Aug. 6-9, 2017, Cleveland, Ohio, USA.